QODL LAB

QOT CENTRE FOR QUANTUM OPTICAL TECHNOLOGIES

UNIVERSITY OF WARSAW

QUANTUM MEMORIES AND SENSORS BASED ON NEUTRAL ATOMS

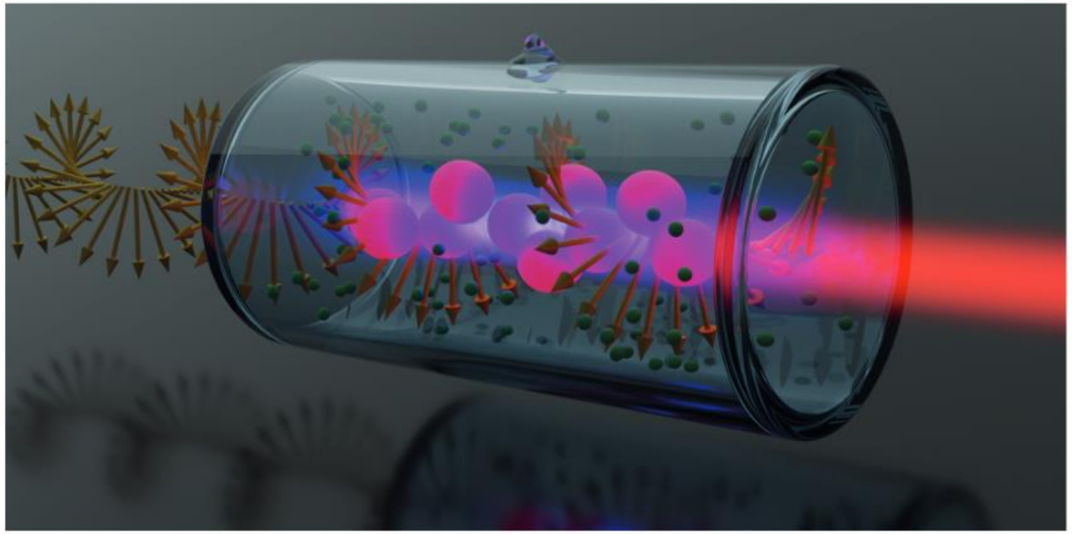

Michał Parniak

Centre for Quantum Optical Technologies

University of Warsaw

qodl.cent.uw.edu.pl

European Funds Smart Growth

Republic of Poland

FNP Foundation for Polish Science

European Union European Regional Development Fund

NATIONAL SCIENCE CENTRE POLAND

2021/43/D/ST2/03114

University of Colorado Boulder| August 18th 2023

Personal introduction

2012-2018

FACULTY OF PHYSICS
UNIVERSITY OF WARSAW

UNIVERSITY OF WARSAW

Cold atoms (MOT),
Quantum memories,
Quantum information

2018-2021

Niels Bohr Institutet

UNIVERSITY OF COPENHAGEN

Cavity quantum
optomechanics,
hot atoms

2021-

QOT CENTRE FOR QUANTUM OPTICAL TECHNOLOGIES

UNIVERSITY OF WARSAW

Rydberg atoms (hot/cold),
analog optical quantum
signal processors (e.g. for
superresolution
spectroscopy)

qodl.cent.uw.edu.pl

Multifunctional quantum memories

Photon spin-wave storage

Photon generation

Spin-wave interference

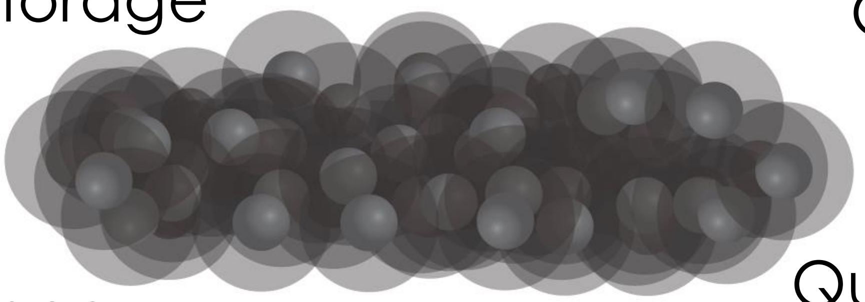

Quantum repeater

Error correction

Quantum gates: linear, nonlinear

Qu**d**it storage: spatial, temporal

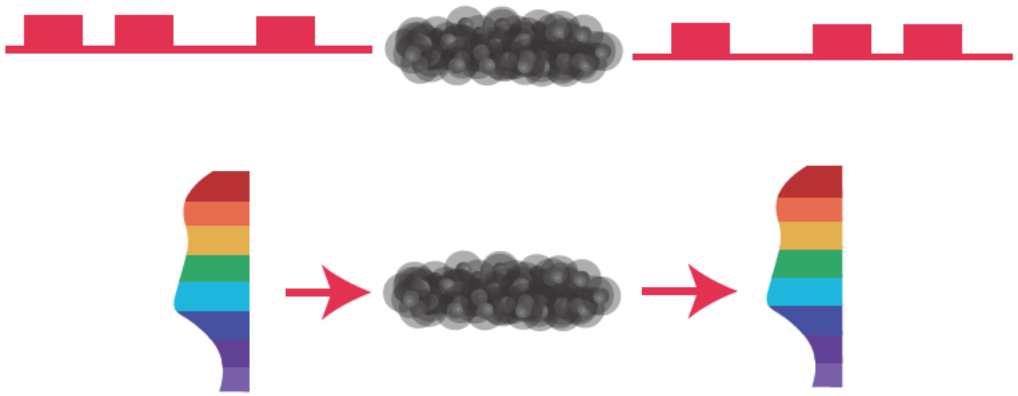

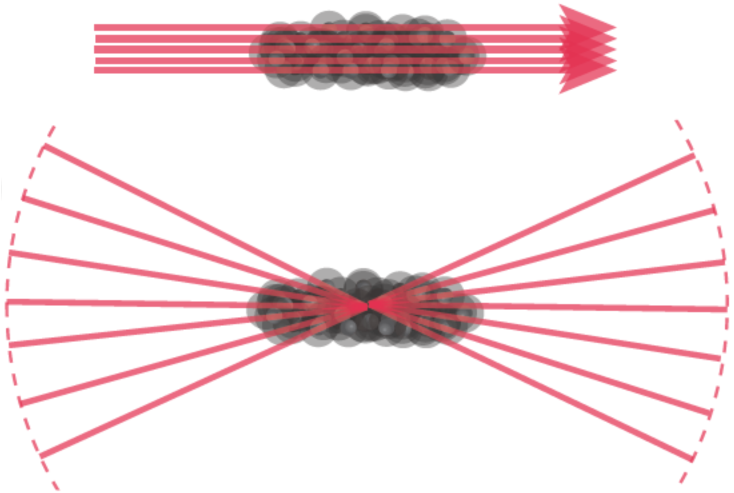

Raman interface

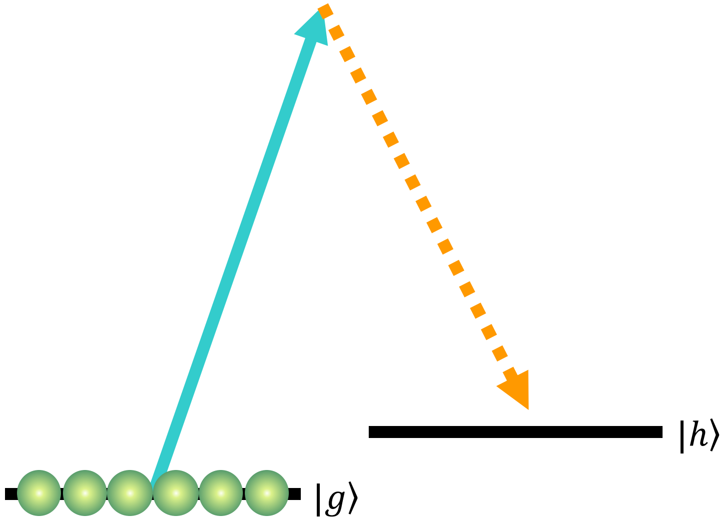

two-mode squeezed state creation via off-resonant **Raman scattering**

quantum memory

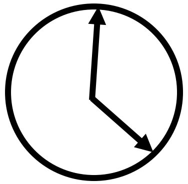

spin-wave

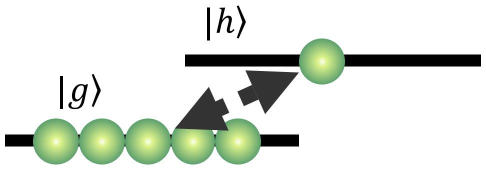

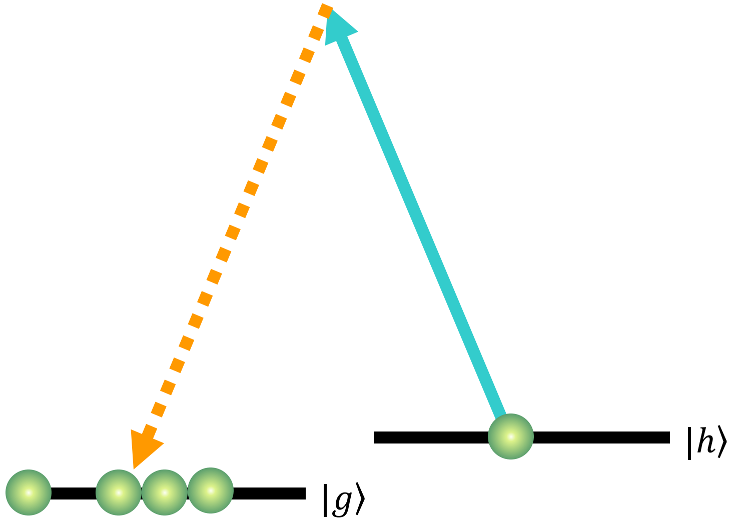

readout stage after storage time results in **anihilation of spin-wave**

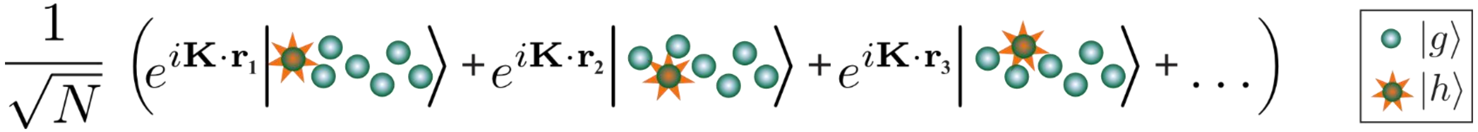

Wavevector Multiplexing

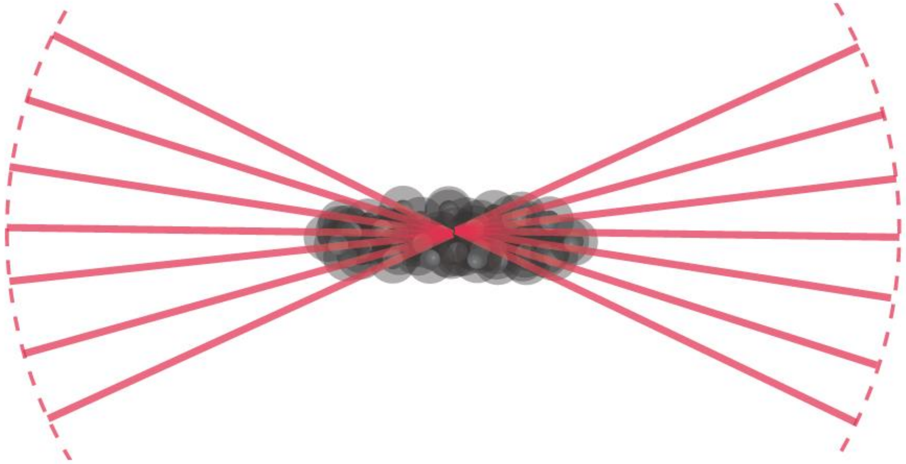

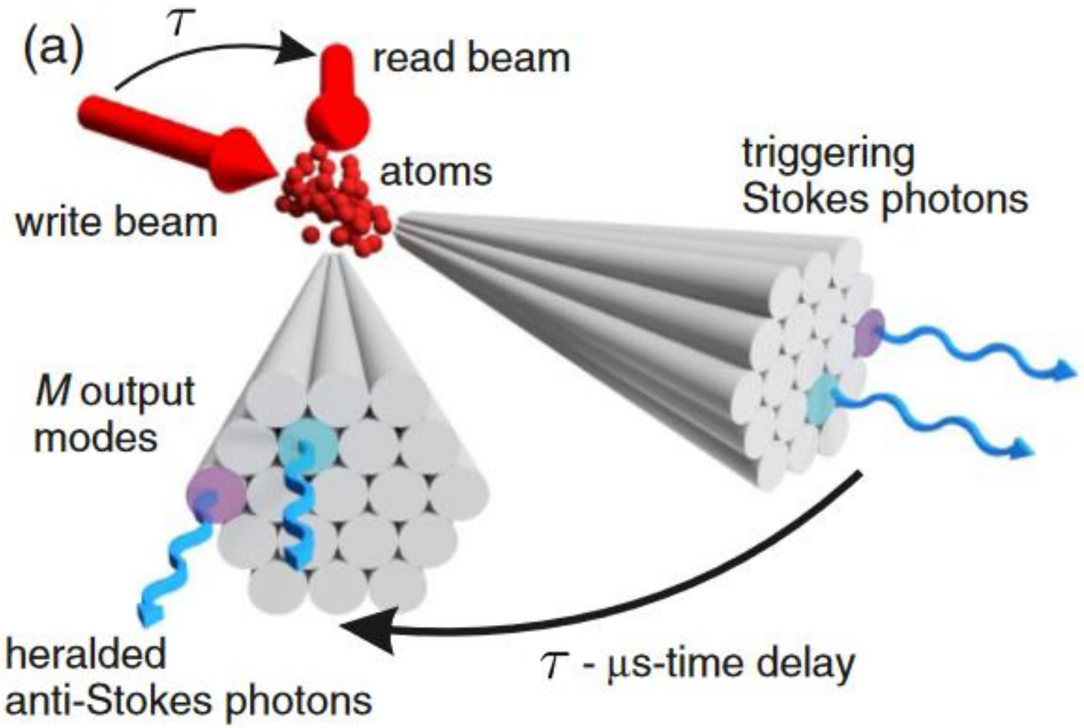

Radosław Chrapkiewicz, Michał Dąbrowski, and Wojciech Wasilewski
Phys. Rev . Lett. 118, 063603

Deterministic single and multi-photons

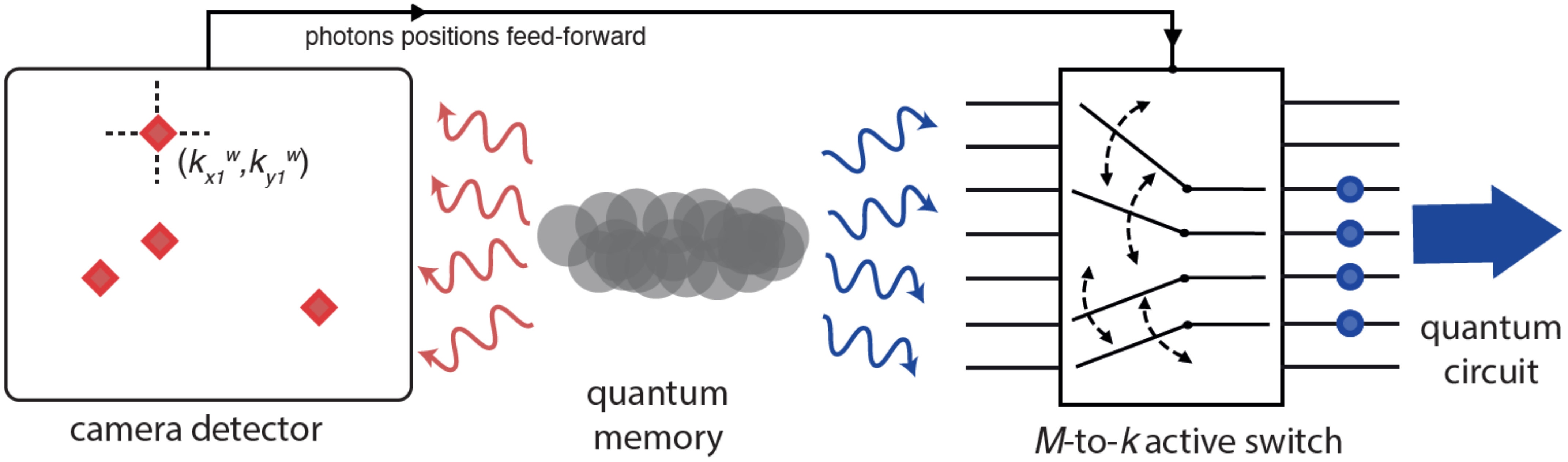

MP, M. Dąbrowski, M. Mazelanik, A. Leszczyński, M. Lipka, W. Wasilewski, Nat. Commun **8**, 2140 (2017)

I-sCMOS camera

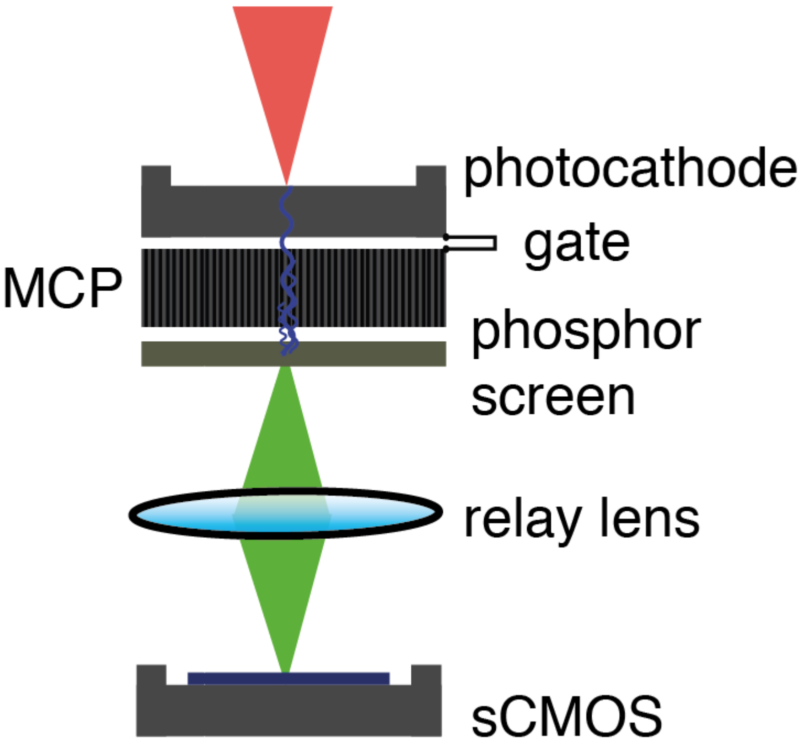

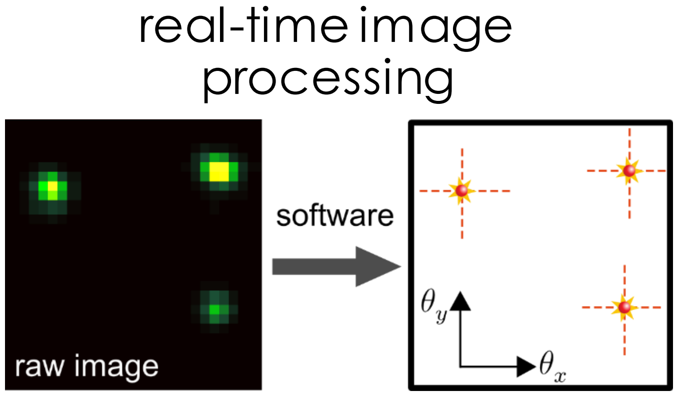

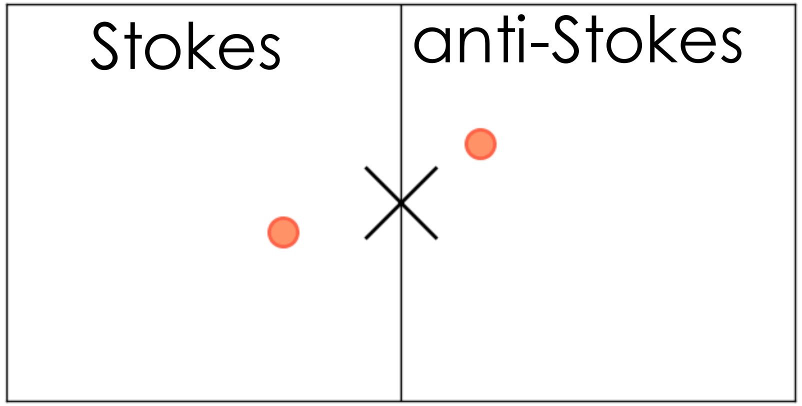

R. Chrapkiewicz, M. Jachura, K. Banaszek, W. Wasilewski, Nat. Photonics **10**, 576 (2016)
M. Jachura, R. Chrapkiewicz, W. Wasilewski, R. Demkowicz-Dobrzański, K. Banaszek, Nat. Commun. **7**, 11411(2016)
MP, M. Dąbrowski, M. Mazelanik, A. Leszczyński, M. Lipka, W. Wasilewski, Nat. Commun. **8**, 2140 (2017)

Photon number correlations

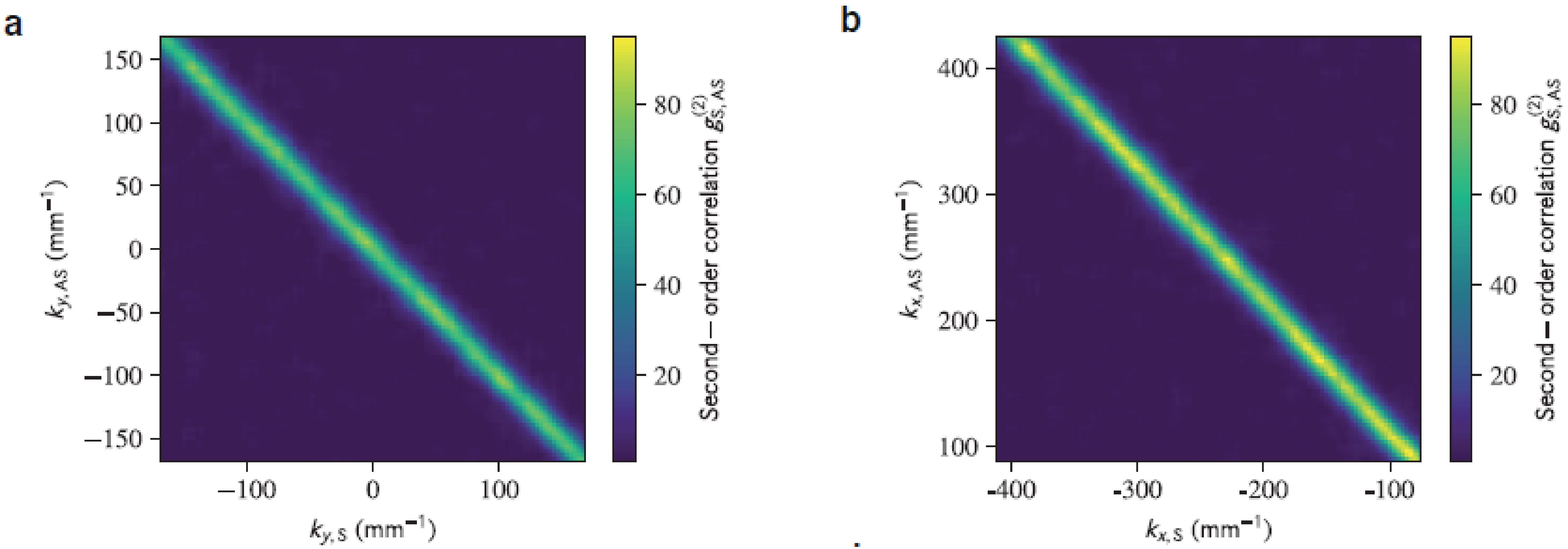

non-classical correlations

$$g^{(2)} = \frac{\langle n_S n_{AS} \rangle}{\langle n_S \rangle \langle n_{AS} \rangle} = 72 \pm 5 \gg 2$$

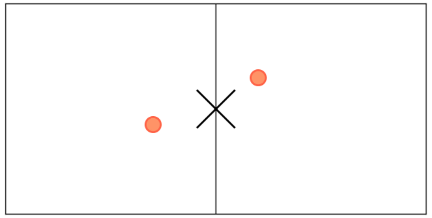

- **>500 modes**
- **>50 μs storage**

Nat. Commun **8**, 2140 (2017)

New system

Custom FPGA data processing

New custom high-voltage gating module

Now 100.000 frames per second, **~10 microseconds from detection to information**

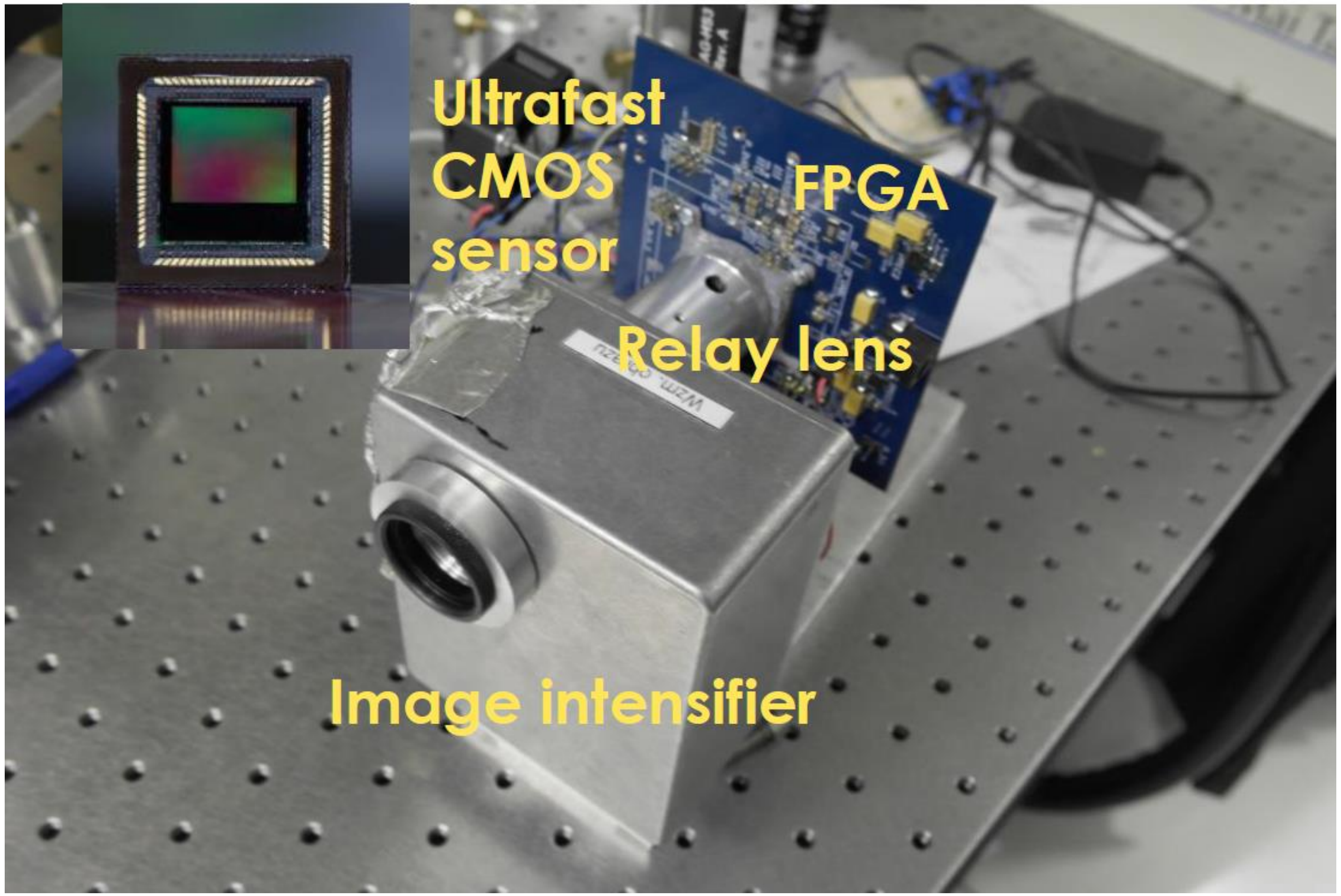

Optics Letters 46, 3009-3012 (2021)

Photon rate gains

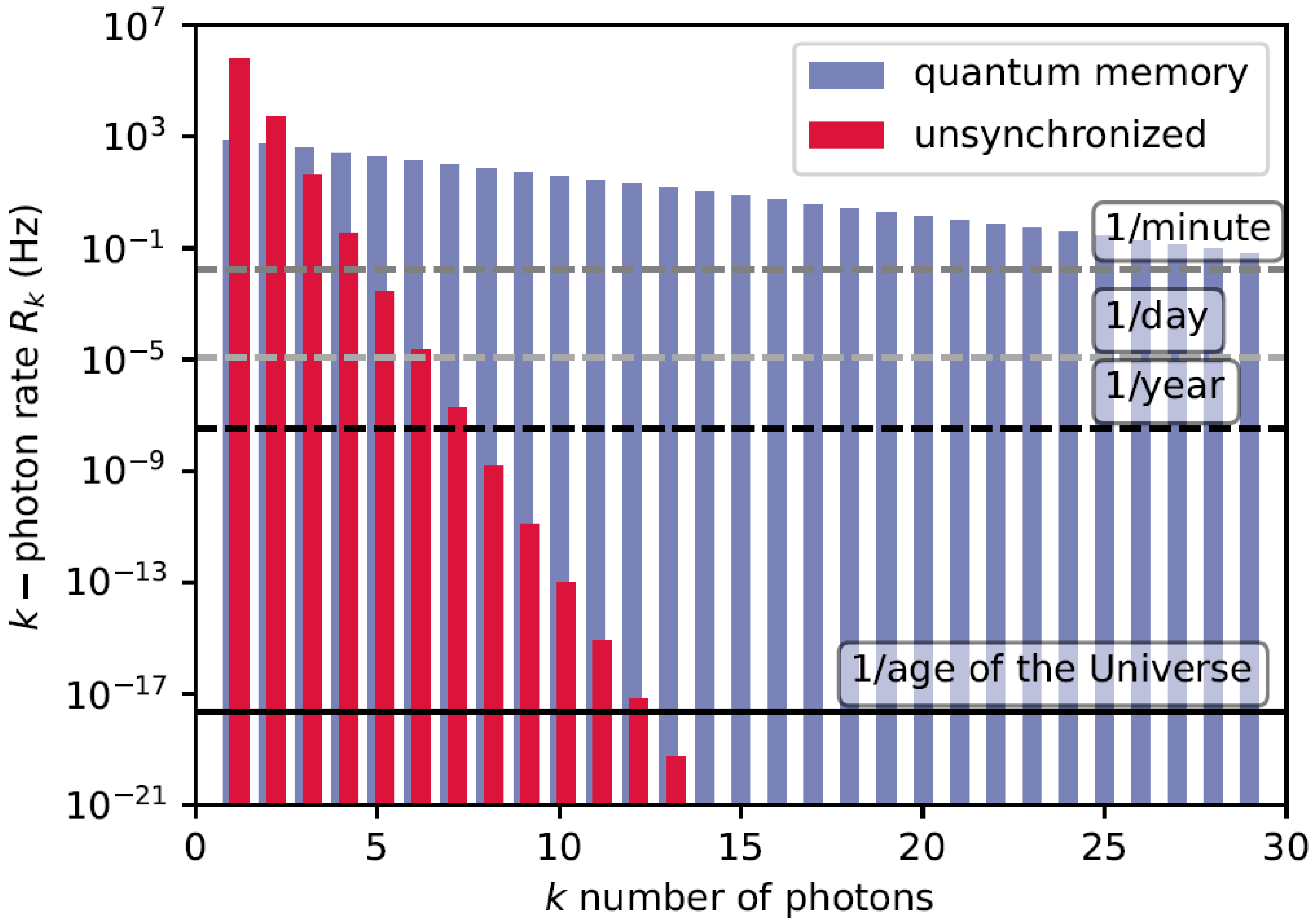

1 kHz rep. rate quantum memory

vs

80 MHz rep. rate SPDC

Temporal multiplexing

Gradient echo memory (GEM)

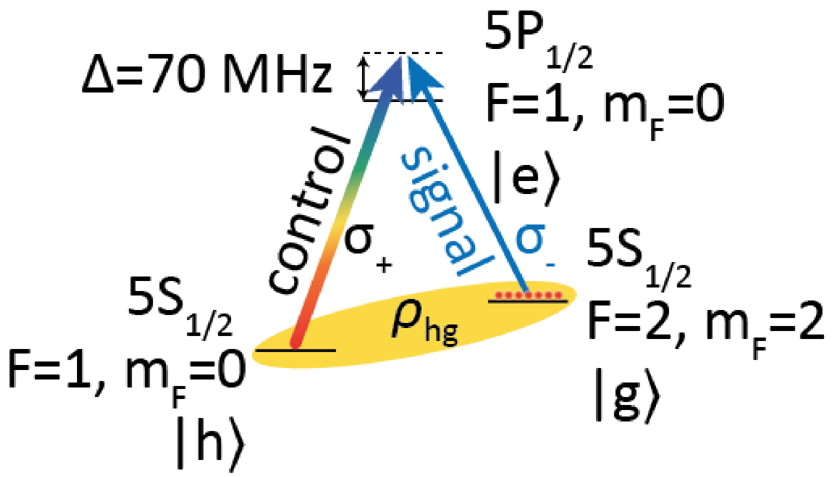

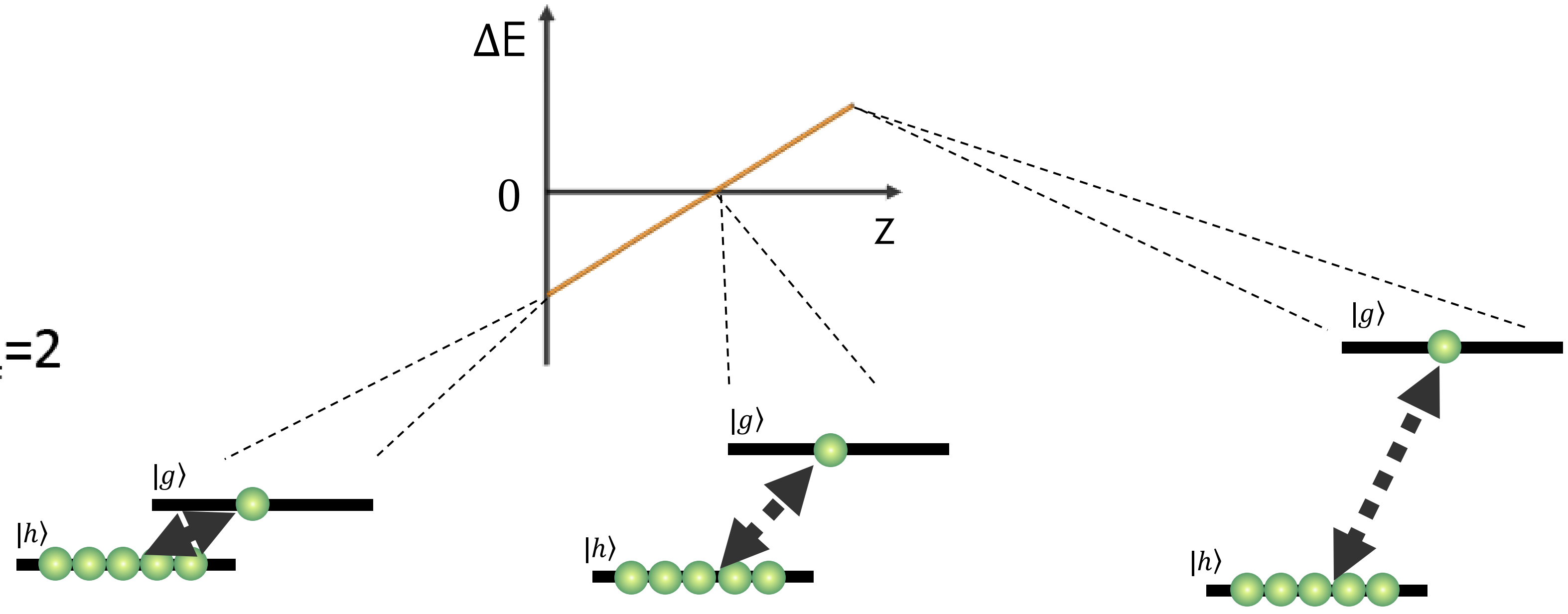

$$\frac{\partial \check{\rho}_{hg}(z,t)}{\partial t} = \frac{i}{\hbar}\frac{\Omega^*(t) d A(z,t)}{4\Delta - 2i\Gamma} - \frac{1}{2\tau}\check{\rho}_{hg}(z,t) + i\delta_{\mathrm{tot}}(z,t)\check{\rho}_{hg}(z,t),$$

$$\frac{\partial A(z,t)}{\partial z} = -i\frac{\hbar\Omega(t)\check{\rho}_{hg}(z,t)/d + A(z,t)}{2\Delta + i\Gamma}\frac{\Gamma}{2} g n(z),$$

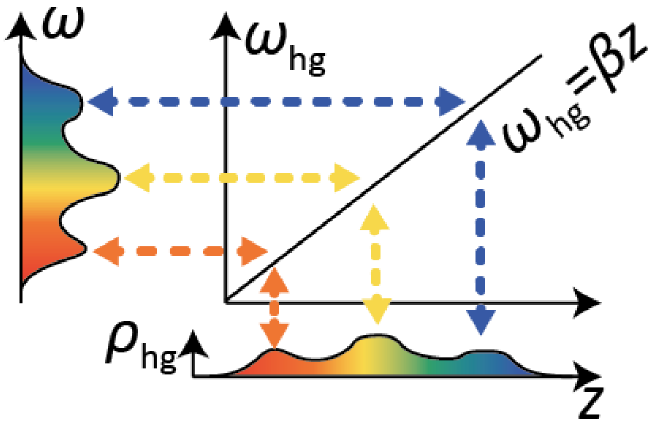

Hosseini et al., Nature 461, 241 (2009)

Spin-wave phase modulation (GEM)

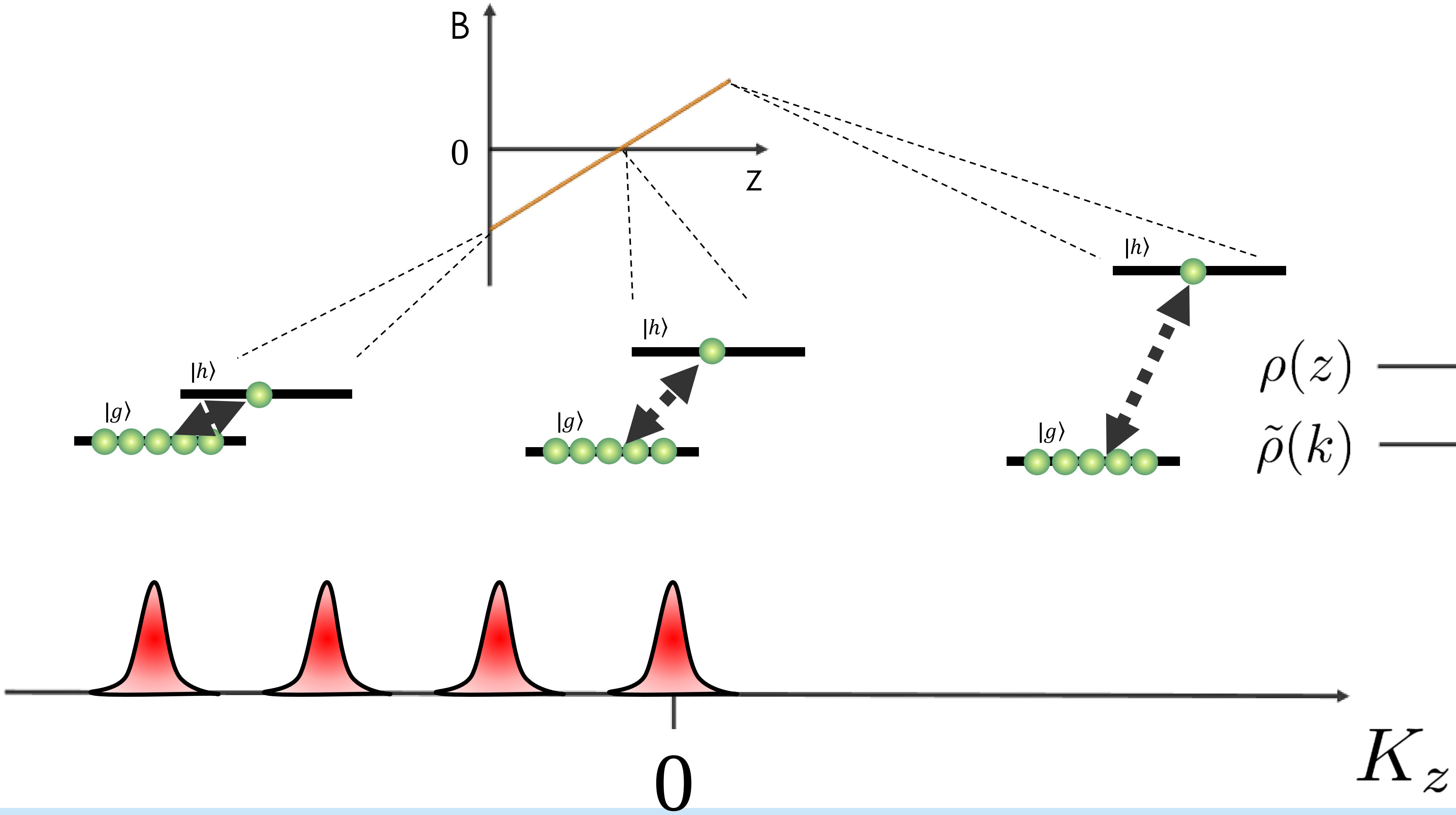

$$\rho(z) \longrightarrow \rho(z)e^{i\delta kz}$$
$$\tilde{\rho}(k) \longrightarrow \tilde{\rho}(k-\delta k)$$

ac-Stark spin-wave phase modulation

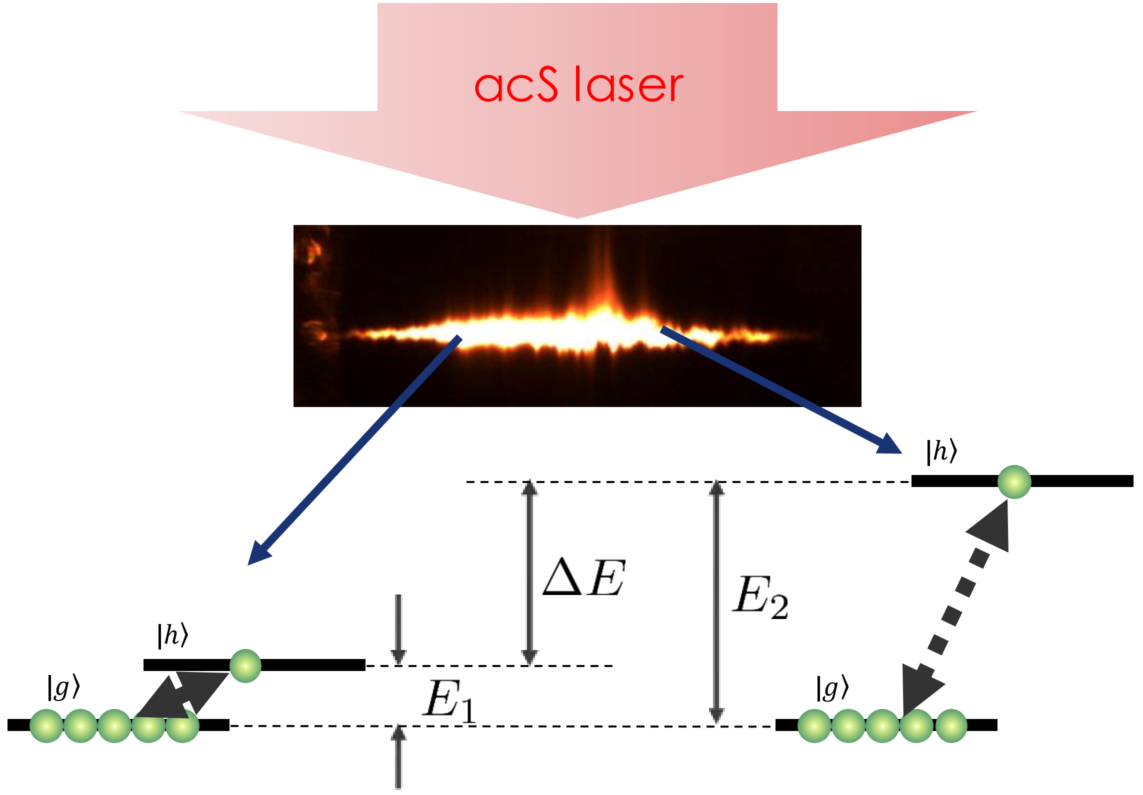

$$\Delta\varphi(y,z) = \Delta E(y,z)T/\hbar$$

Differential phase accumulated during free evolution

Fictitious magnetic fields

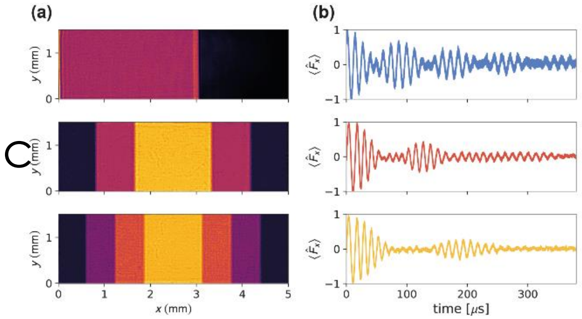

Opt. Lett. 43, 1147 (2018)

Spin-wave Hong-Ou-Mandel interference

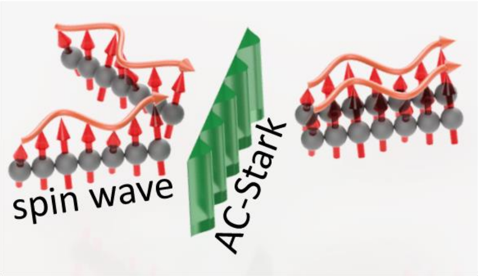

Phys. Rev. Lett. **122**, 063604 (2019)

Spin-wave processor of stored optical pulses

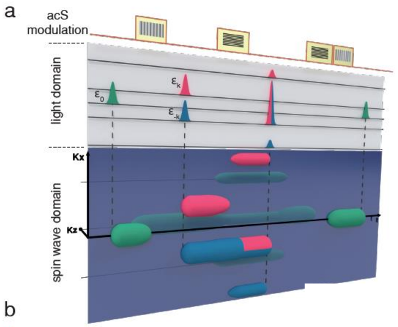

npj Quantum Information **5**, 22 (2019)

ac-Stark GEM

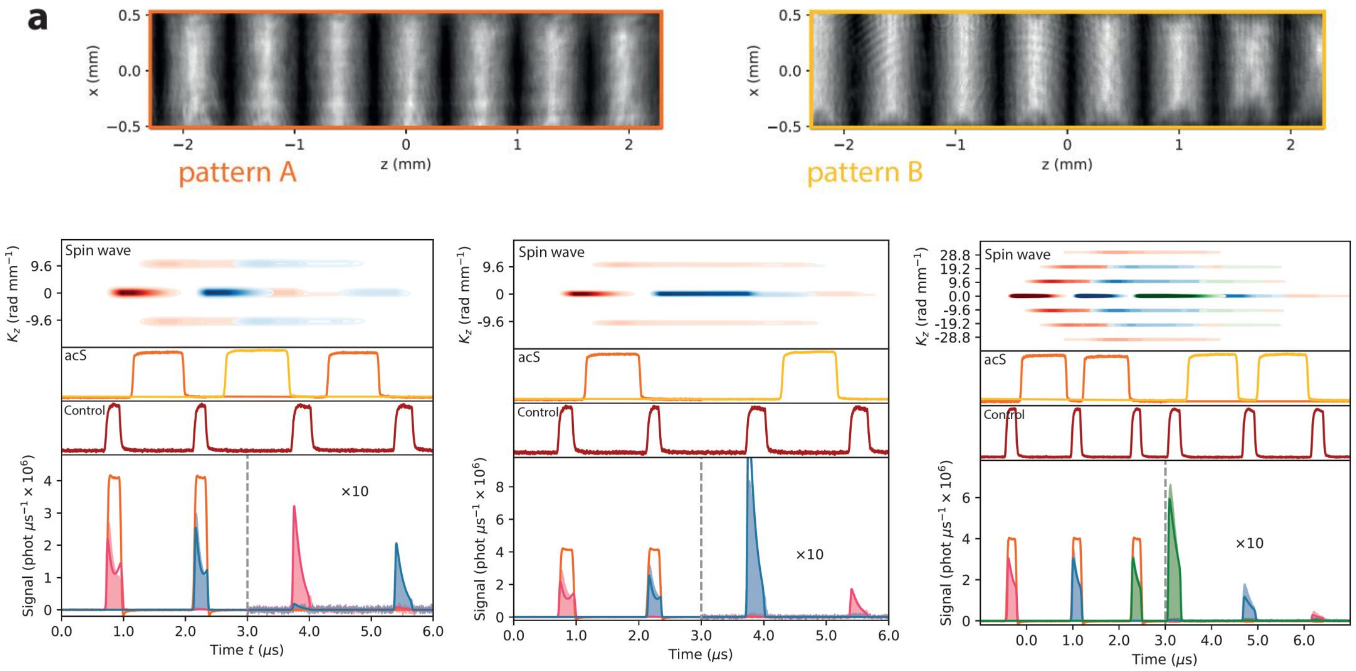

a
pattern A
pattern B
x (mm)
z (mm)
Spin wave
acS
Control
K_z (rad mm^{-1})
Signal (phot µs^{-1} × 10^6)
×10
Time t (µs)
Time (µs)

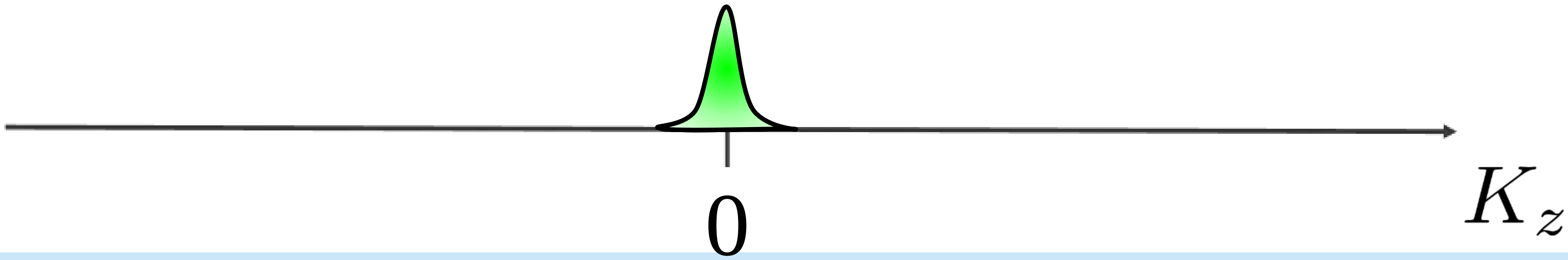

0
K_z

Spin-wave splitter

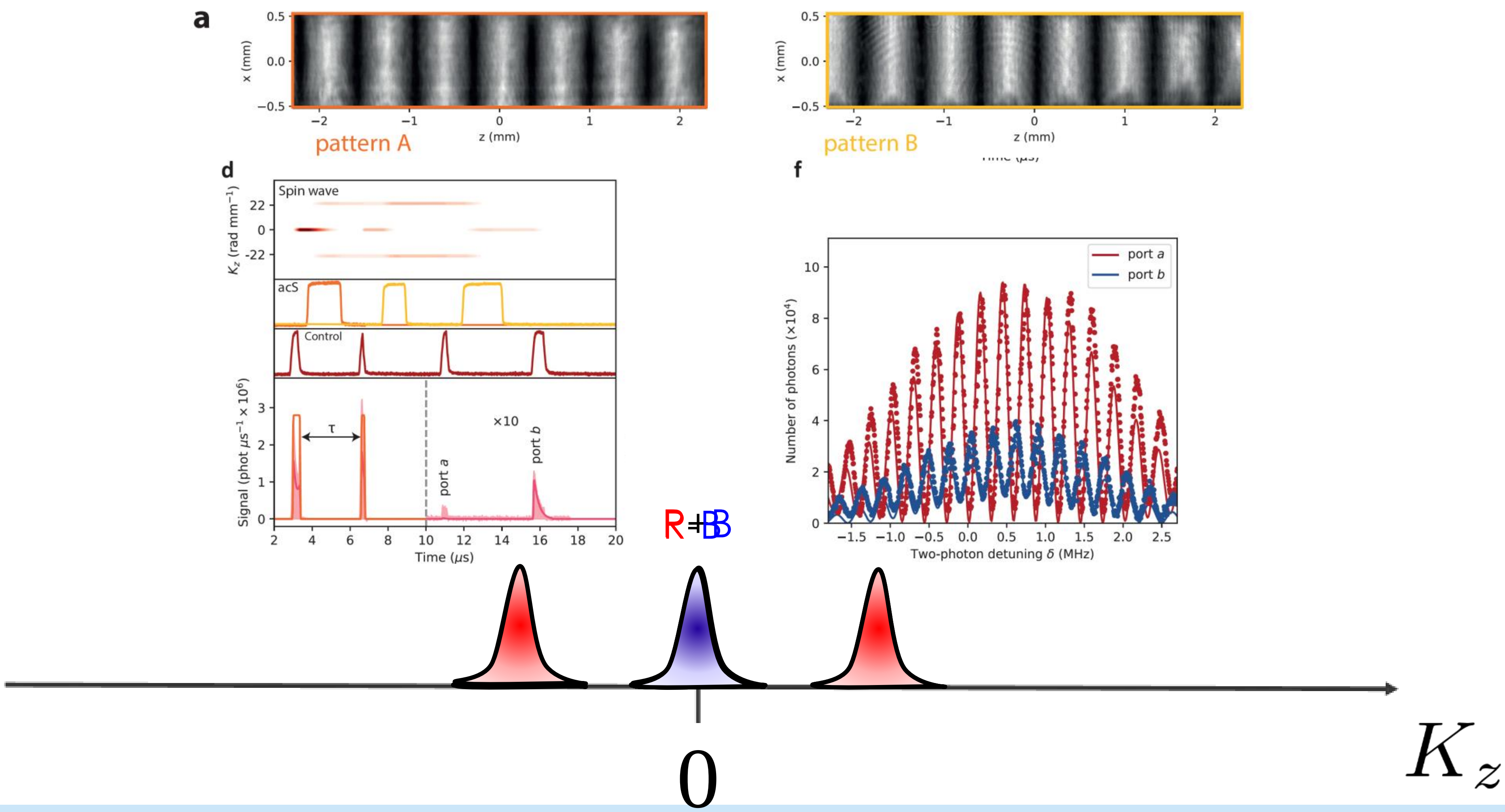

Time-lens and spectro-spatial mapping

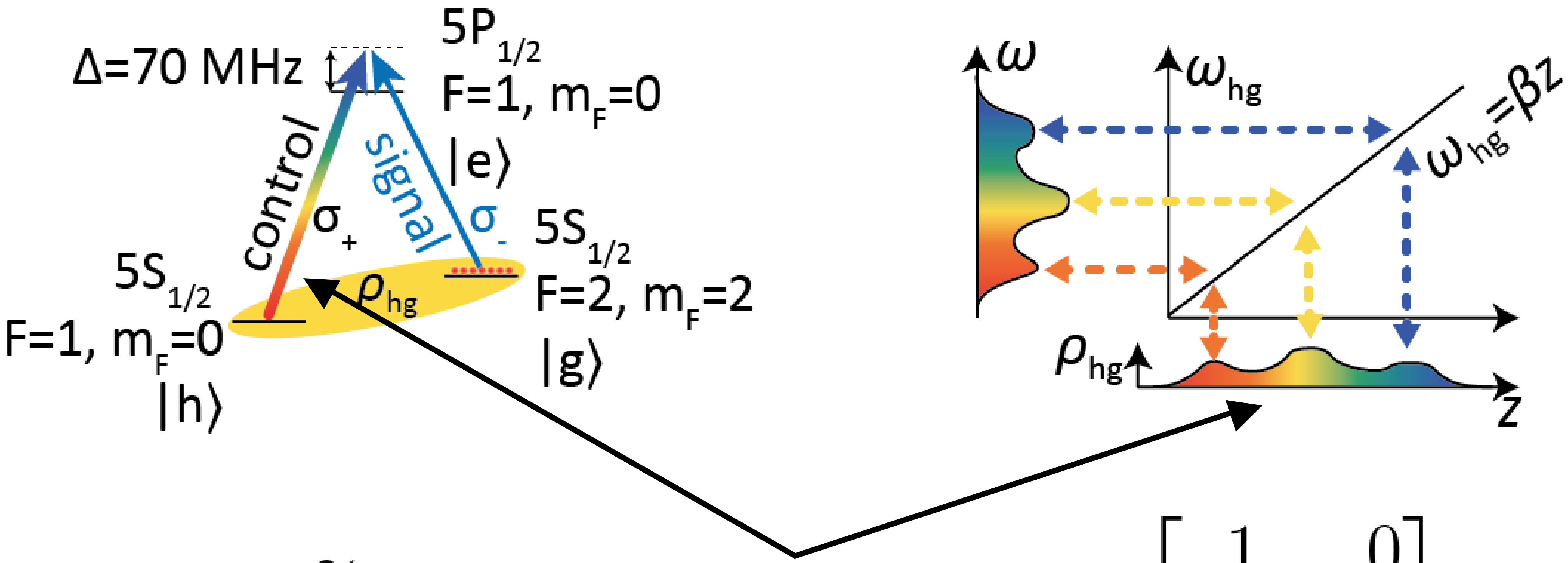

$$\rho_{hg}(z) \propto \widetilde{A}(\beta z)$$

Time-lens realized
by chirped control field

$$\delta\omega(t) = \alpha t$$

$$\begin{bmatrix} 1 & 0 \\ -\frac{1}{f_t} & 1 \end{bmatrix}$$

Far-field temporal imaging

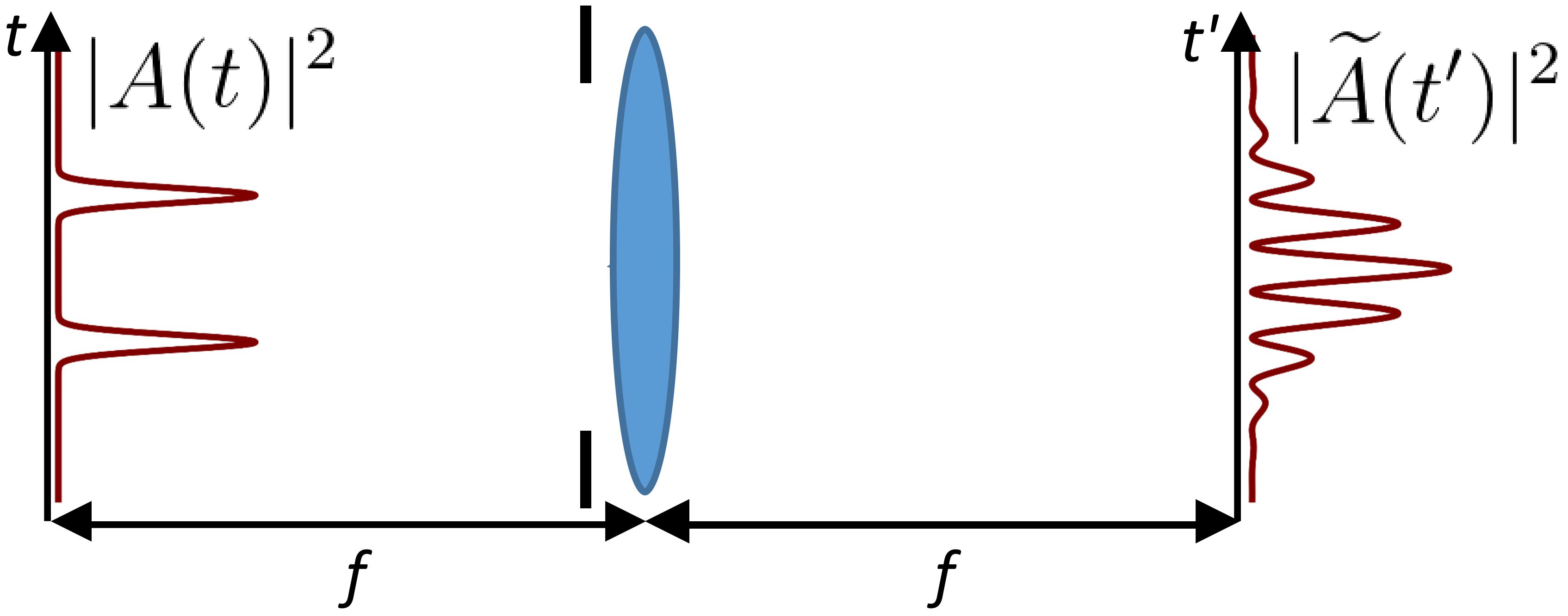

$$|\widetilde{A}(t')|^2 = |\mathcal{F}_t[A(t)](t')|^2$$

Temporal imaging

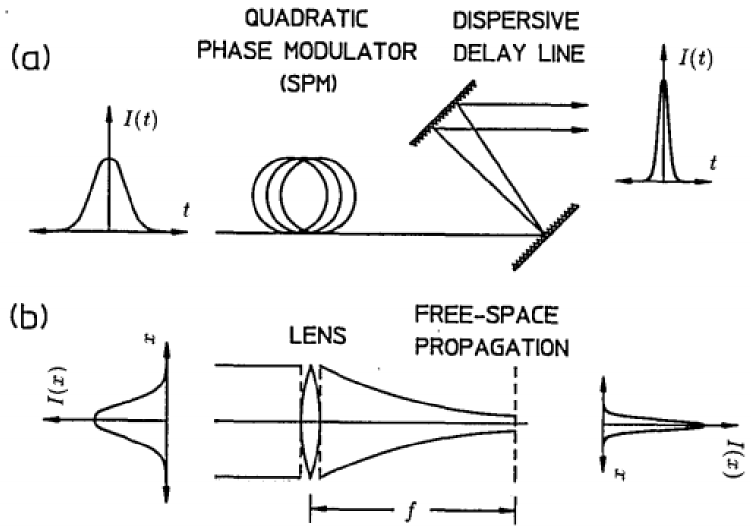

Opt. Lett. 14, 630 (1989)

- Spectral conversion
- Bandwidth manipulation
- Temporal ghost imaging
- Characterization of the time-frequency entanglement
- Manipulation of field-orthogonal temporal modes

Existing solutions are compatible with solid-state emission (high bandwith, low spectral resolution)

No solution for narrowband atomic emission

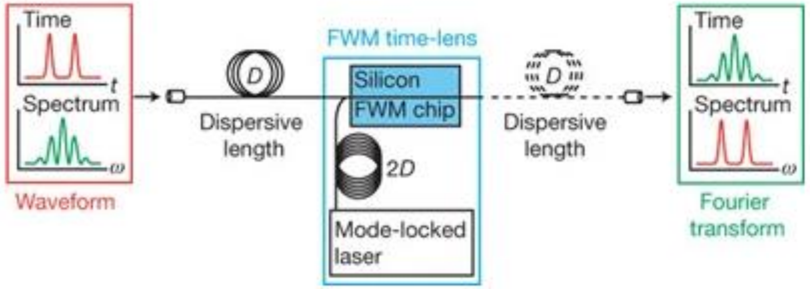

Nature 456, 81–84 (2008)

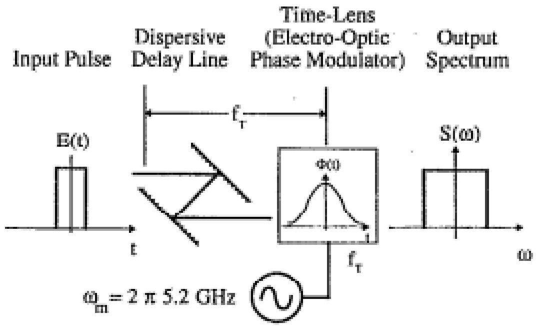

Appl. Phys. Lett. 64, 270–272 (1994)

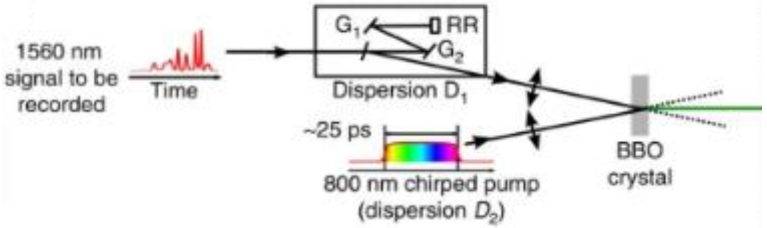

Nat. Commun. 7, 13136 (2016)

Temporal propagation

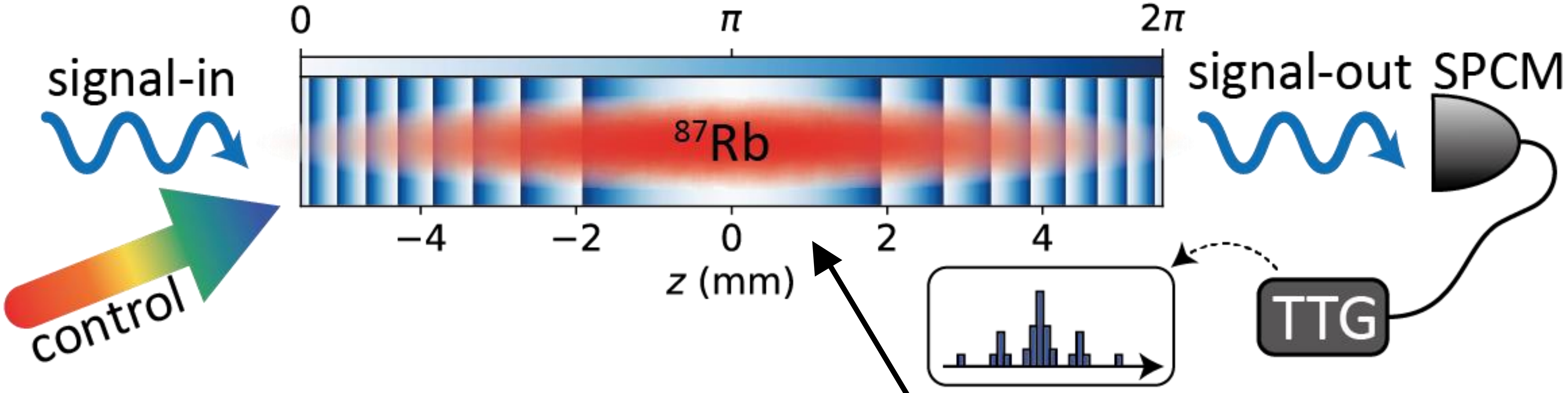

Temporal „free-space" propagation
– a quadratic phase in frequency

$$\tilde{A}(\omega) = \mathcal{F}_t[A(t)](\omega)$$
$$\tilde{A}(\omega) \rightarrow \tilde{A}(\omega)\exp[-i(f_\mathrm{t}/\omega_0)\omega^2]$$

Thanks to spectro-spatial mapping the temporal propagation is realized by imposing a quadratic phase (Fresnel) profile onto the atomic coherence ρ_{hg}

Optica **7**, 203-208 (2020)

FF-TI (QMTI) - Rotating Wigner function

$$W(t,\omega) = 1/\sqrt{2\pi}\int_{-\infty}^{\infty} A(t+\xi/2)A^*(t-\xi/2)\exp(-i\omega\xi)$$

$$\begin{bmatrix} t' \\ \frac{\omega'}{\omega_0} \end{bmatrix} = \begin{bmatrix} 1 & 0 \\ -\frac{1}{f_\mathrm{t}} & 1 \end{bmatrix} \begin{bmatrix} 1 & f_\mathrm{t} \\ 0 & 1 \end{bmatrix} \begin{bmatrix} 1 & 0 \\ -\frac{1}{f_\mathrm{t}} & 1 \end{bmatrix} \begin{bmatrix} t \\ \frac{\omega}{\omega_0} \end{bmatrix} = \begin{bmatrix} 0 & f_\mathrm{t} \\ -\frac{1}{f_\mathrm{t}} & 0 \end{bmatrix} \begin{bmatrix} t \\ \frac{\omega}{\omega_0} \end{bmatrix}$$

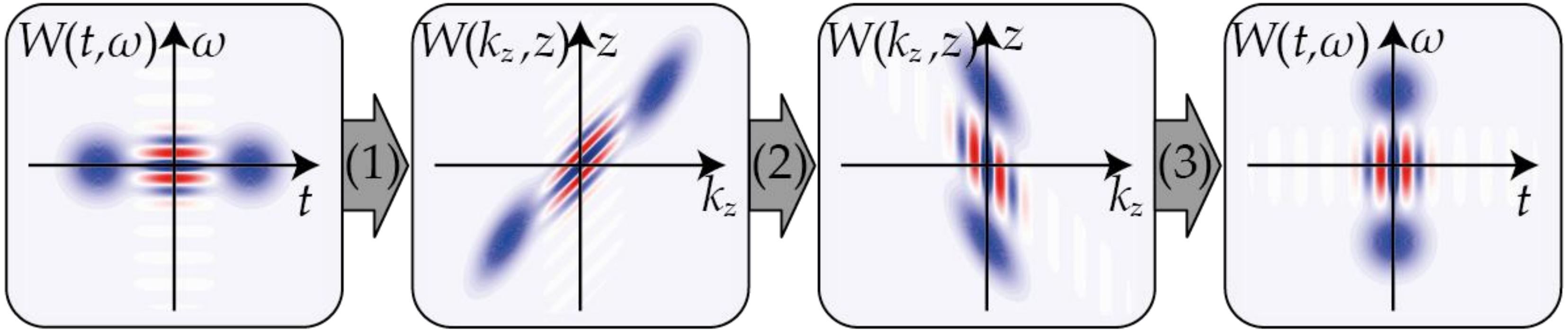

Example input/output

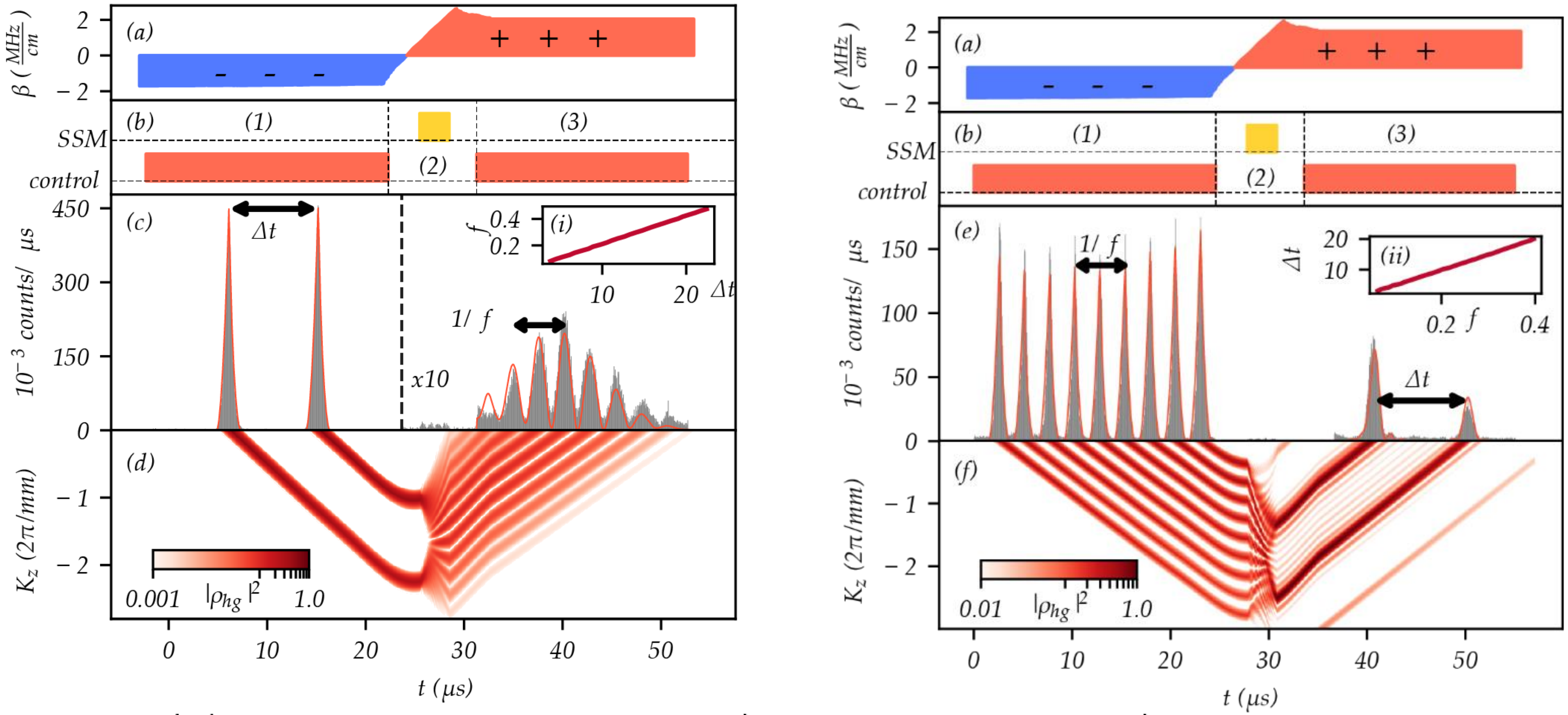

$$\left(\left(\widetilde{A}(\alpha t)\exp(-i(\alpha/2)t^2)\right) * \zeta(\beta t) * \zeta(\beta t)\right)\exp(i(\alpha/2)t^2)$$

Optica **7**, 203-208 (2020)

Rotation by arbitrary angle = the FrFT

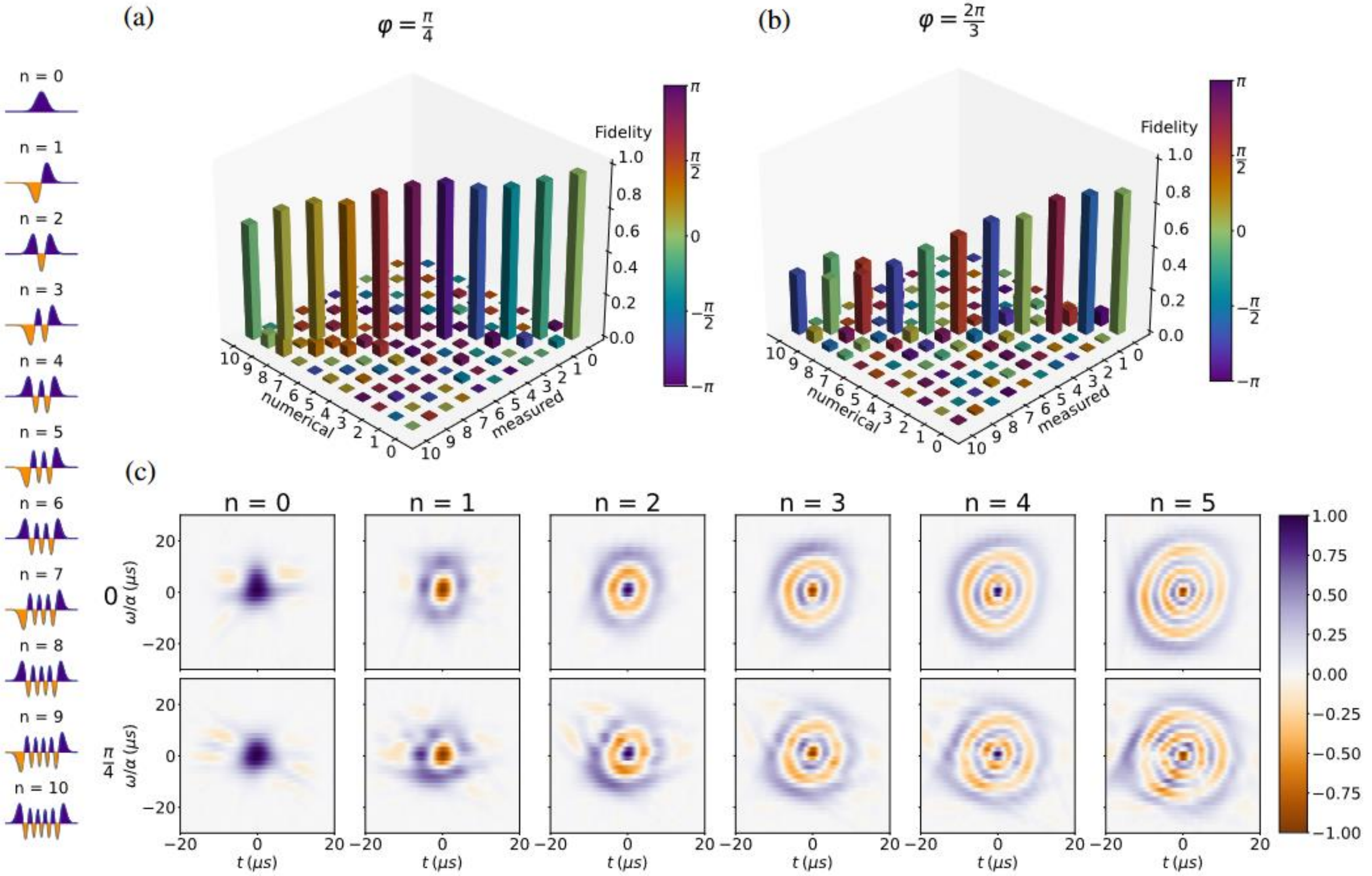

B. Niewelt et al., Phys. Rev. Lett. 130, 240801 (2023)

Rotation by arbitrary angle = the FrFT

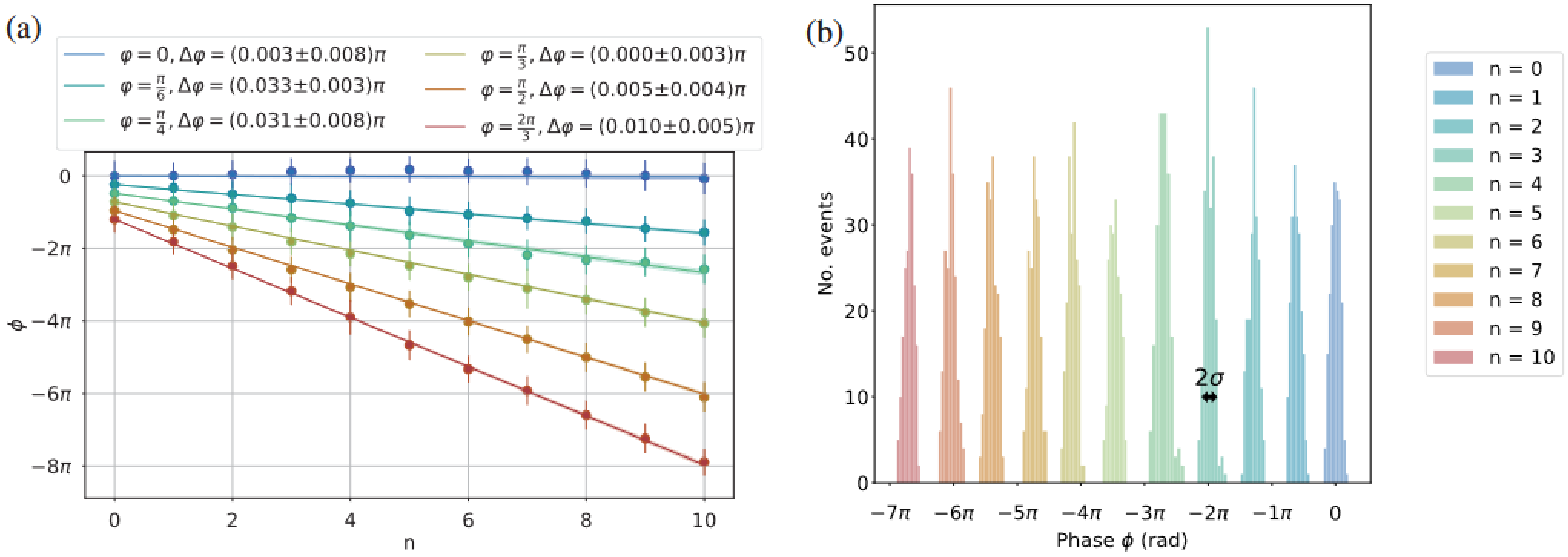

B. Niewelt et al., Phys. Rev. Lett. 130, 240801 (2023)

Imaging resolution - Rayleigh Criterion

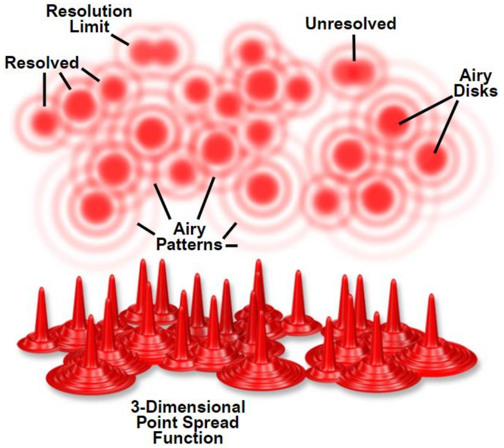

$$\theta = 1{\cdot}2197 \frac{\lambda}{2R}$$

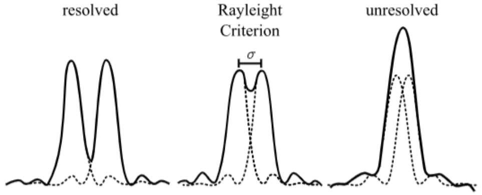

$$\sigma = \frac{0.61\lambda}{\mu \sin\gamma} = \frac{0.61\lambda}{NA}$$

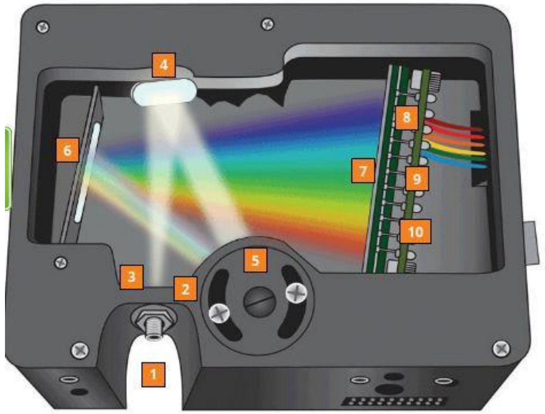

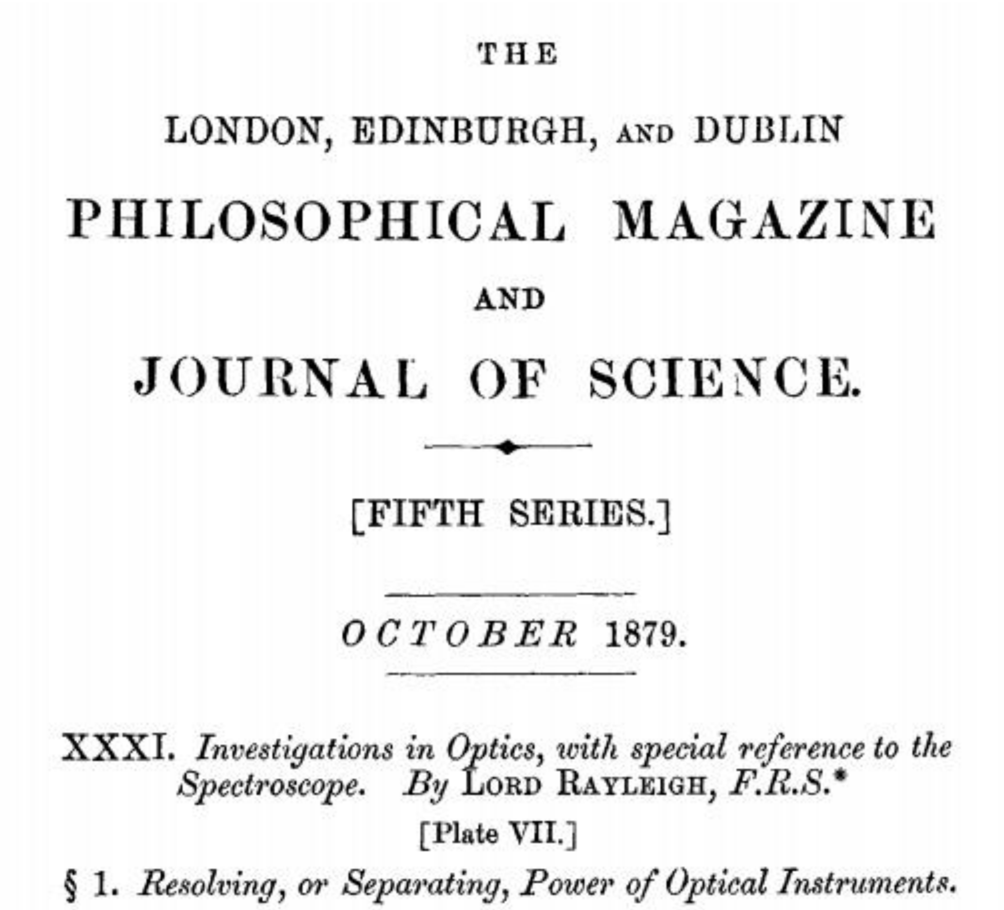
THE

LONDON, EDINBURGH, AND DUBLIN

PHILOSOPHICAL MAGAZINE

AND

JOURNAL OF SCIENCE.

[FIFTH SERIES.]

OCTOBER 1879.

XXXI. *Investigations in Optics, with special reference to the Spectroscope.* By LORD RAYLEIGH, *F.R.S.**

[Plate VII.]

§ 1. *Resolving, or Separating, Power of Optical Instruments.*

Rayleigh Limit

Two point sources:

$$|u(x+\varepsilon/2)|^2 + |u(x-\varepsilon/2)|^2$$

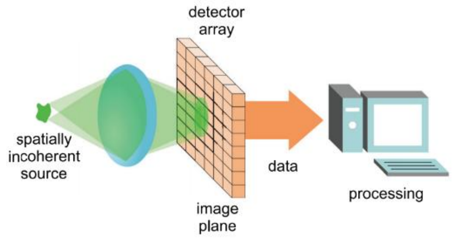

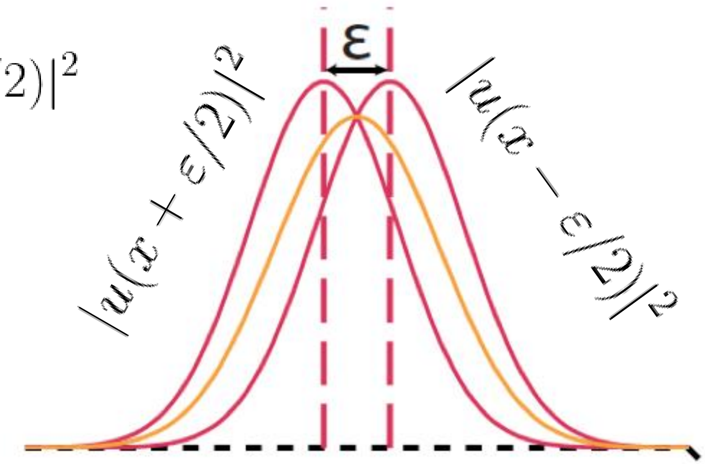

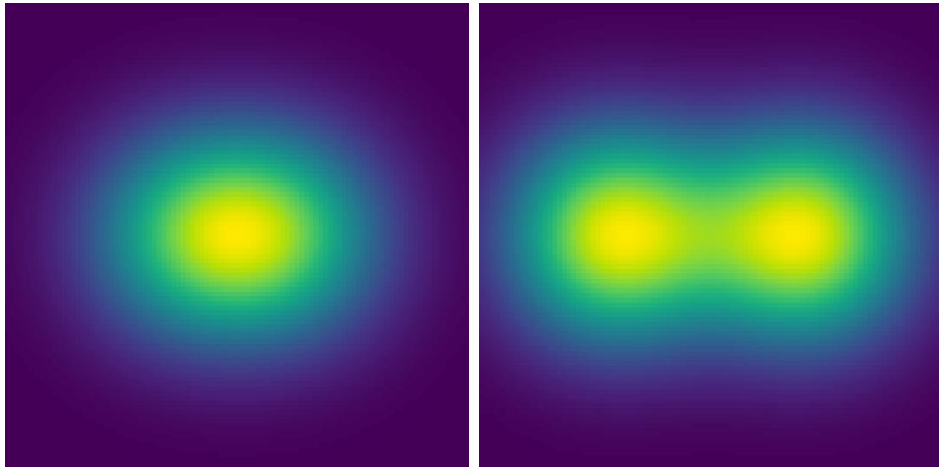

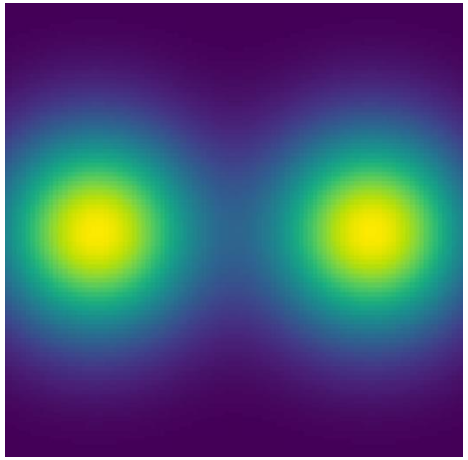

$$\mathcal{F}_{\mathrm{DI}} \approx \varepsilon^2/8$$

Cramér–Rao bound (CRB)

$$\Delta^2\hat{\varepsilon} \geq \frac{1}{\mathcal{F}}, \mathcal{F} = \int \frac{1}{p_\varepsilon(x)} \left(\frac{\partial}{\partial\varepsilon} p_\varepsilon(x)\right)^2 \mathrm{d}x$$

Precision (per photon)

$$(\Delta^2\varepsilon)^{-1}_{\mathrm{DI}} = \frac{\varepsilon^2}{8},$$

Fisher information

$$F(\theta) = \sum_r p(r|\theta) \left(\frac{\partial}{\partial\theta} \log p(r|\theta) \right)^2$$

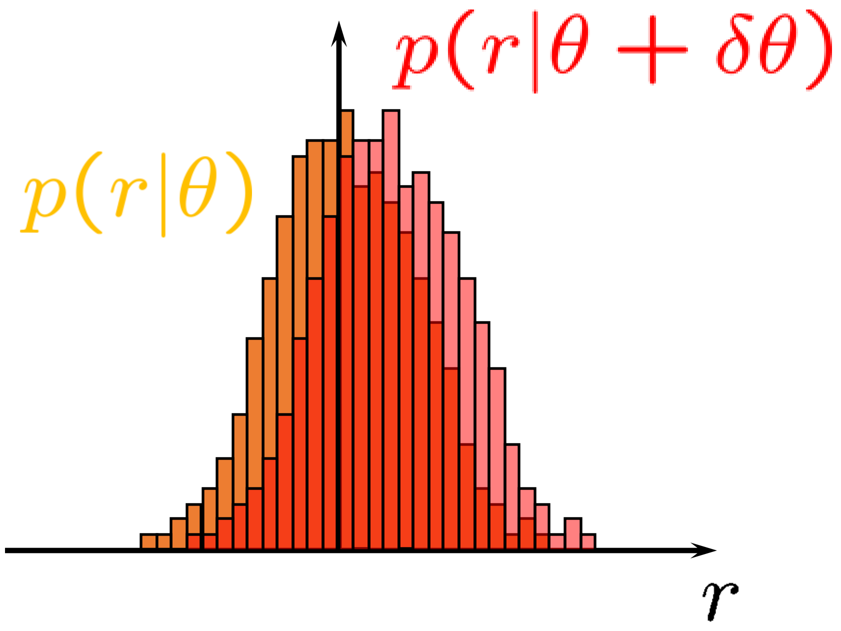

Cramér-Rao bound:
for unbiased estimators

$$\Delta\theta \geq \frac{1}{\sqrt{NF(\theta)}}$$

$$(\Delta^2\theta)^{-1} \leq F(\theta)N$$

Beating the Rayleigh Limit more conventionally

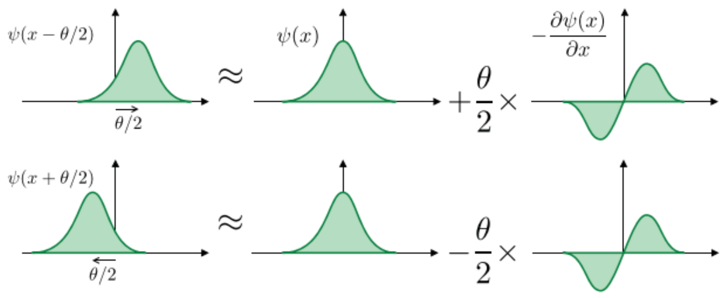

SLI

via $\mathcal{F}_{\text{SLIVER}} \approx \frac{1}{4} - \frac{\varepsilon^2}{32}$ etry)

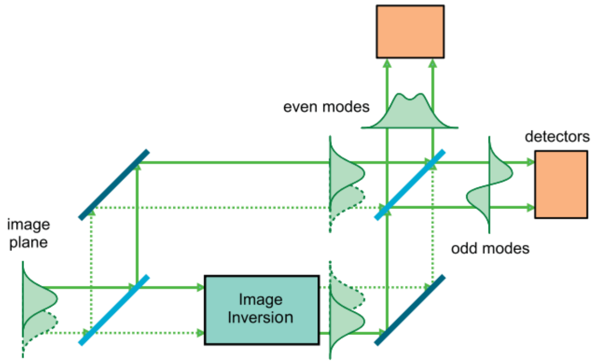

SPADE (spatial-mode demultiplexing)

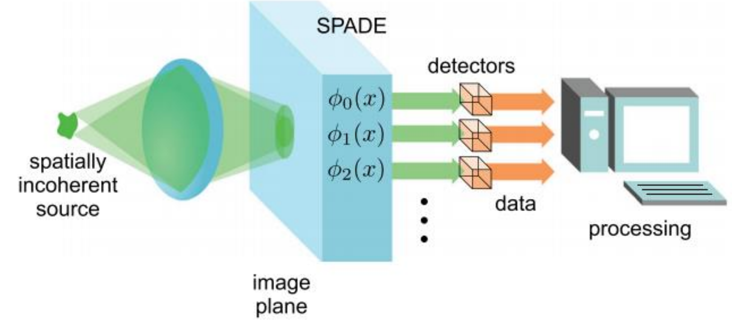

SPLICE (super-resolved position localization by inversion of coherence along an edge)

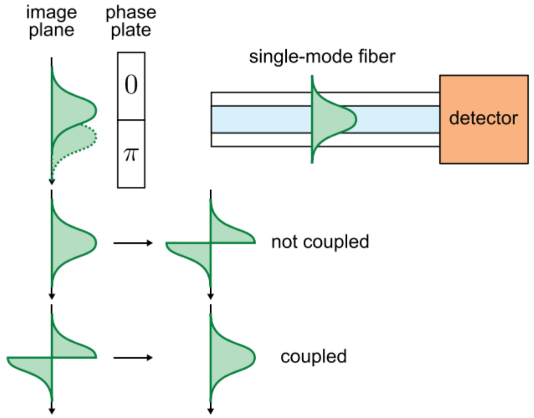

Contemporary Physics, 60:4, 279-298

Nature Communications **13**, 691 (2022)

Two incoherent sources

$$\tilde{I}(\omega) = \tfrac{1}{2}\left(|\tilde{\psi}(\omega - \delta\omega/2)|^2 + |\tilde{\psi}_{-}(\omega + \delta\omega/2)|^2\right)$$

$$\tilde{\psi}(\omega) = \tilde{\psi}_{\blacktriangle}(\omega) = \left(\sqrt{2\pi}\sigma\right)^{-1/2} \exp\left(-\frac{\omega^2}{4\sigma^2}\right)$$

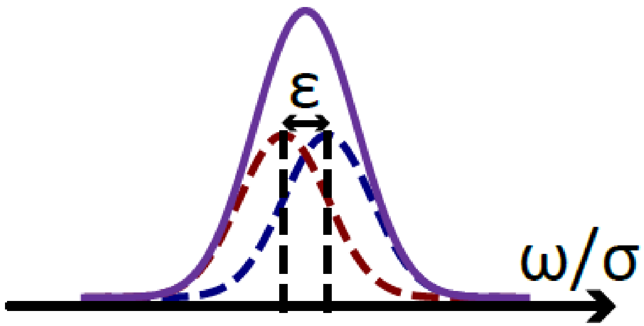

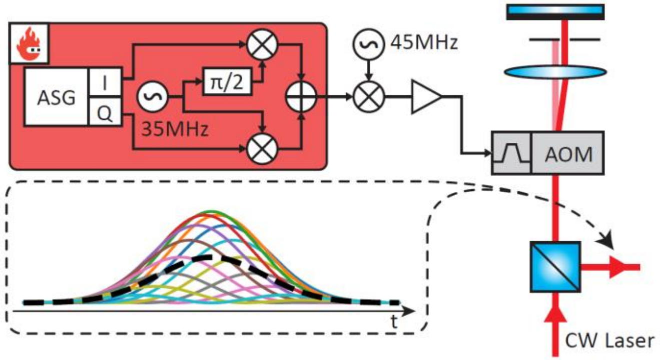

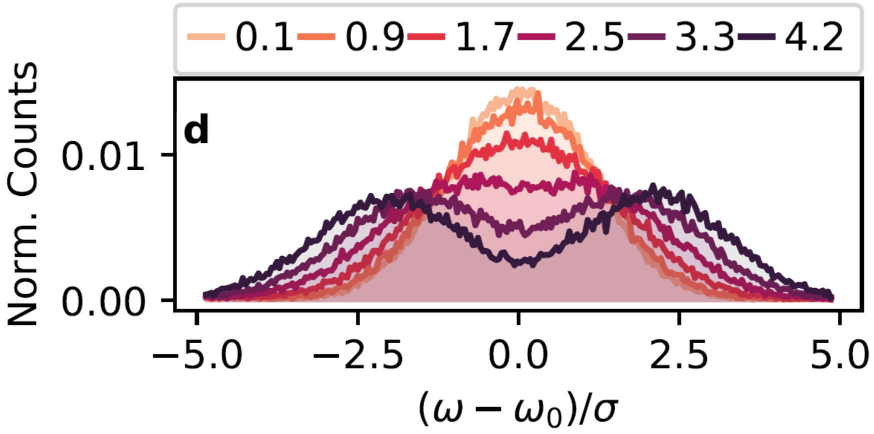

$$\mathcal{S}_{\varphi}(\omega) = \frac{1}{\sqrt{2}}\left(\tilde{\psi}_{\blacktriangle}(\omega - \sigma\varepsilon/2) + e^{i\varphi}\tilde{\psi}_{\blacktriangle}(\omega + \sigma\varepsilon/2)\right)$$

$$\mathcal{W}_{\mathcal{S}}(t,\omega) = \psi_{\blacktriangle}^2(t)(\tilde{\psi}_{\blacktriangle}^2(\omega - \sigma\varepsilon/2) + \tilde{\psi}_{\blacktriangle}^2(\omega + \sigma\varepsilon/2))$$

Nature Communications **13**, 691 (2022)

PuDTAI
Pulse-division time-axis-inversion interferometer

$1/\sqrt{2}(\mathcal{S}(\omega) + \mathcal{S}(-\omega))$

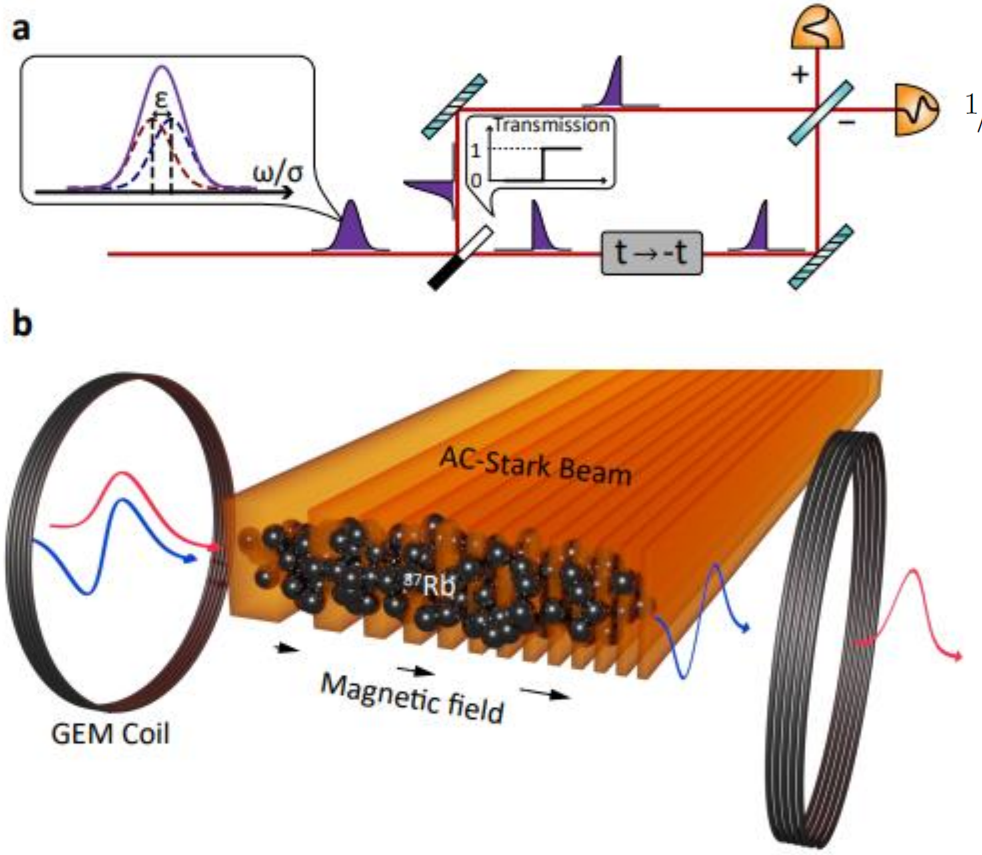

$1/\sqrt{2}(\mathcal{S}(\omega) - \mathcal{S}(-\omega))$

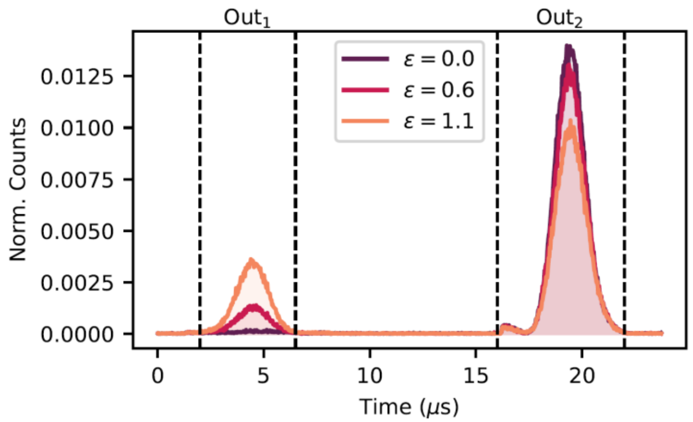

For real space imaging:
Wavefront-division
image-inversion
interferometer

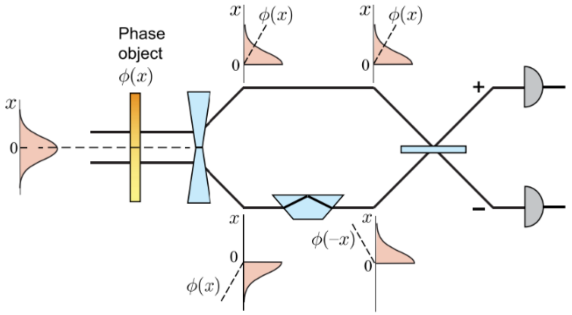

Phys. Rev. A 102, 013712 (2020)

PuDTAI in phase space

$$\mathcal{W}(z,k_z)=\frac{1}{\sqrt{2\pi}}\int \varrho_{hg}(z+\xi/2)\varrho^*_{hg}(z-\xi/2)\exp(-ik_z\xi)\mathrm{d}\xi$$

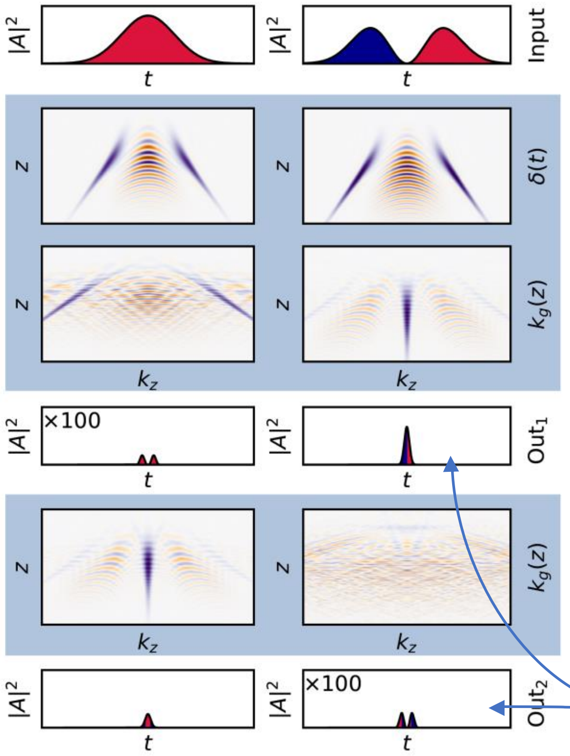

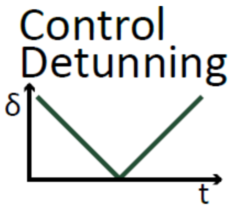

$$\delta(t) = \alpha|t|$$

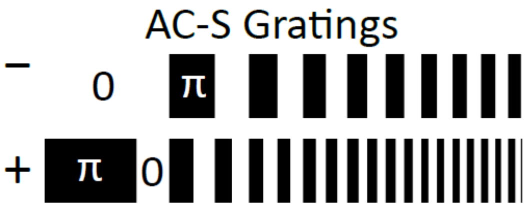

$$k_g = \zeta z \quad k_g = 2\zeta z$$

The interference happens in the Fourier domain

For the first half of the pulse:

$$\mathcal{A}_-(t)=\begin{cases}\mathcal{A}(t) & t<0\\ 0 & t\geq 0\end{cases}$$

$$k_z \to k_z' = \zeta z$$

$$z \to z' = z - \frac{1}{\zeta}k_z$$

Separation estimation

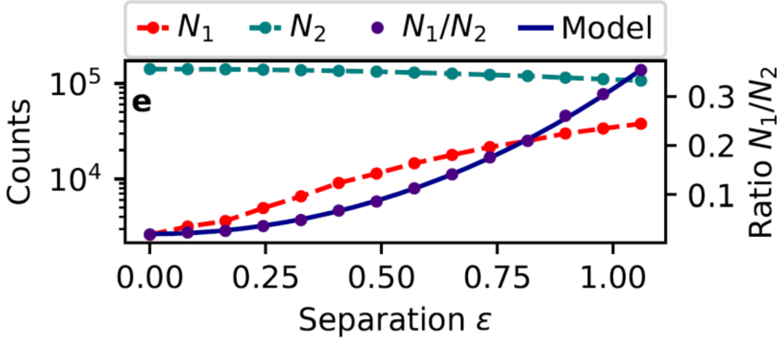

$$p_1 = \eta_1 \eta_1^{\mathfrak{A}} \frac{1}{2}\left(1 - \mathcal{V}_1 e^{-\frac{\epsilon^2}{8}}\right) \rightarrow N_1$$

$$p_2 = \eta_2 \eta_2^{\mathfrak{A}} \frac{1}{2}\left(1 + \mathcal{V}_2 e^{-\frac{\epsilon^2}{8}}\right) \rightarrow N_2$$

$$\rightarrow \hat{\varepsilon}(N_1/N_2)$$

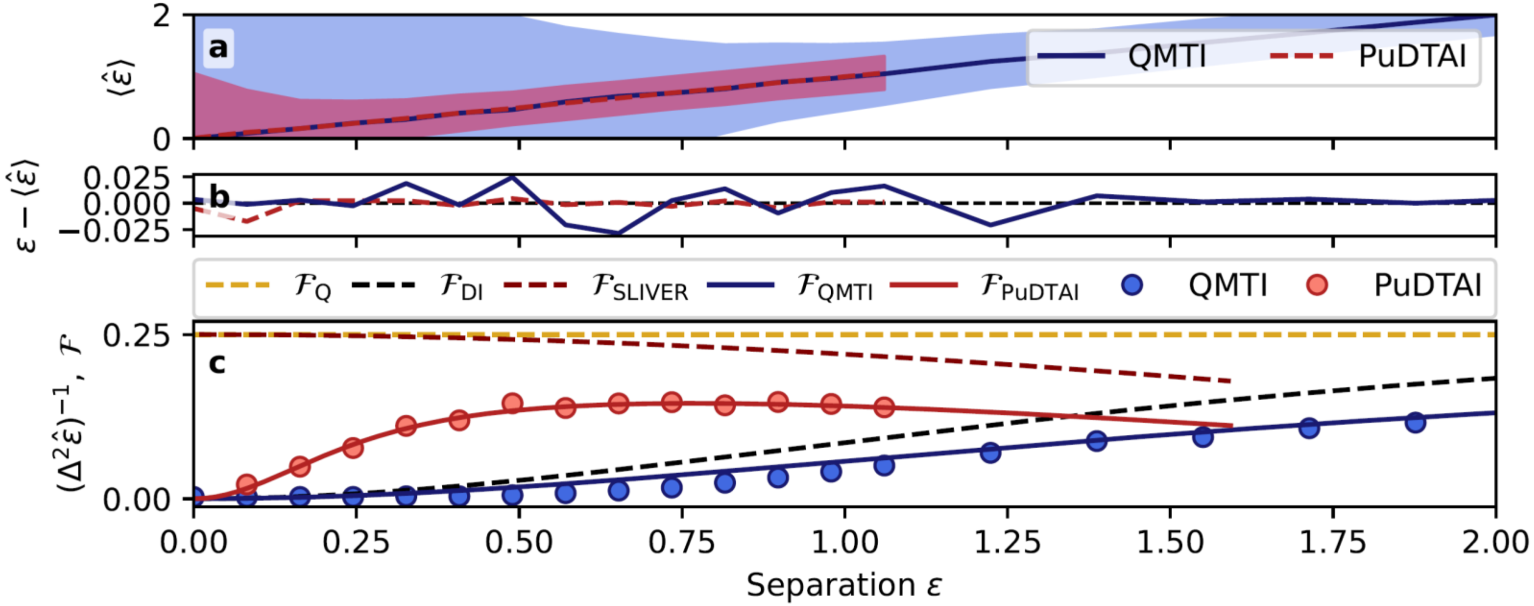

Maximum likelihood estimation in both cases

QMTI raw data:

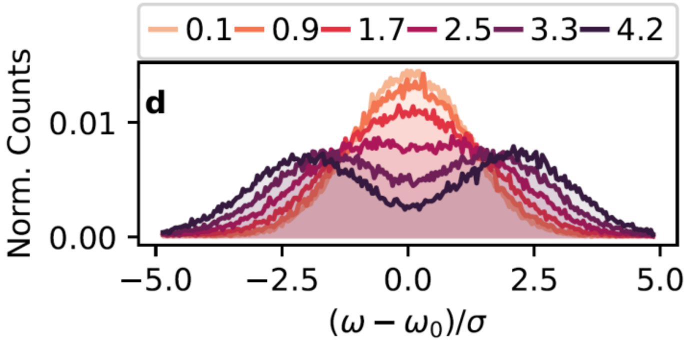

Ultranarrowband optical spectroscopy

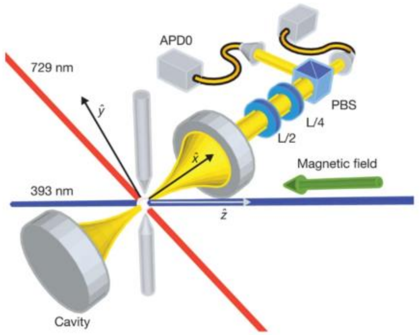

Single ions <100kHz

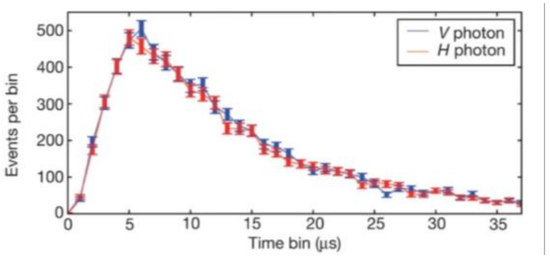

Nature **485**, 482–485(2012)

Hot and cold atoms MHz-kHz

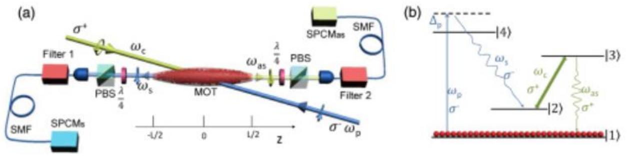

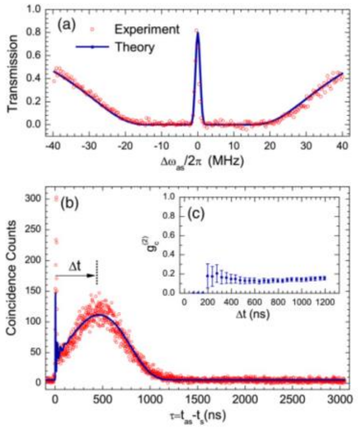

Optica **1**, pp. 84-88 (2014)

Optomechanical systems ~10kHz

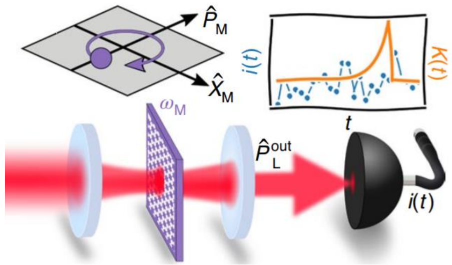

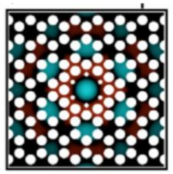

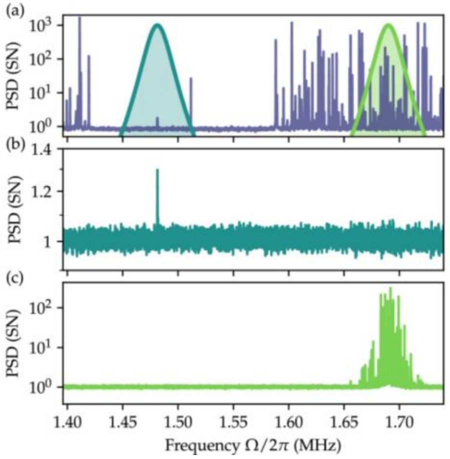

Optica **7**, 718-725 (2020)

Nature Communications **13**, 691 (2022)

Comparison

Our approach: PuDTAI

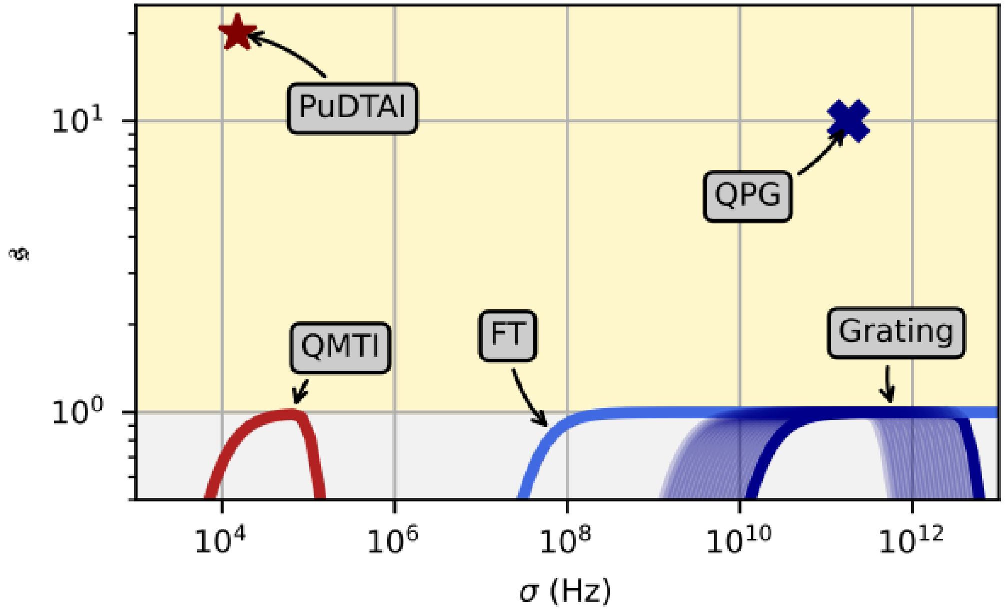

Superresolution parameter:

$$\mathfrak{s} = \lim_{\varepsilon \to 0} (\mathcal{F}/\mathcal{F}_{\mathrm{DI}})$$

Quantum Pulse Gate (QPG) - SPADE

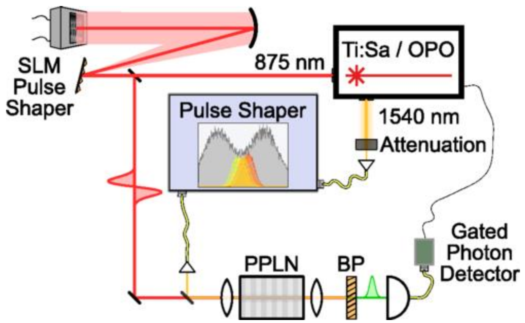

Phys. Rev. Lett. 121, 090501 (2018)

Homodyne/Heterodyne (under development)

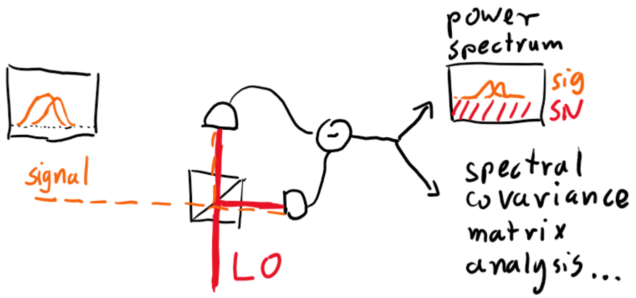

Phys. Rev. A 102, 063526 (2020)

The three-way splitter

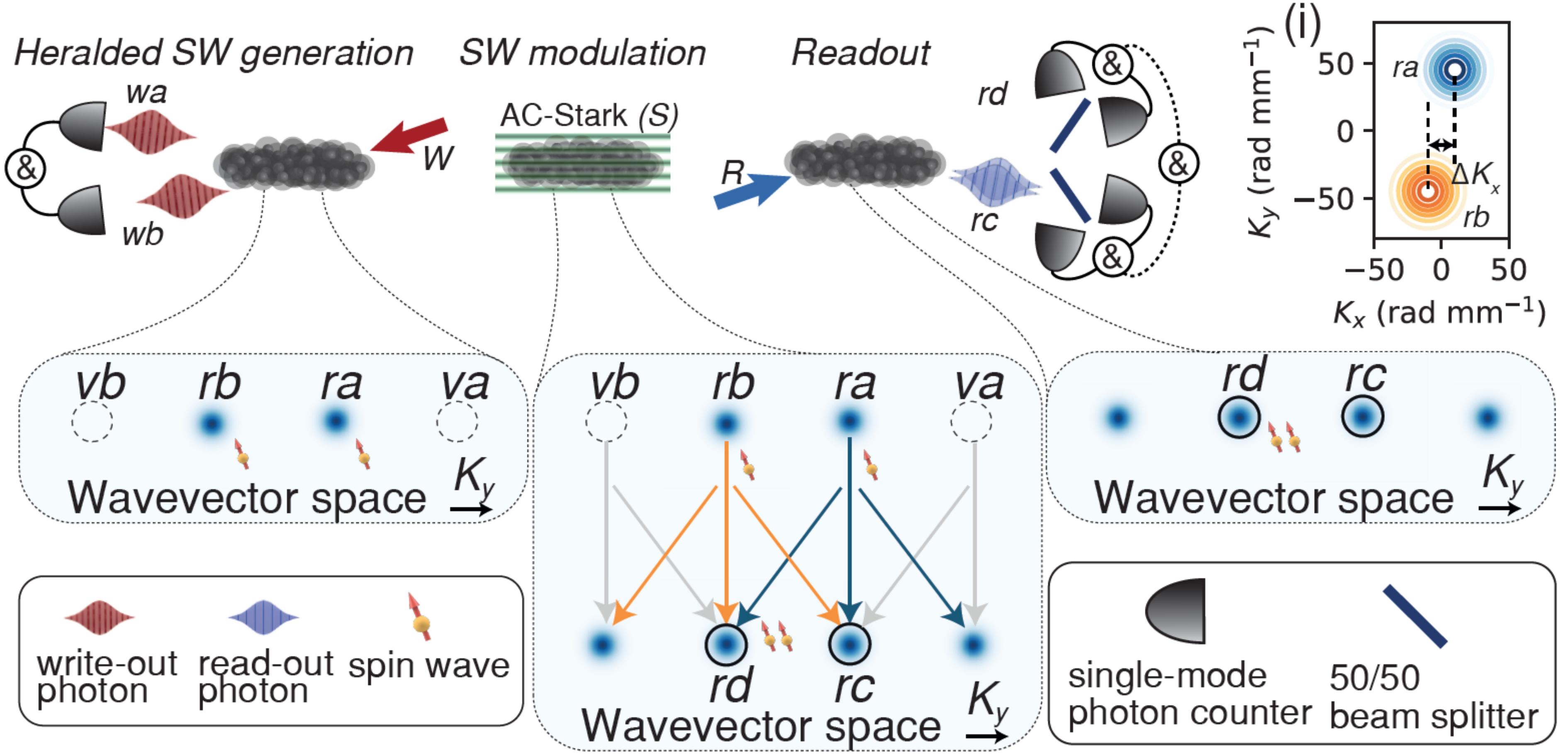

Phys. Rev. Lett. **122**, 063604 (2019)

Hong-Ou-Mandel effect

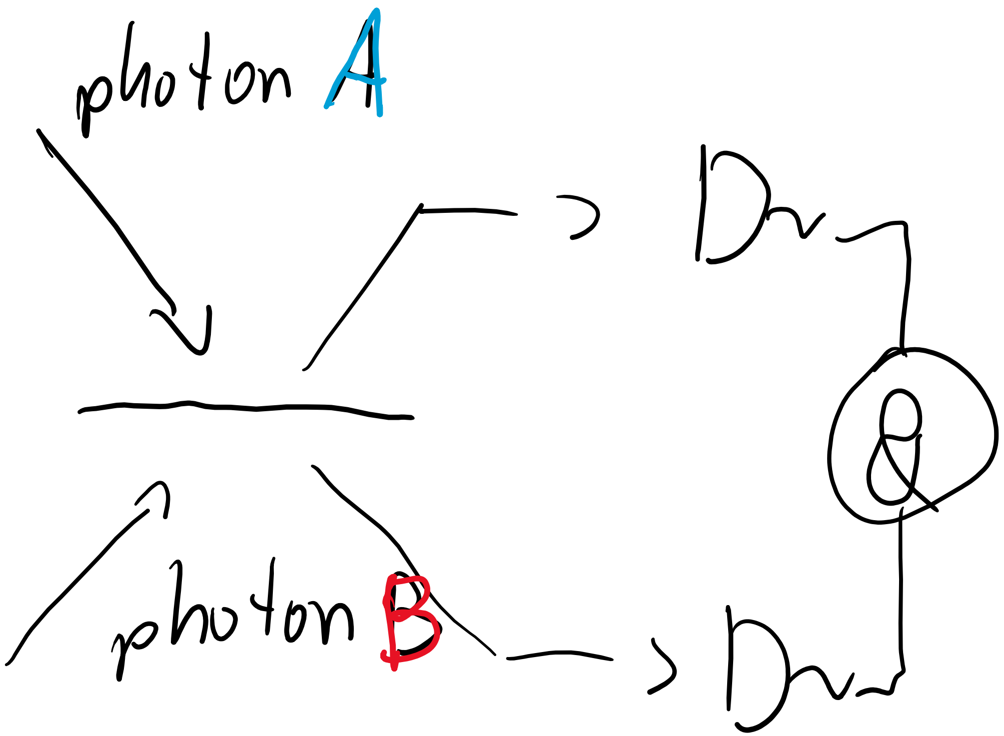

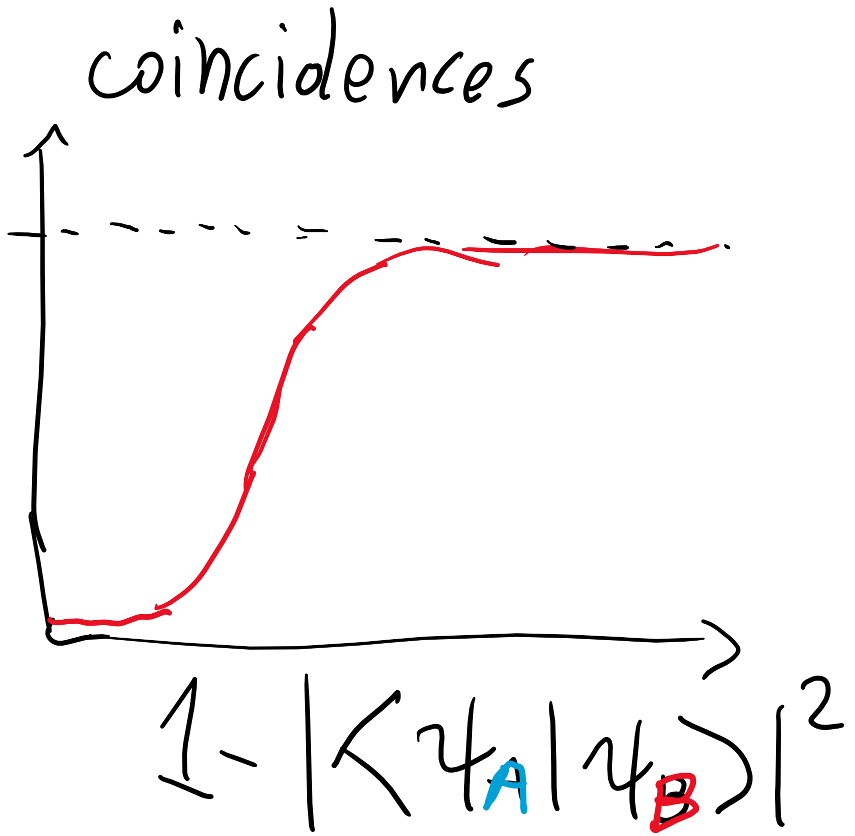

BS matrix $= \frac{1}{\sqrt{2}}\begin{pmatrix} 1 & -1 \\ 1 & 1 \end{pmatrix}$

Hong-Ou-Mandel interference

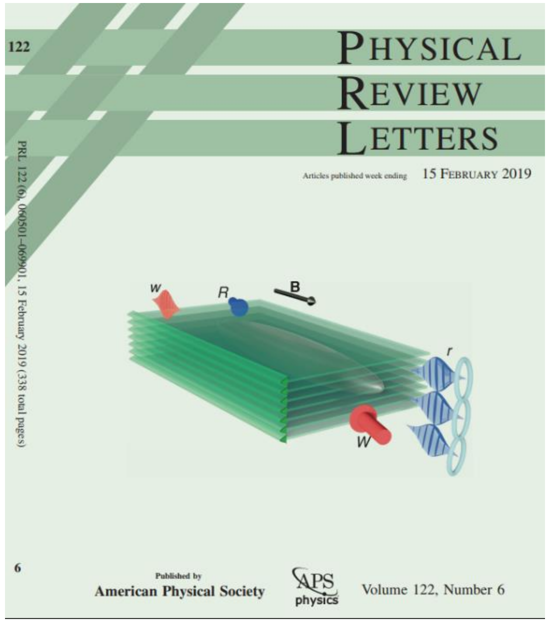

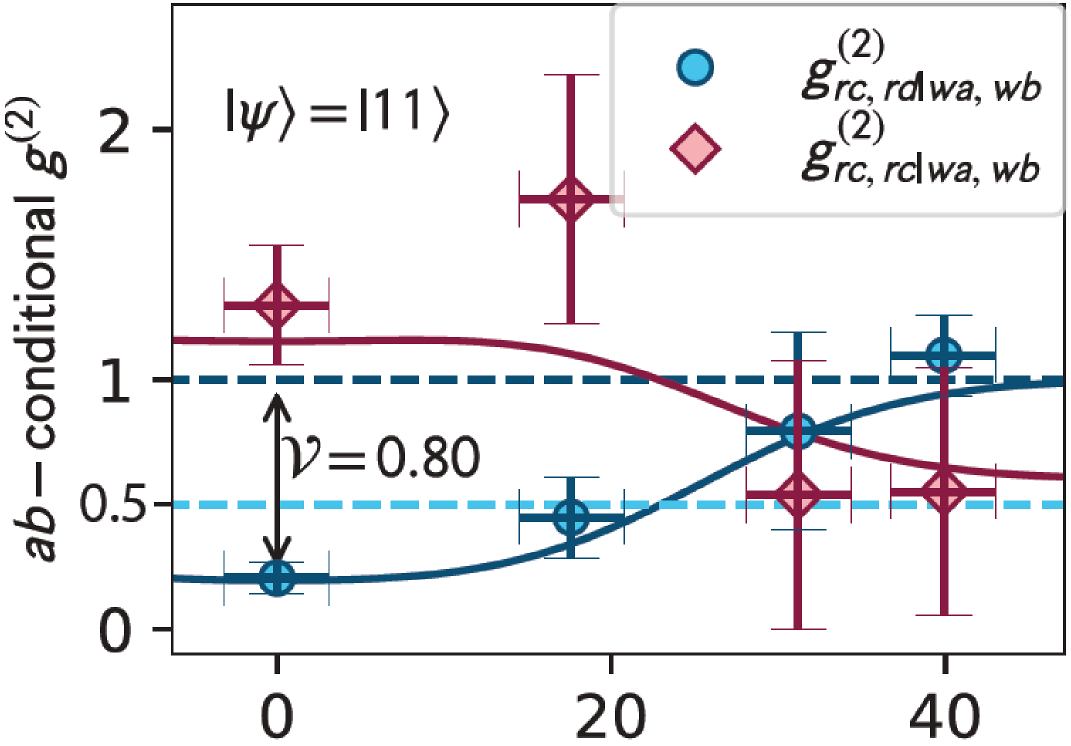

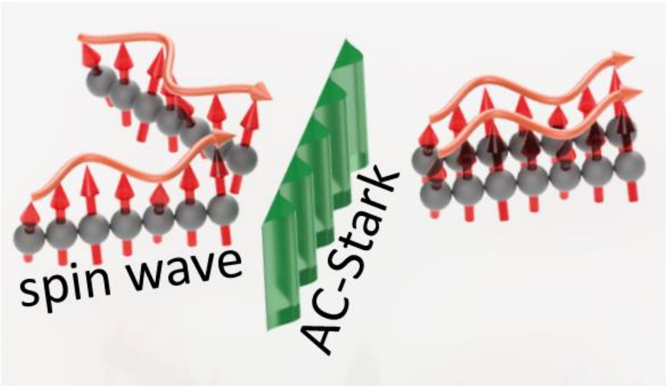

80% visibility at the moment limited by photon purity: with weak coherent states we observed interferometric visibility of >95%

Phys. Rev. Lett. **122**, 063604 (2019)

Atom-embedded photonic (co)processor

- **Wavevector-multiplexed quantum memory**
- **Spin-wave-based interferometric processor for stored light**
- **Multiplexed quantum repeaters**

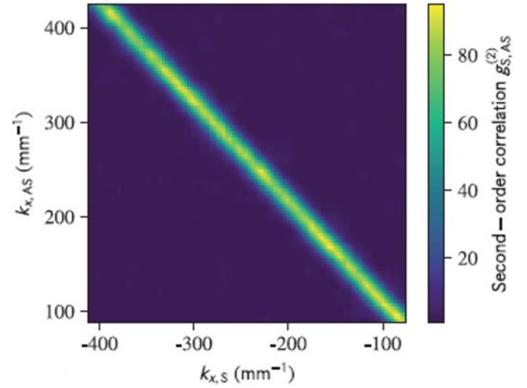

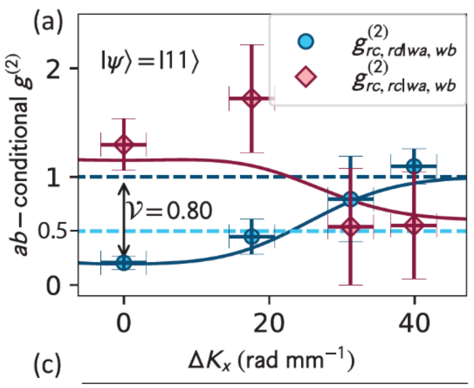

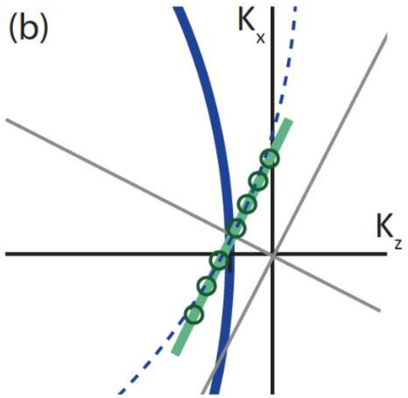

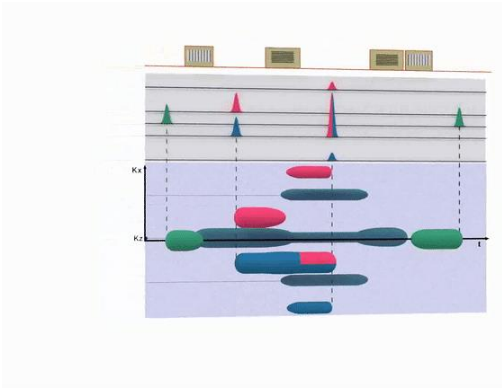

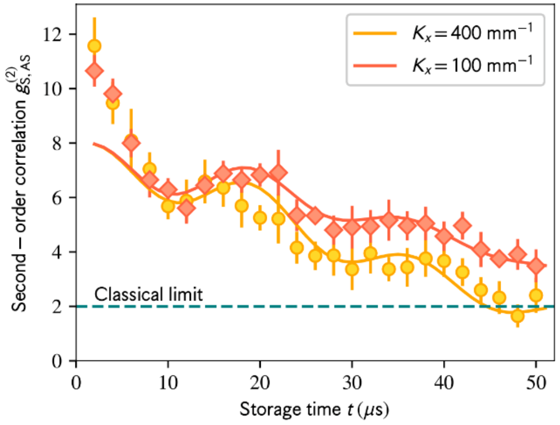

Applications of quantum transduction

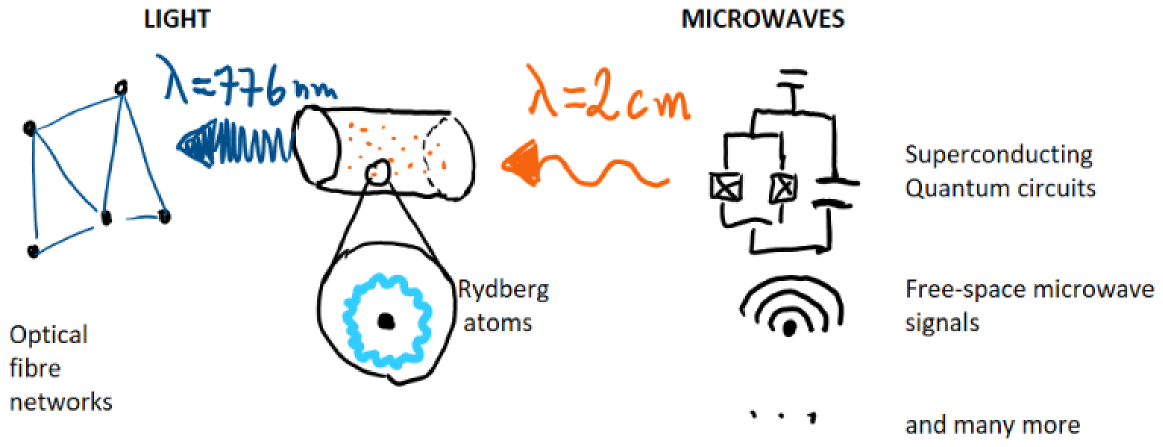

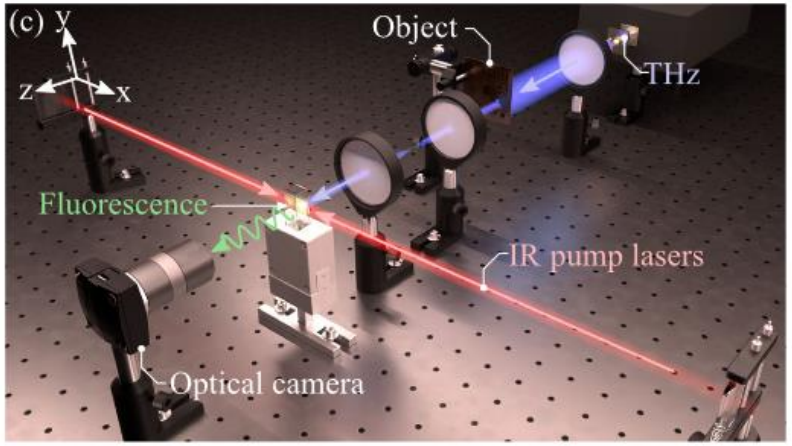

L. A. Downes et al., Phys Rev X 10, 011027 (2020) (Durham)

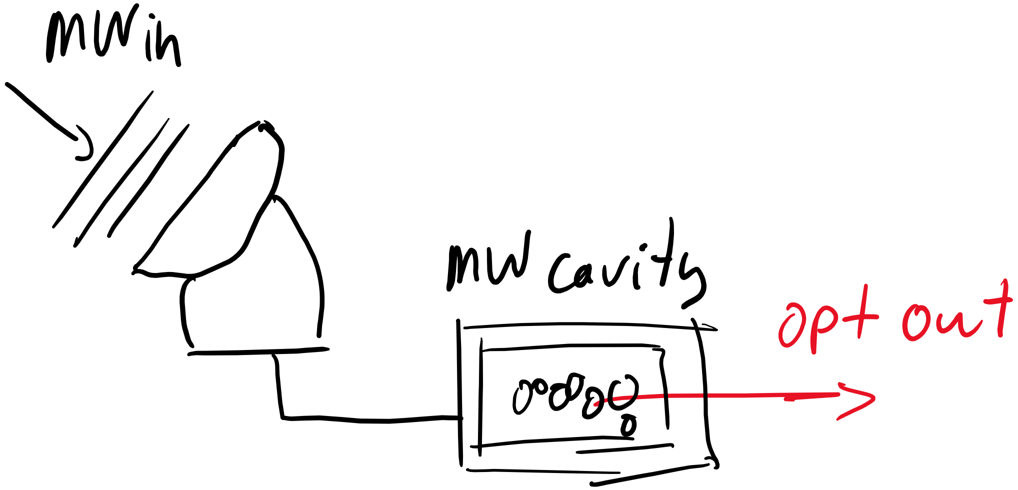

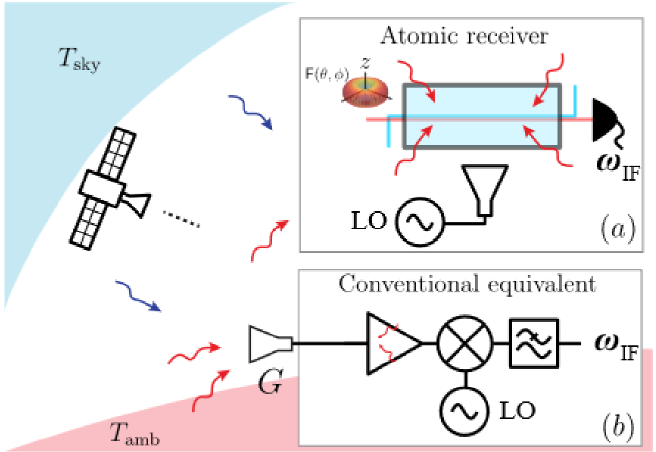

G. Santamaria Botello et al., arXiv:2209.00908 (CU Boulder)

Other approaches - examples

Λ system

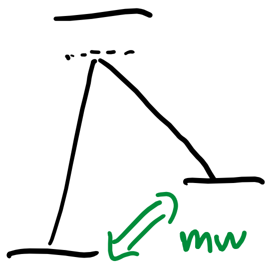

(very low dipole moment)

Ground state atoms, RE ions, …

opto-electro-mechanics

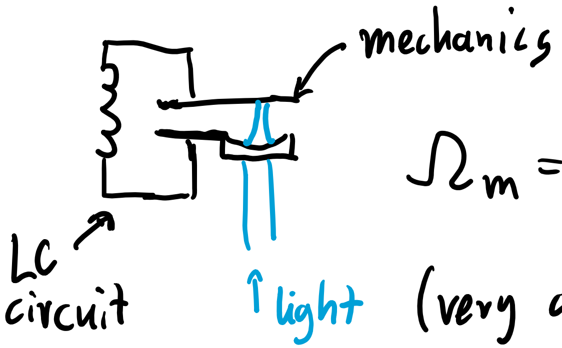

$\Omega_m = \Omega_{LC}$

(very complex)

Si or SiN resonators, …

Nature Phys. **16**, 69–74 (2020)
(Delft)
Nature Phys. **10**, 321–326 (2014)
(JILA Boulder)

Electro-optics

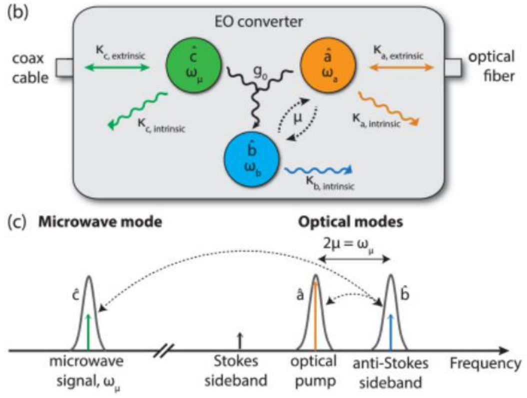

LN resonator, …

Optica 7, 12, 1737-1745 (2020)
(Stanford)

Opto-magnonics

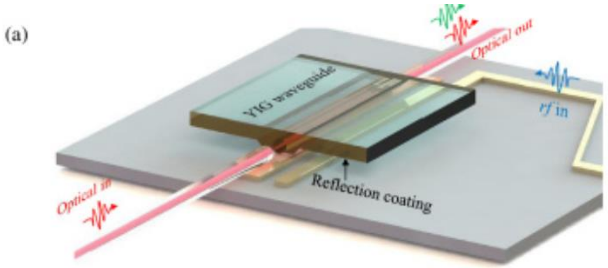

Optica 7, 10, 1291 (2020)
(Yale)

Other approaches – Rydberg atoms

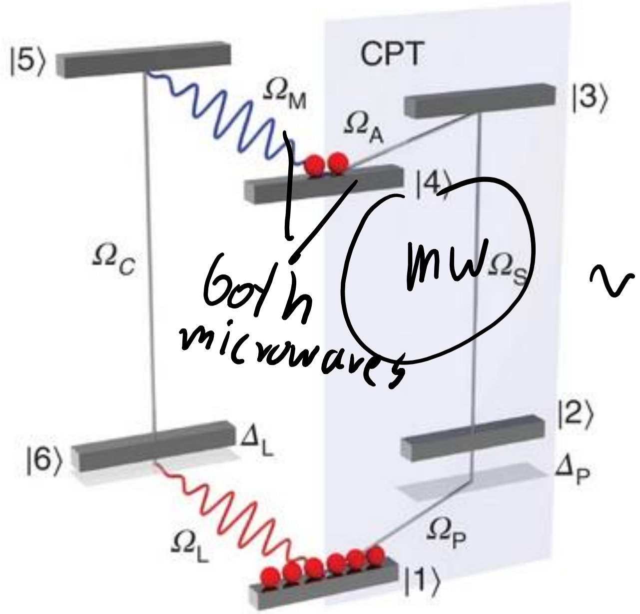

both microwaves
mw ~ atoms ~ light

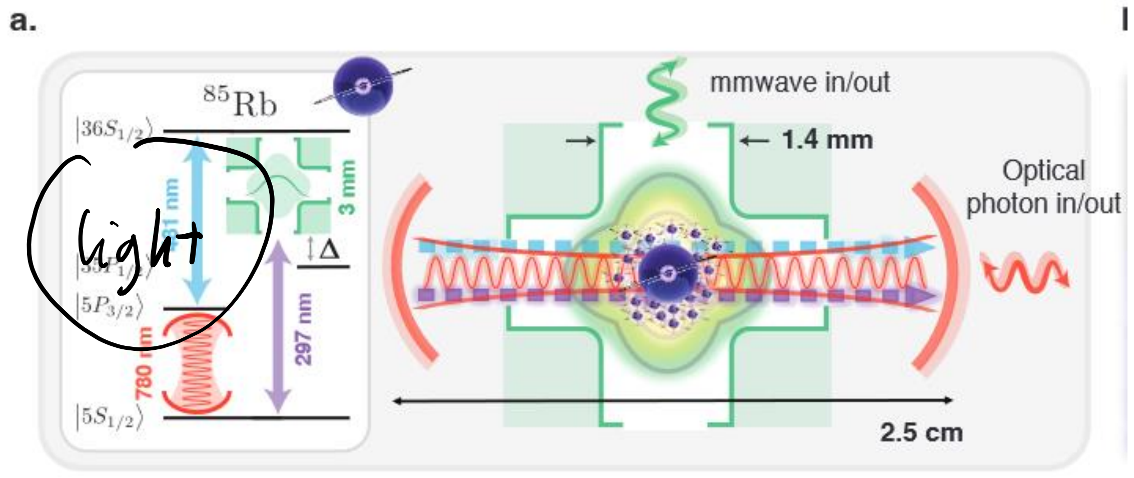

A. Kumar et al., Nature **615**, 614 (2023) (Stanford/Chicago)

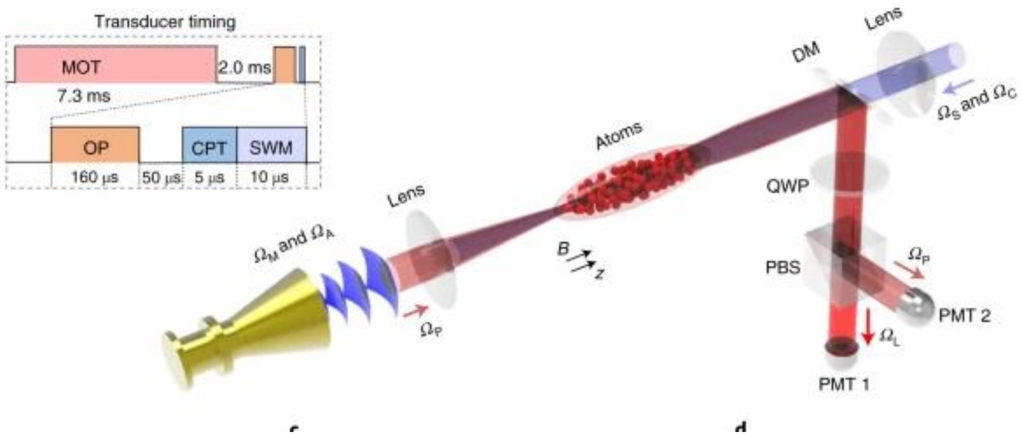

Nat. Photon. **16**, 291–296 (2022) (SCNU Guangzhou)

Other approaches

MW + mechanics

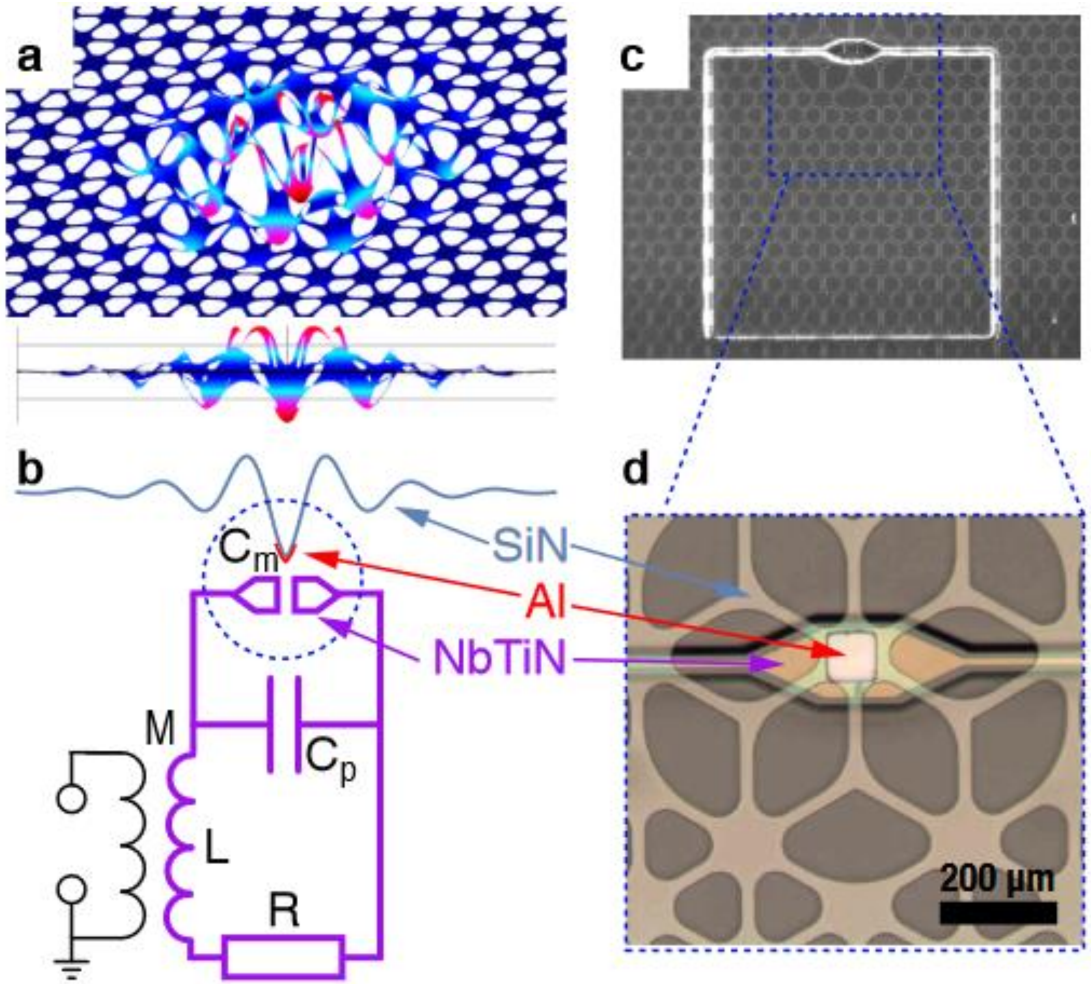

Nat Commun 13, 1507 (2022) (NBI Copenhagen)

optomechanics

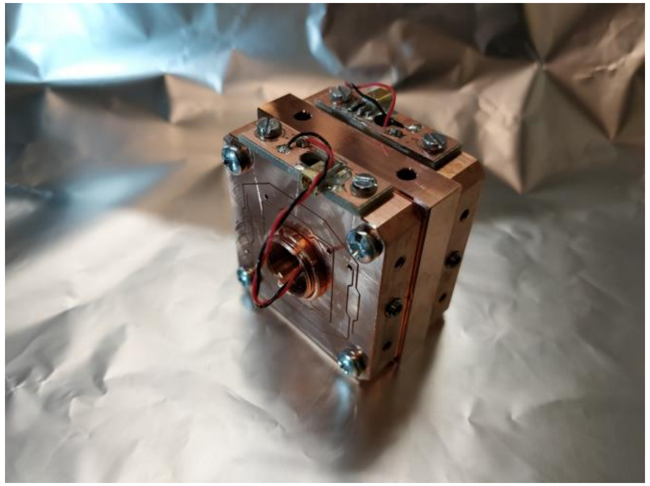

assembly

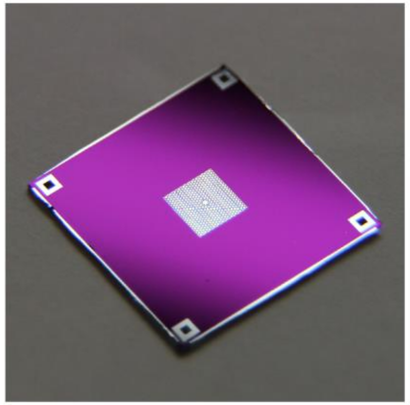

membrane

I. Galinskiy, Y. Tsaturyan, MP, E. S. Polzik, Optica 7, 718 (2020)
R.A Thomas, MP, et al., Nature Physics **17**, 228–233 (2021)

Rabi frequency and EIT sensing

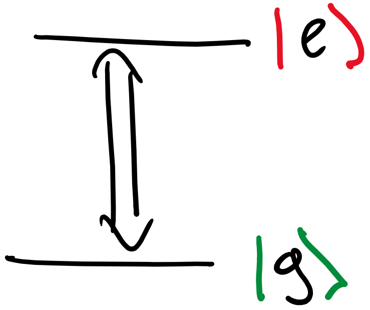

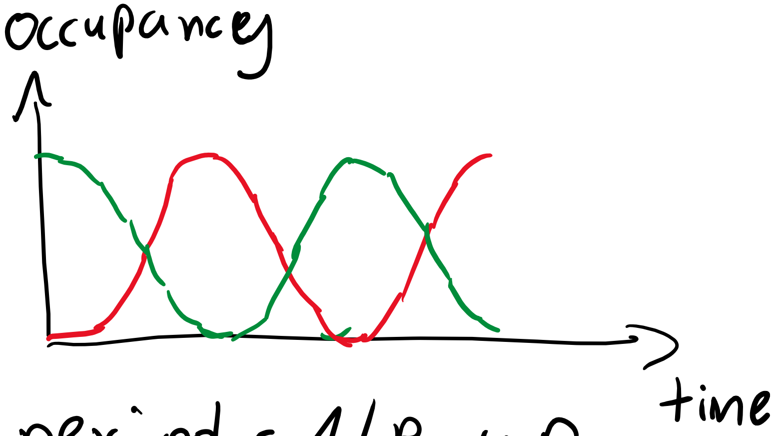

period = 1/Rabi frequency

$$\Omega_R = \frac{E \cdot d}{\hbar}$$

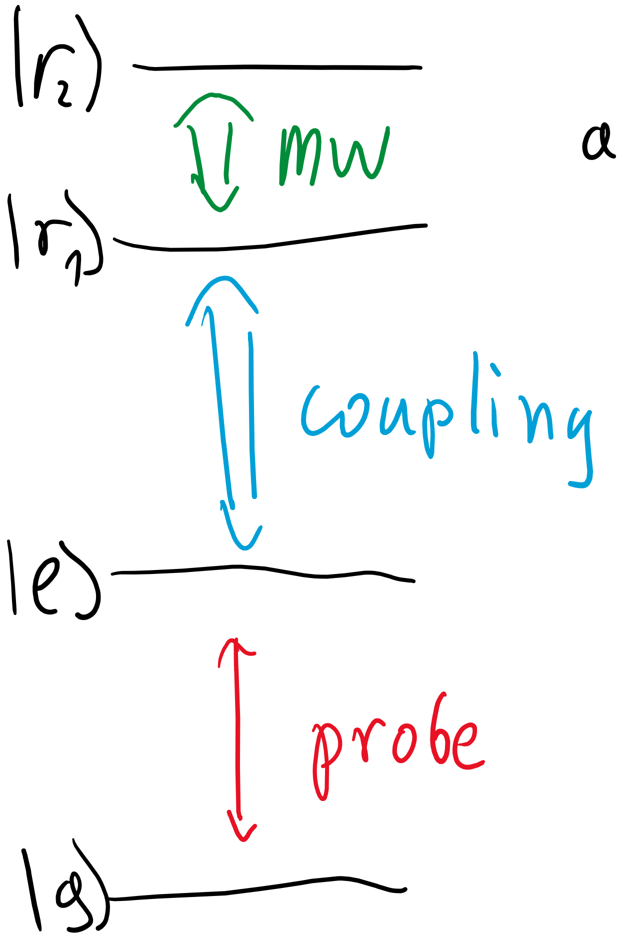

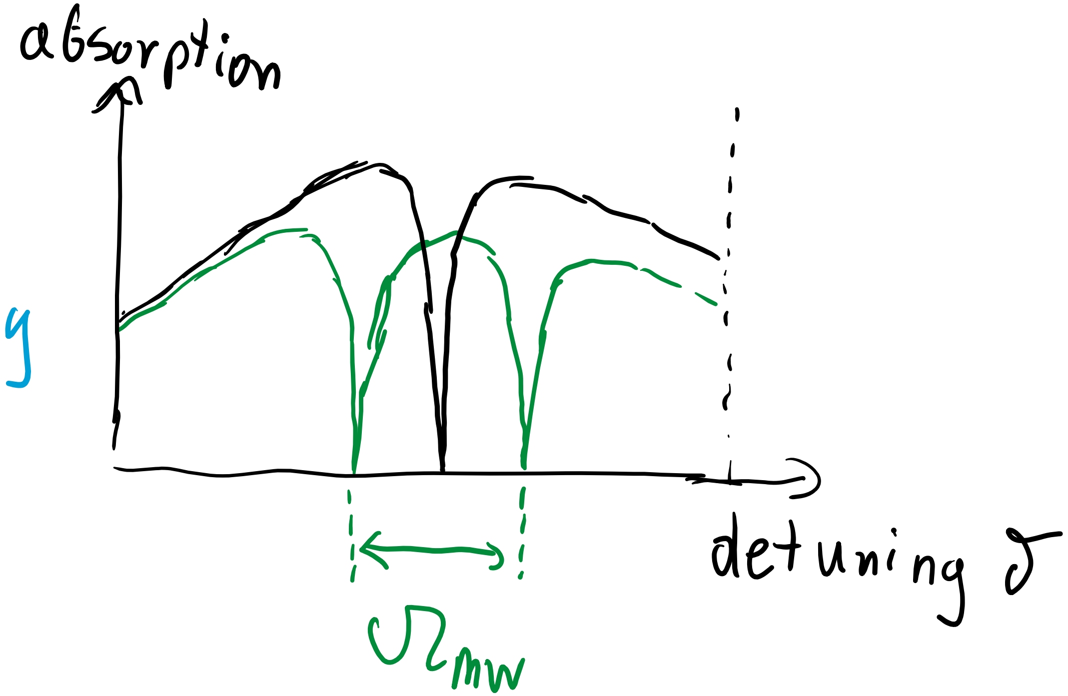

Rydberg electrometry

Frequency splitting
- Rabi frequency - **measured with respect to a frequency reference**

$$\Omega = \frac{d_x E_0}{\hbar}$$

Electric field amplitude **E**
Dipole moment **d**

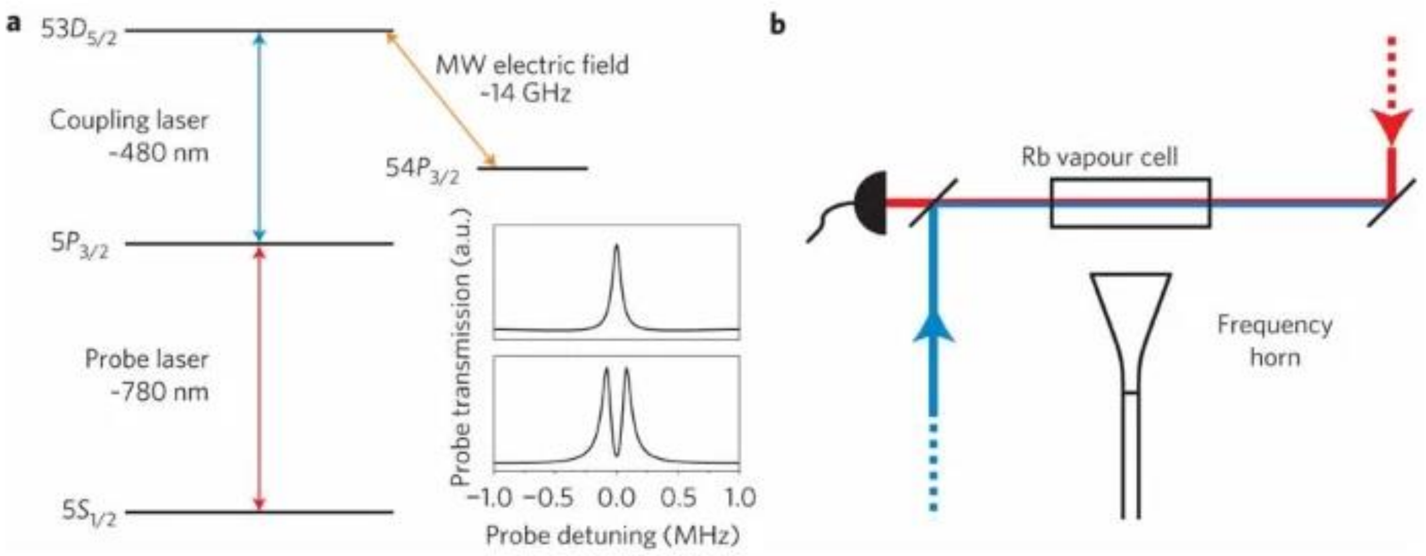

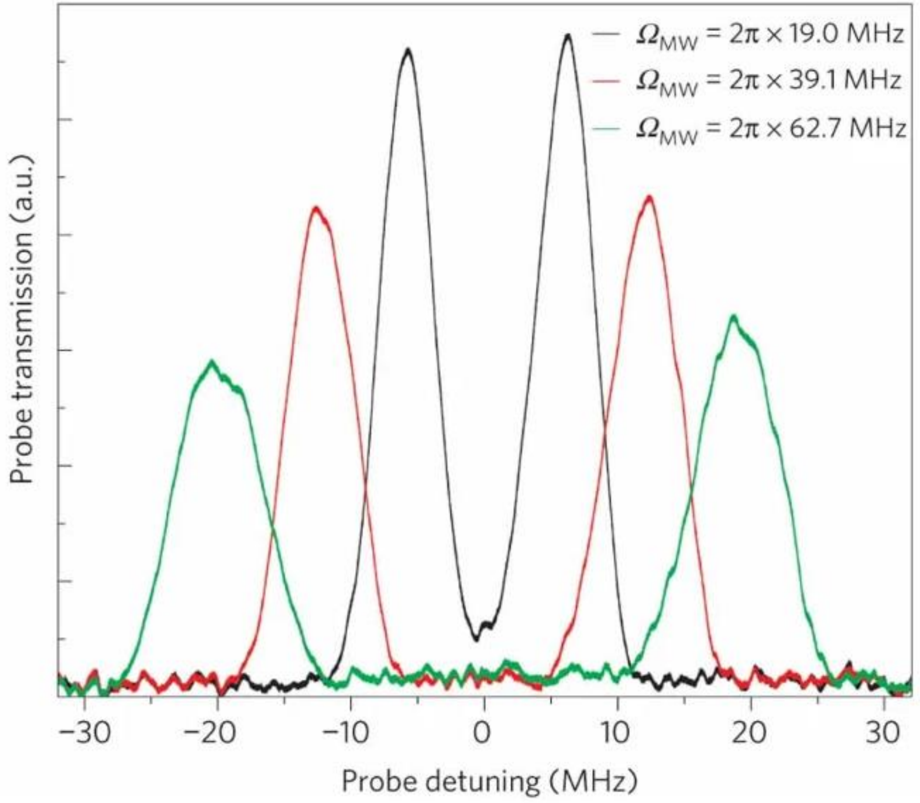

Sedlacek et al., Nature Physics **8**, 819–824 (2012) (Oklahoma/Stuttgart)

Practical electrometers

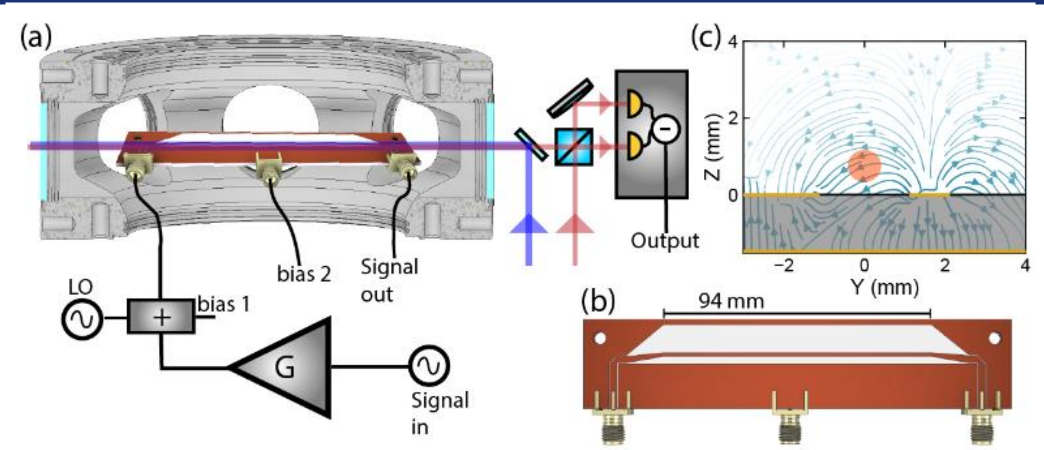

D. Meyer et al., PR Applied **15**, 014053 (2020) (ARL Maryland)

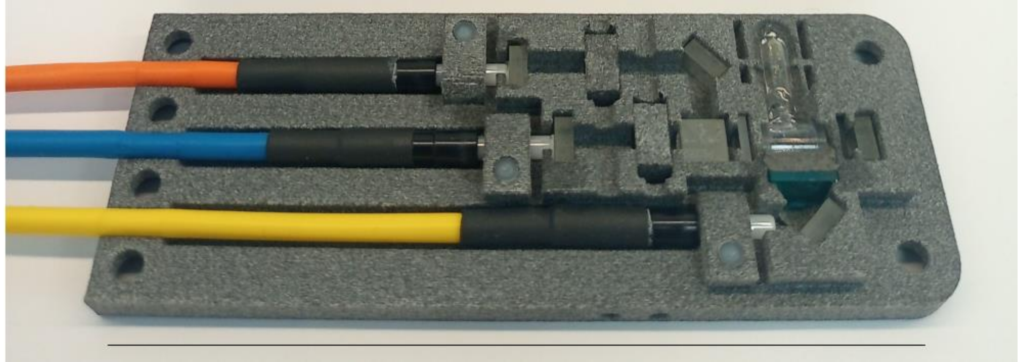

Future: all-fiber laser system?

Example atomic magnetometer by our collaborators from University of Copenhagen
H. Stærkind et al., arXiv:2208.00077 (2022)

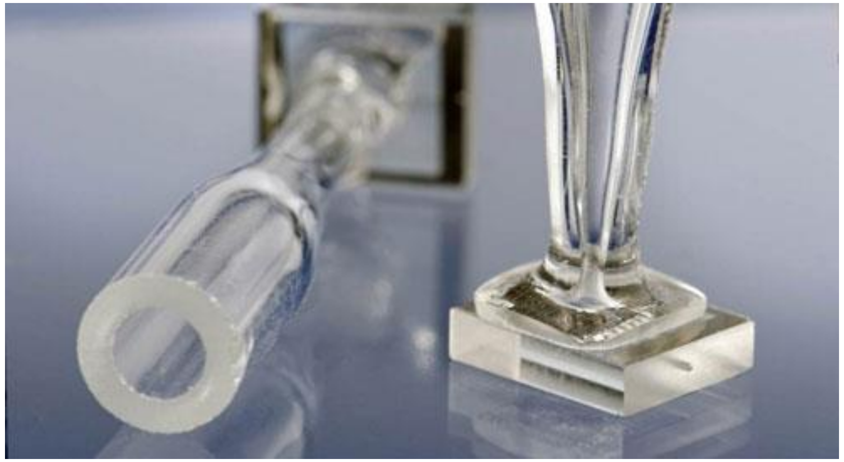

Soon: smaller cel

Future: miniaturized assembly

Potential: all-glass/fiber/plastic microwave receiver, insensitive to EMI

Microwave-to-optical conversion

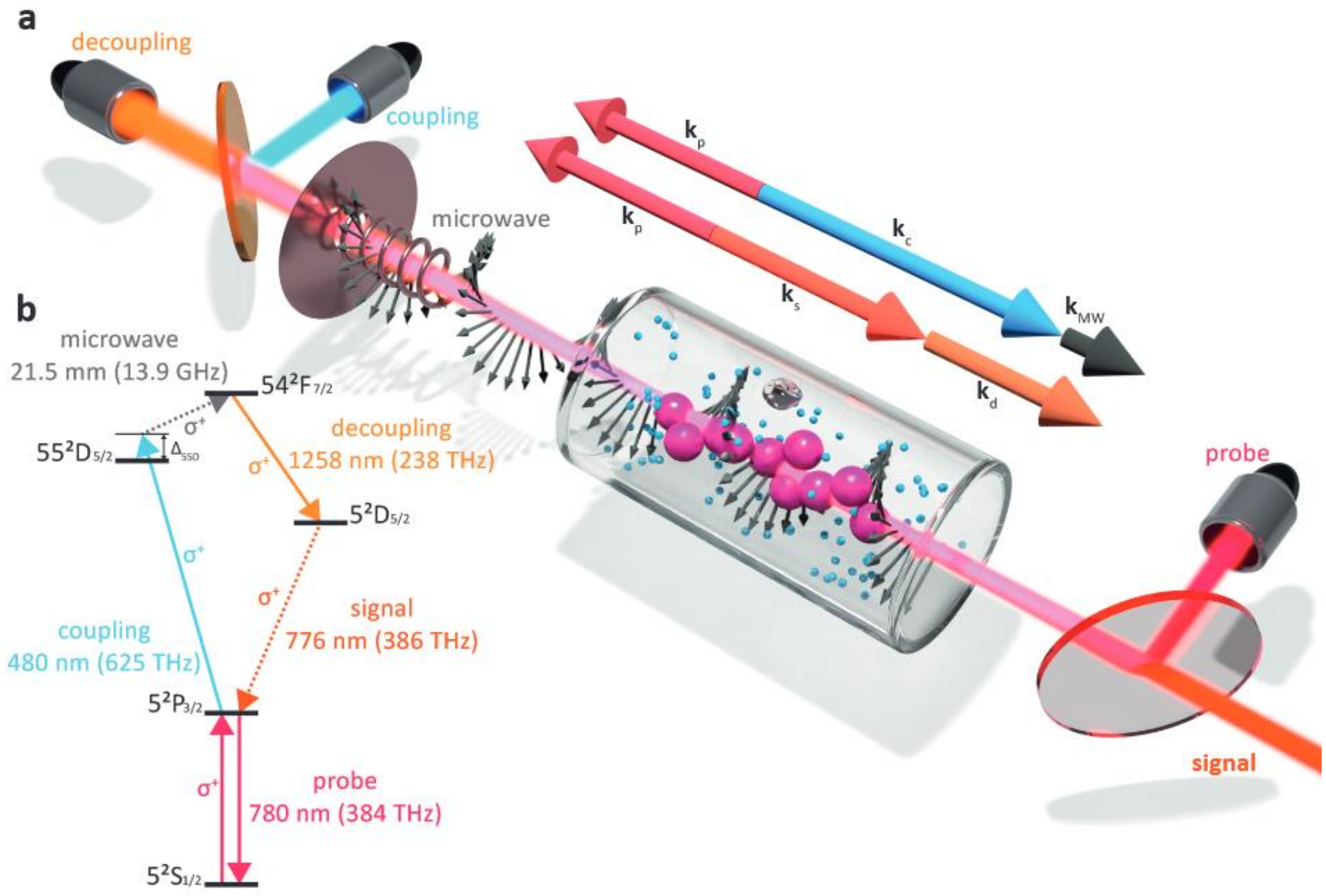

S. Borówka,
U. Pylypenko, M. Mazelanik, **MP**,
arXiv:2302.08380

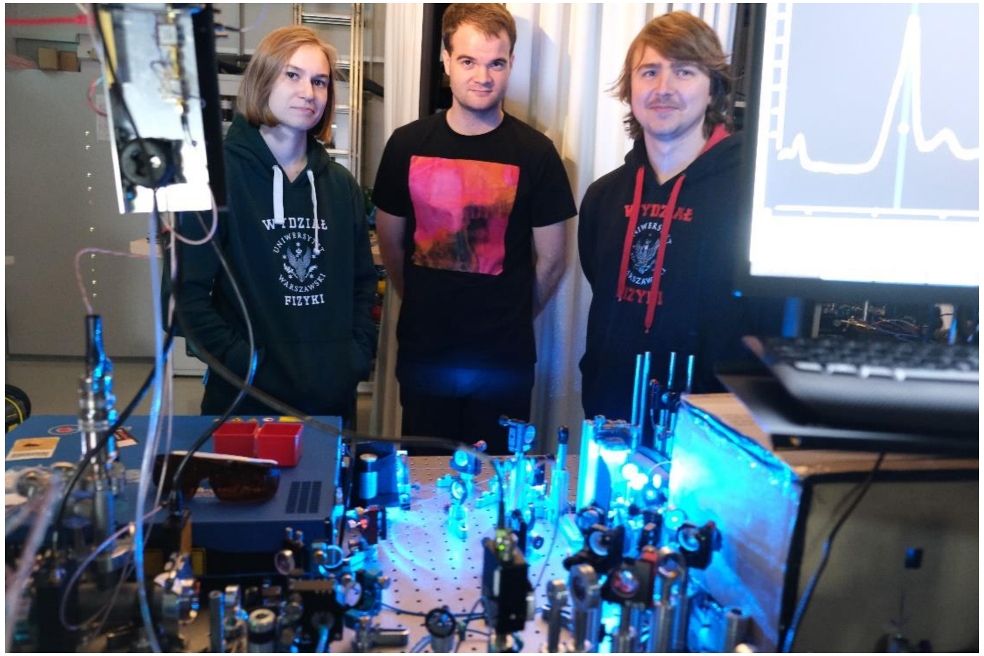

Experimental setup

arXiv:2302.08380

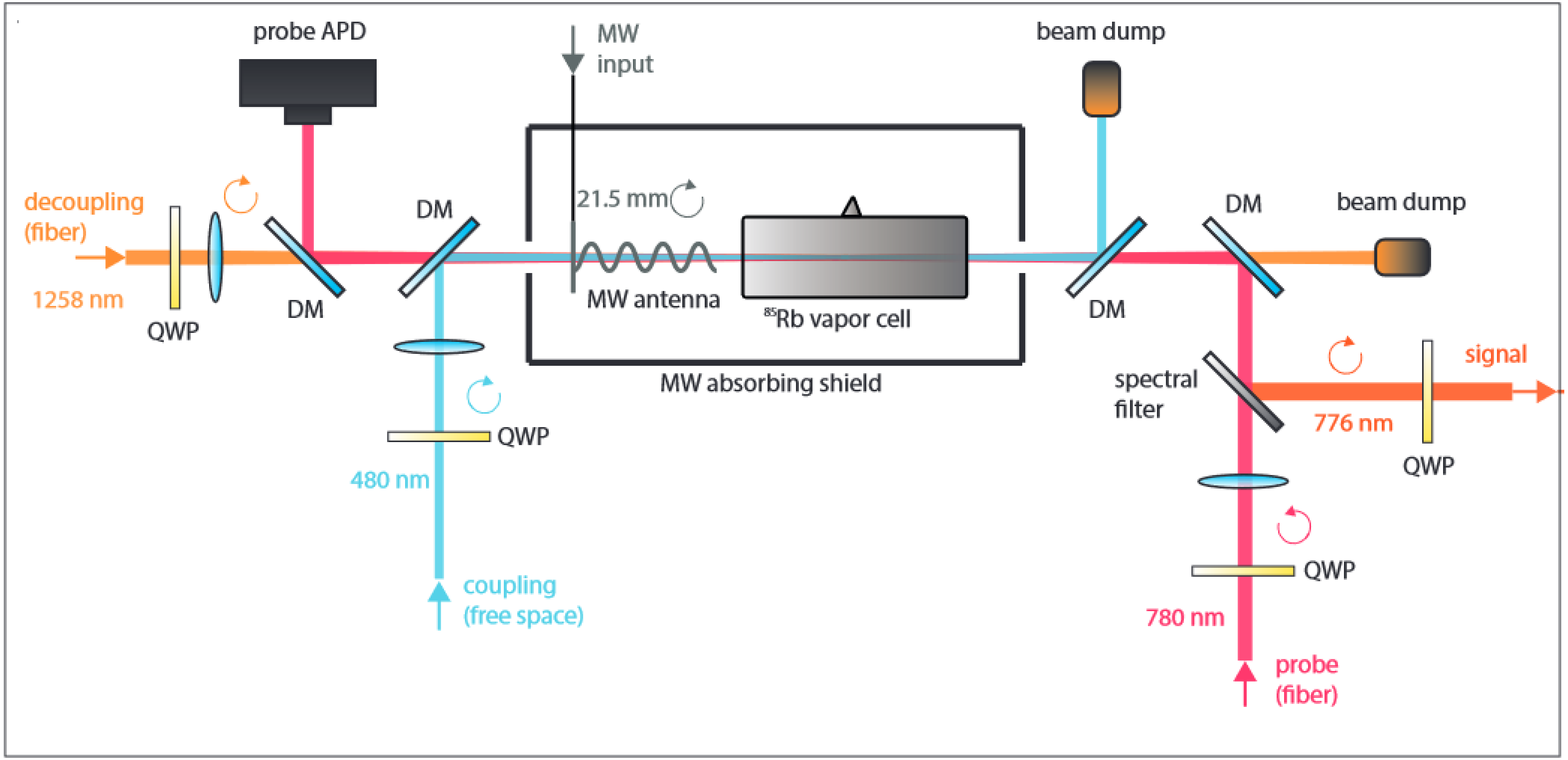

Experimental setup

arXiv:2302.08380

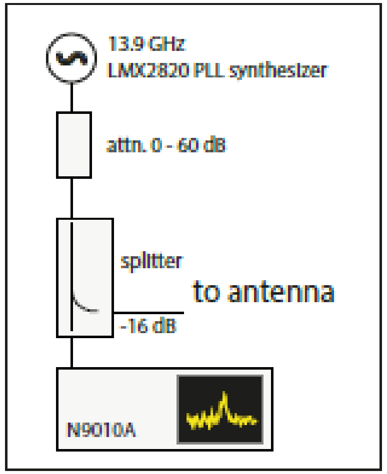

Laser system - cavity transfer locks

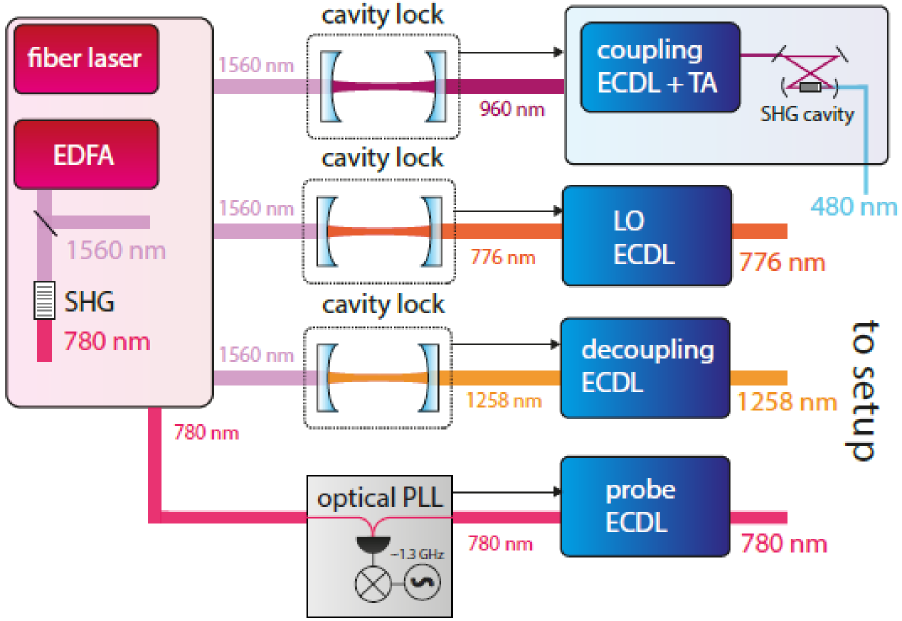

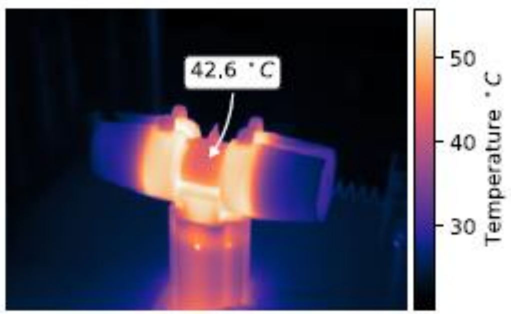

3D printed plastic
heater with air-channels

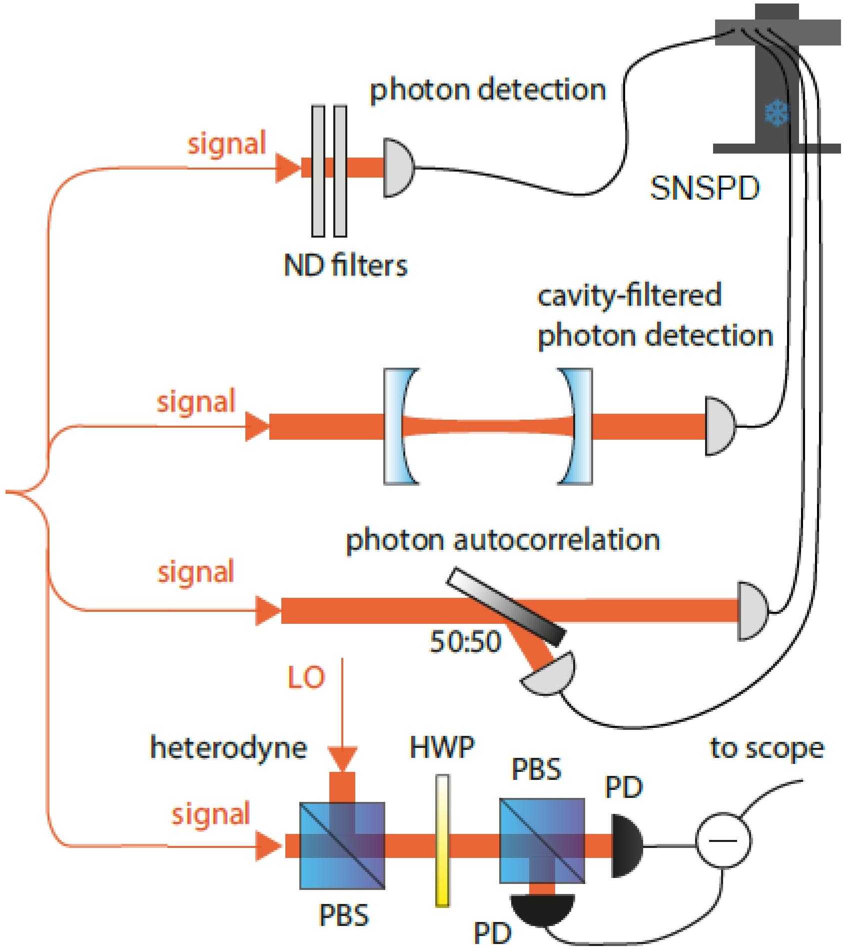

EIT & conversion

arXiv:2302.08380

Simulation

Experiment

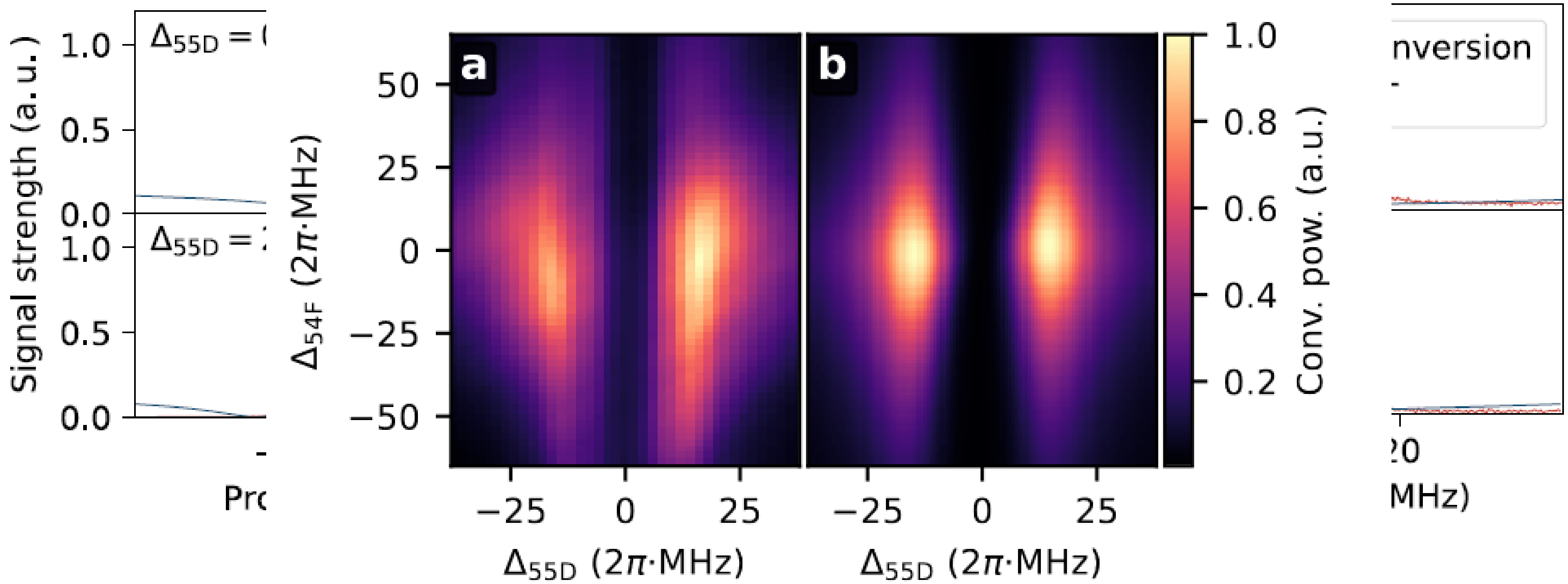

on resonance

off-resonant

Photon counting and efficiency

arXiv:2302.08380

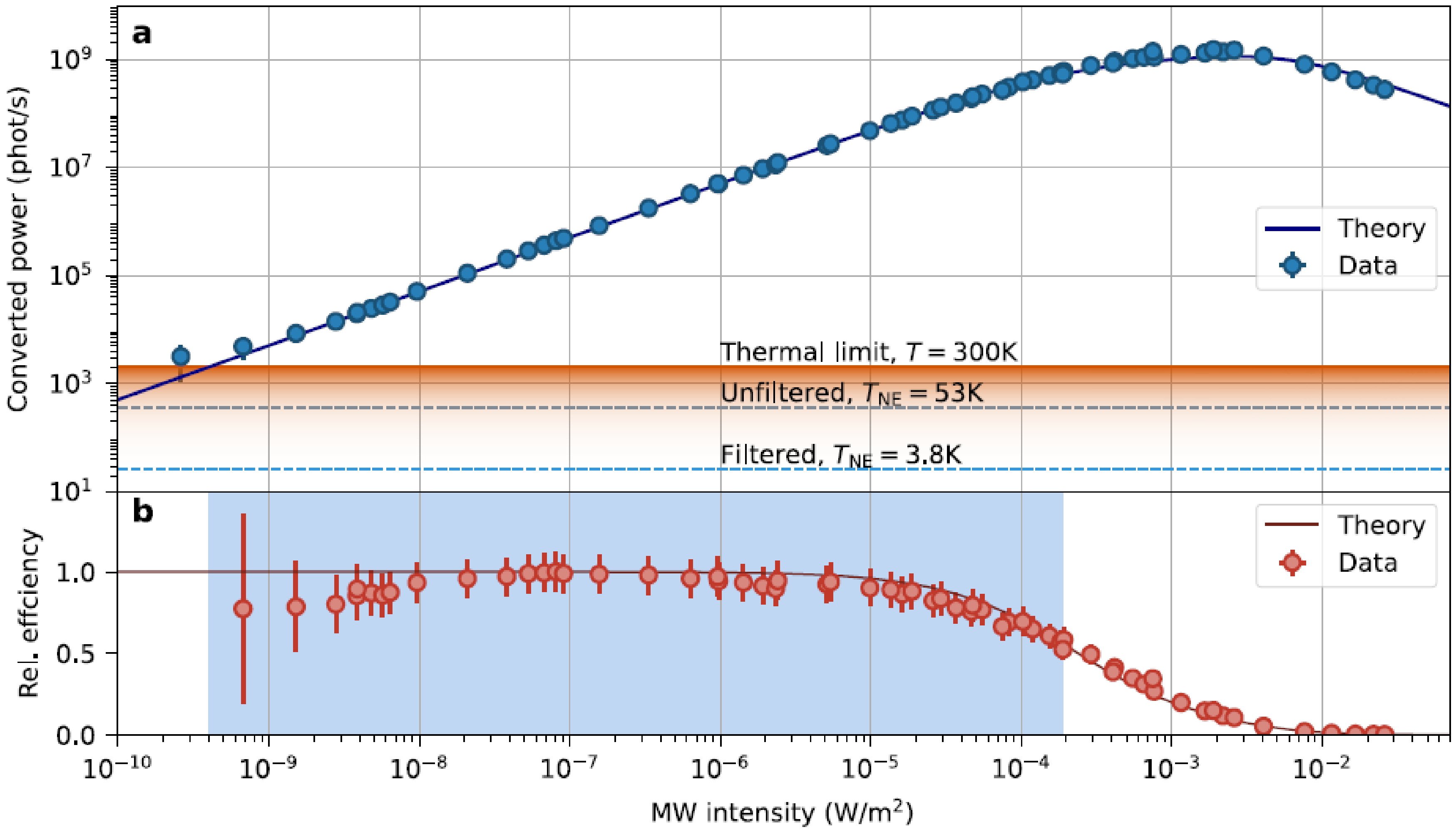

Thermal noise

arXiv:2302.08380

$$\langle E_{\text{eff}}^2 \rangle = \frac{\omega^2 \langle \mathcal{E} \rangle}{\pi^2 c^3 \varepsilon_0} \frac{1}{4\pi} \int_0^{2\pi} \mathrm{d}\phi \int_0^{\pi} \mathrm{d}\theta \sin(\theta) |\eta(\theta)|^2$$

$$\langle \mathcal{E} \rangle = \frac{\hbar\omega}{e^{\hbar\omega/k_B T} - 1},$$

Antenna profile of the converter (gain G=6.22)

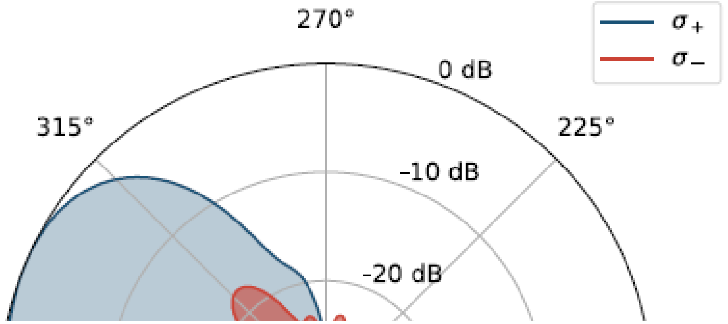

Bandwidth

arXiv:2302.08380

Tunable bandwidth (single laser)

Instantenous bandwidth

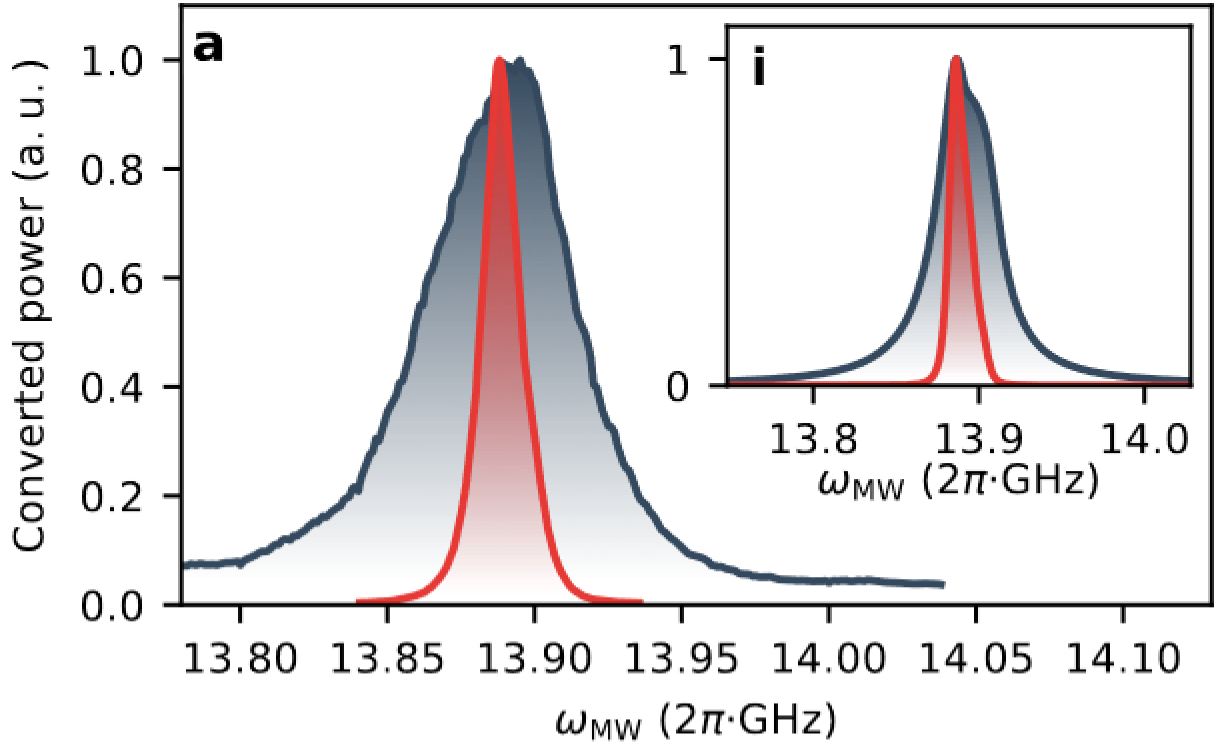

Wiener-Khinchin theorem!

$$g^{(1)}_{\mathrm{th}}(\tau) = \frac{1}{2\pi}\int_{-\infty}^{\infty} |S(\omega)|^2 \, e^{-i\omega\tau} \mathrm{d}\omega,$$

$$g^{(2)}(\tau) = 1 + \frac{1}{4}\left(\left|g^{(1)}_{\mathrm{th}}(\tau) + e^{-i\omega\tau}\right|^2 - 1\right),$$

Tunability

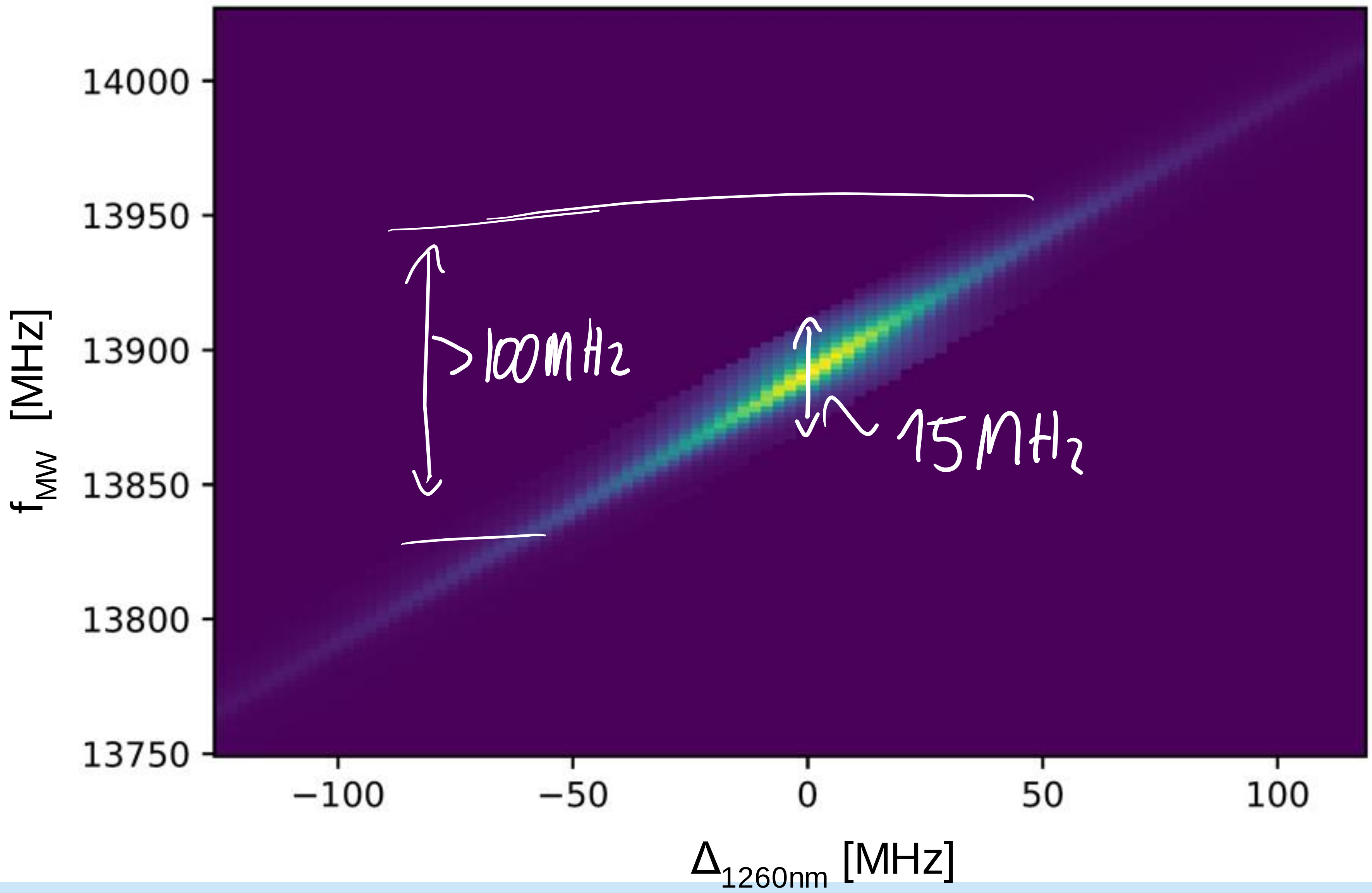

arXiv:2302.08380

Detection with local oscillator

arXiv:2302.08380

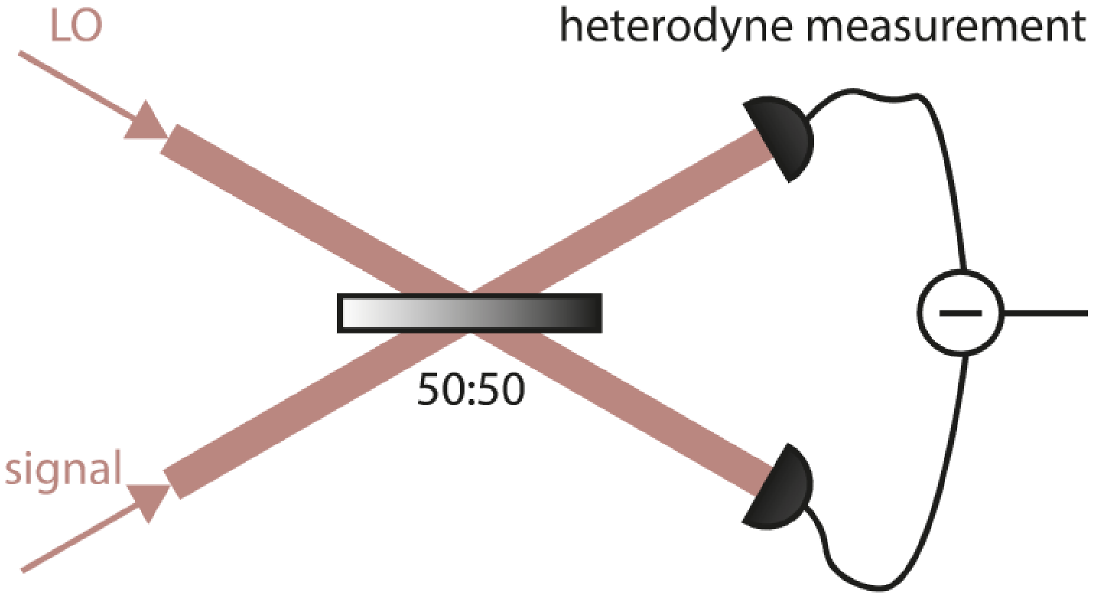

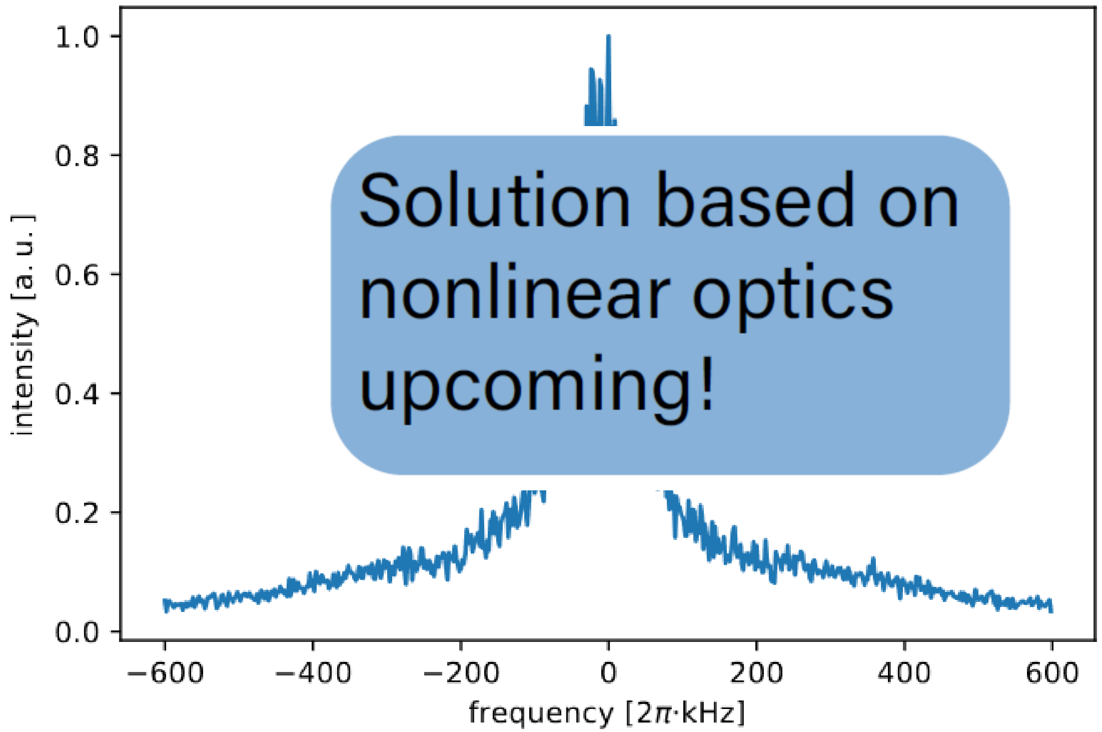

Second-order correlation

arXiv:2302.08380

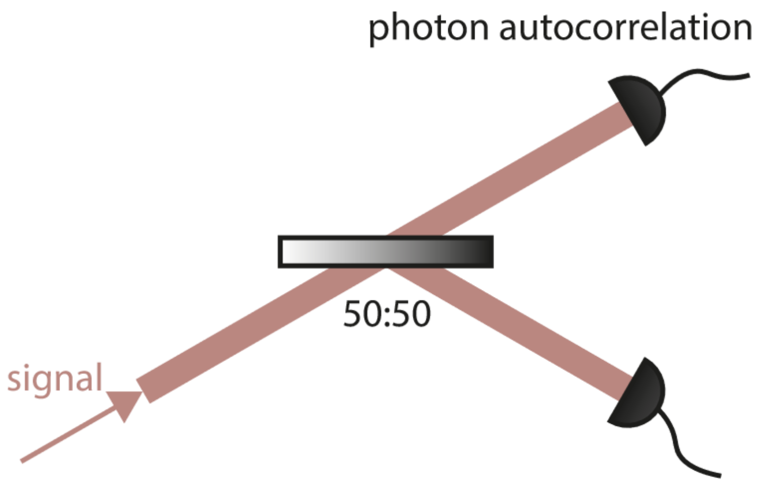

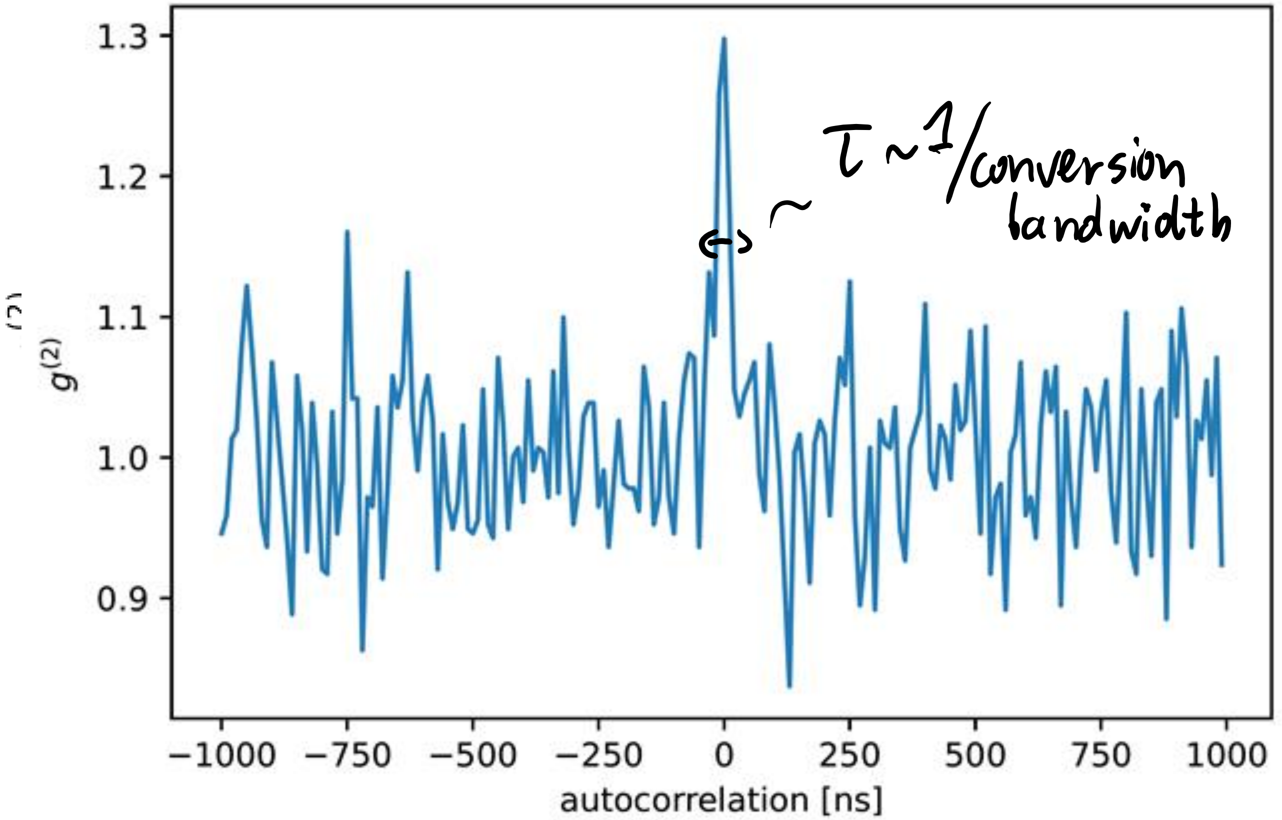

$$g^{(2)}(\tau) = 1 + A\exp(-2|\tau|/\tau_C) = 1 + A\exp(-\Gamma_{opt}|\tau|)$$

Second-order correlation

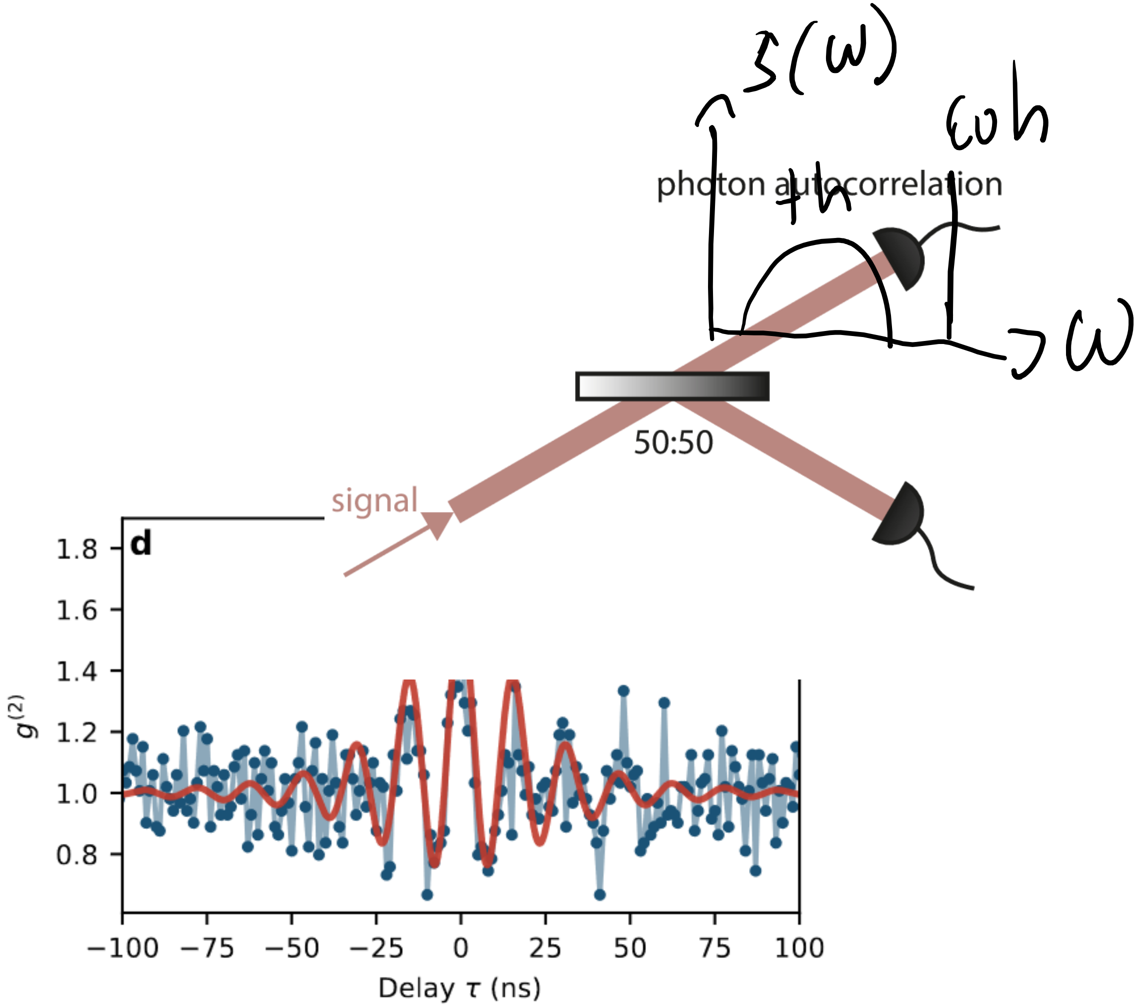

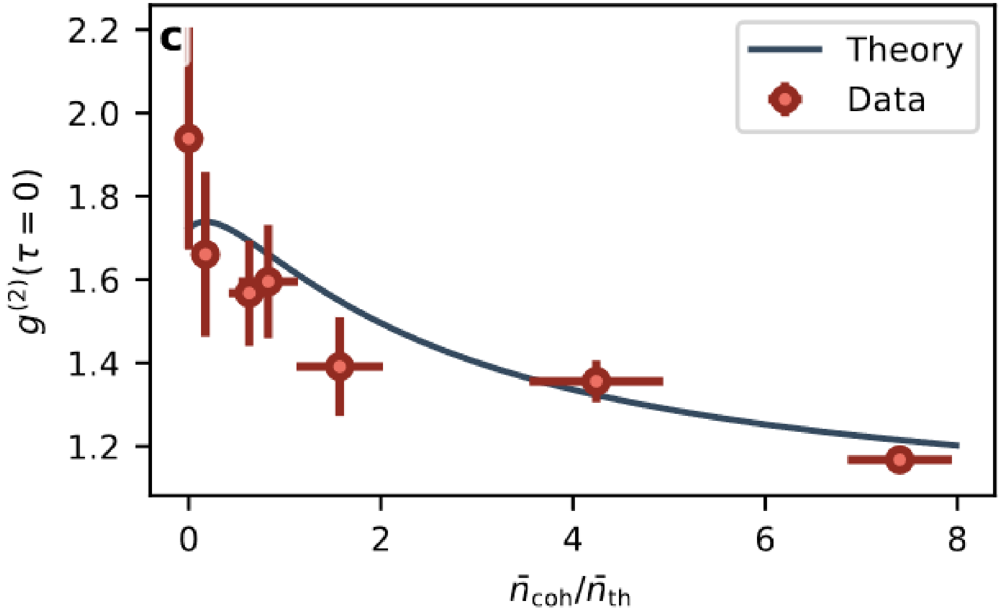

$$g^{(2)}(\tau) = 1 + \frac{\left|\bar{n}_{\mathrm{th}} g^{(1)}_{\mathrm{th}}(\tau) + \bar{n}_{\mathrm{coh}} e^{-i\omega\tau}\right|^2 - \bar{n}^2_{\mathrm{coh}}}{(\bar{n}_{\mathrm{th}} + \bar{n}_{\mathrm{coh}} + \bar{n}_{\mathrm{noise}})^2}$$

arXiv:2302.08380

Residual noise

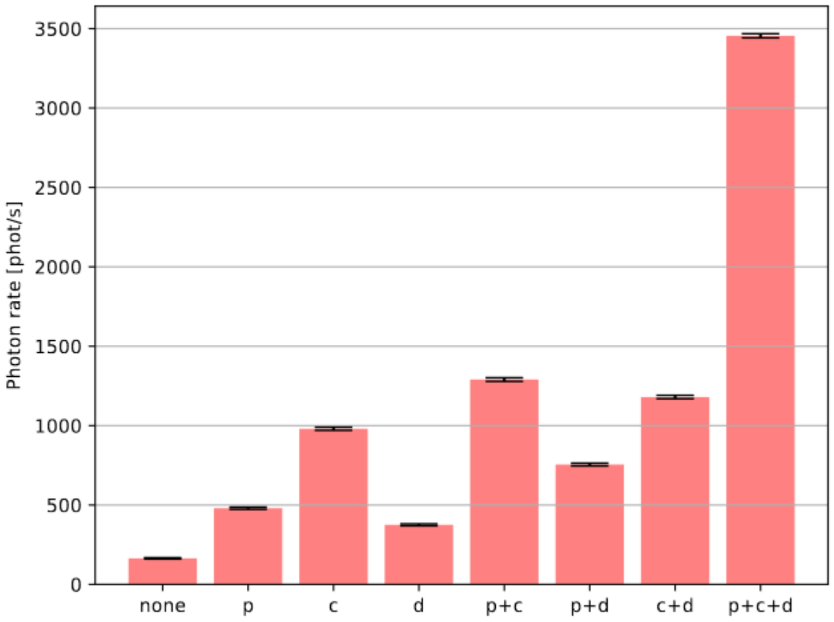

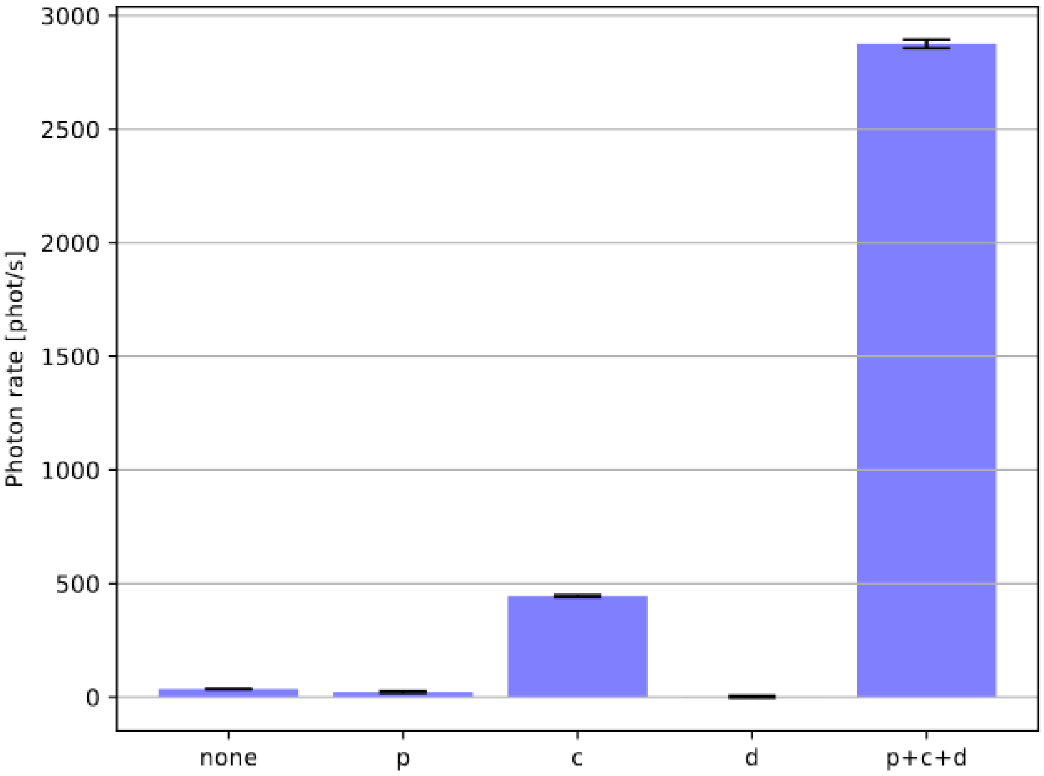

arXiv:2302.08380

Counting of microwave photons

current setup:

free space „atomic antenna"

future

atomic receiver,

but large antenna

... from:

5G/6G networks,

...e (radio astronomy)

Current equivalent noise – due to dark noise – around 4K
Best MW amplifiers at room temperature – 50 K
With cavity, noise can be removed via cooling (readout)

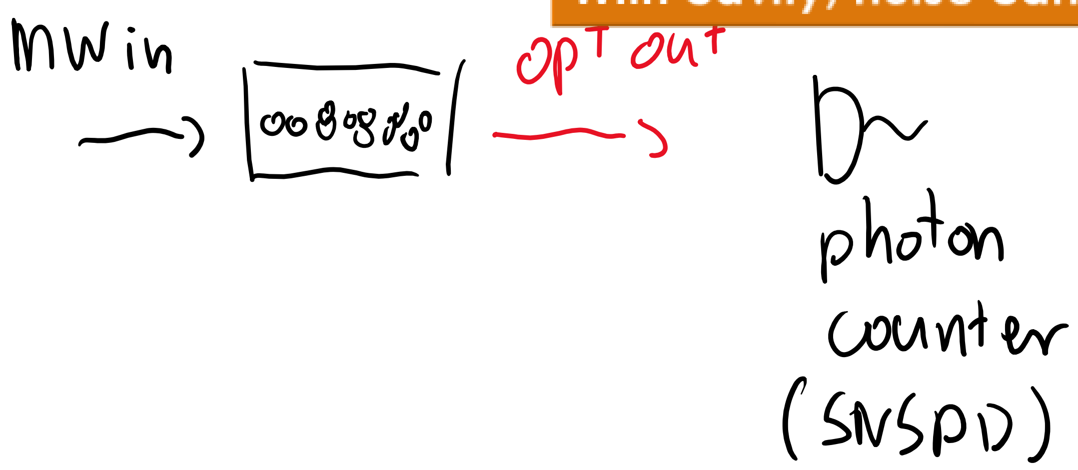

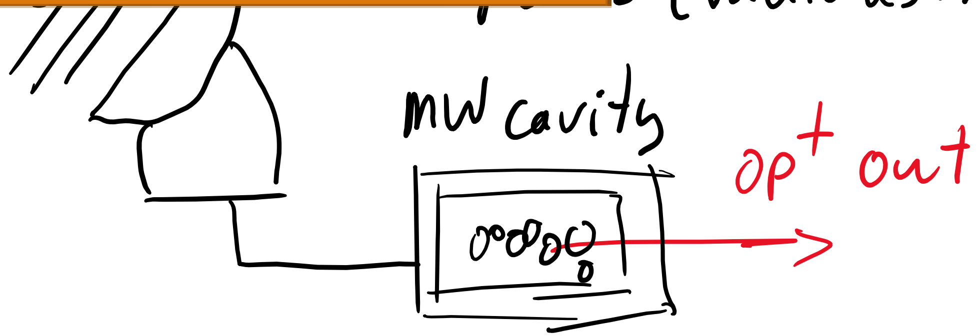

Cooperative enhancement
via radiative cooling

Applications of Rydberg-atom transducer

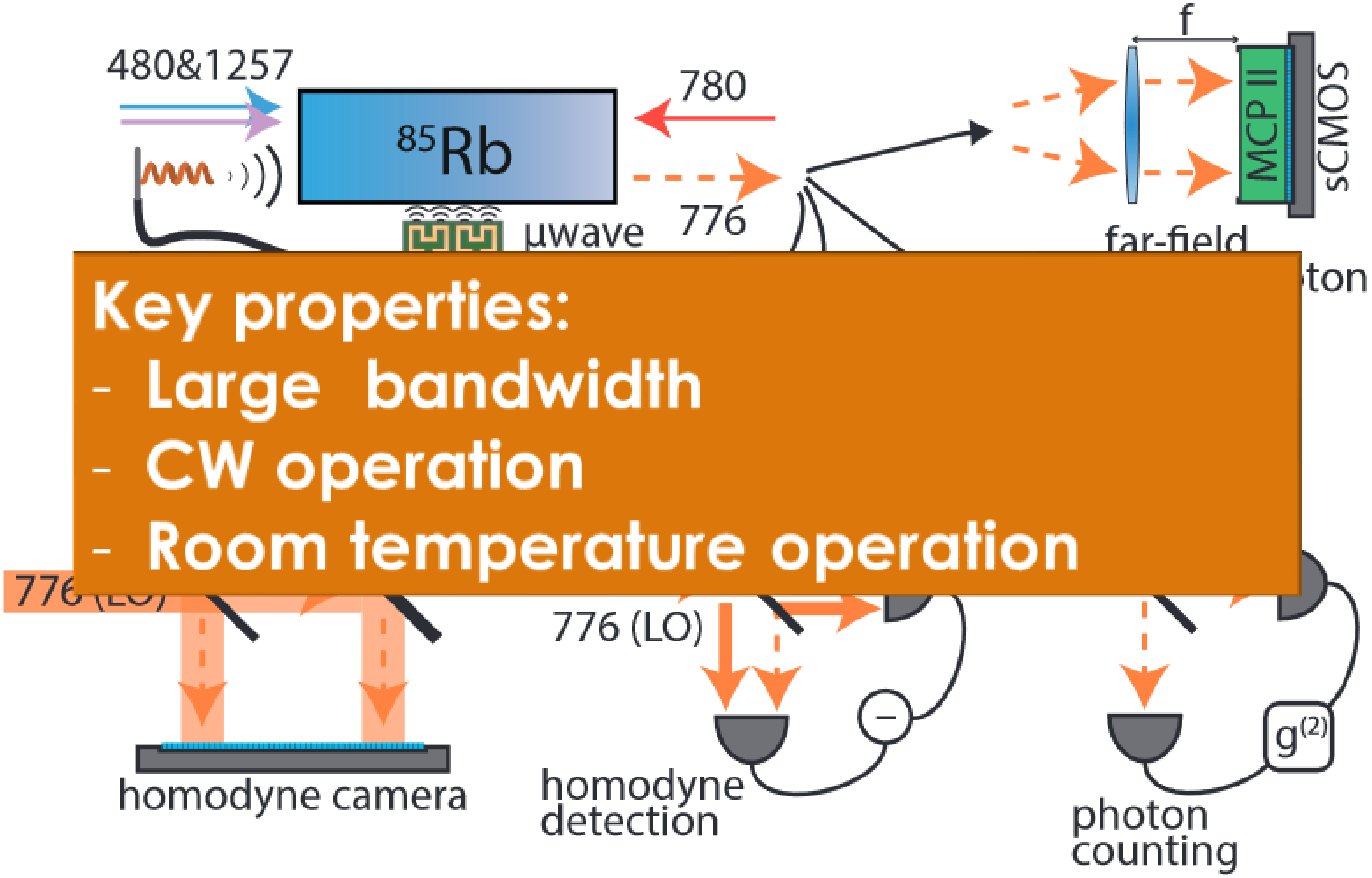

Key properties:

- Large bandwidth
- CW operation
- Room temperature operation

Tomography

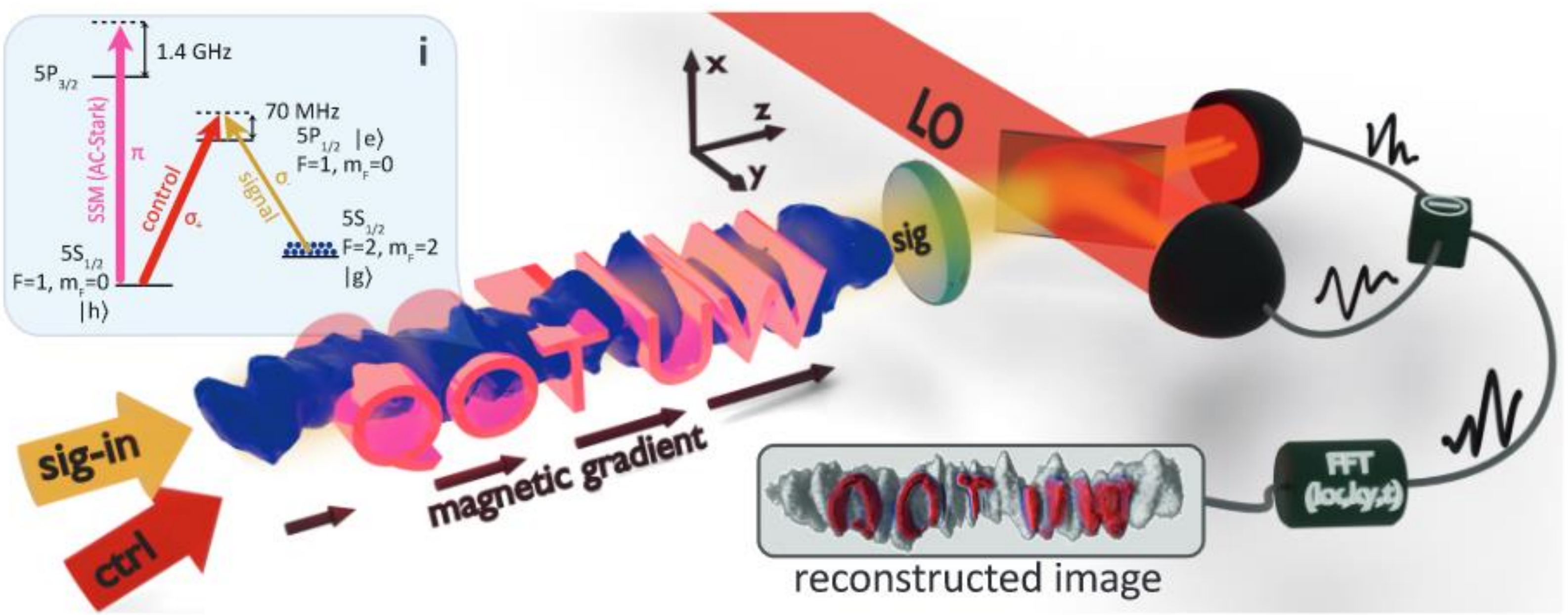
i
1.4 GHz
5P3/2
70 MHz
5P1/2 |e⟩
F=1, mF=0
5S1/2
F=2, mF=2
|g⟩
5S1/2
F=1, mF=0
|h⟩
SSM (AC-Stark)
π
control
σ+
signal
σ-
x
z
y
LO
sig
sig-in
ctrl
magnetic gradient
FFT
reconstructed image

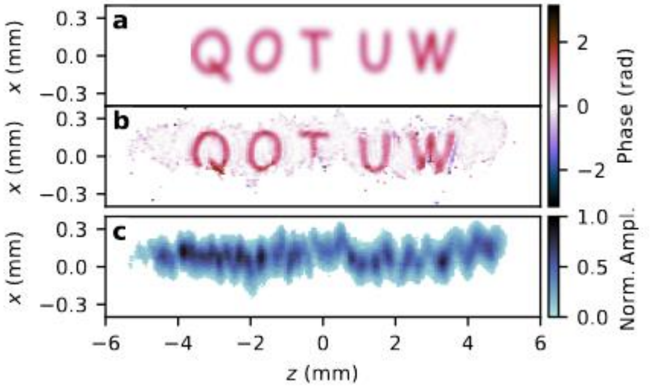
a
b
c
x (mm)
z (mm)
Phase (rad)
Norm. Ampl.

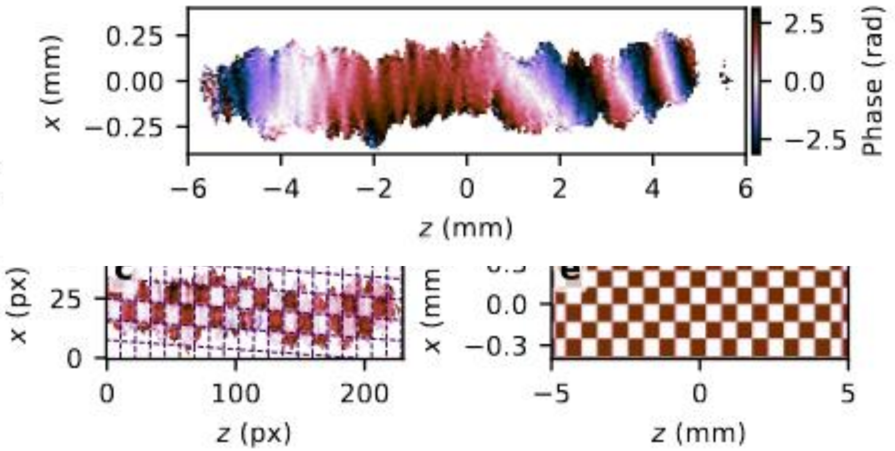
x (mm)
z (mm)
Phase (rad)
x (px)
z (px)
e

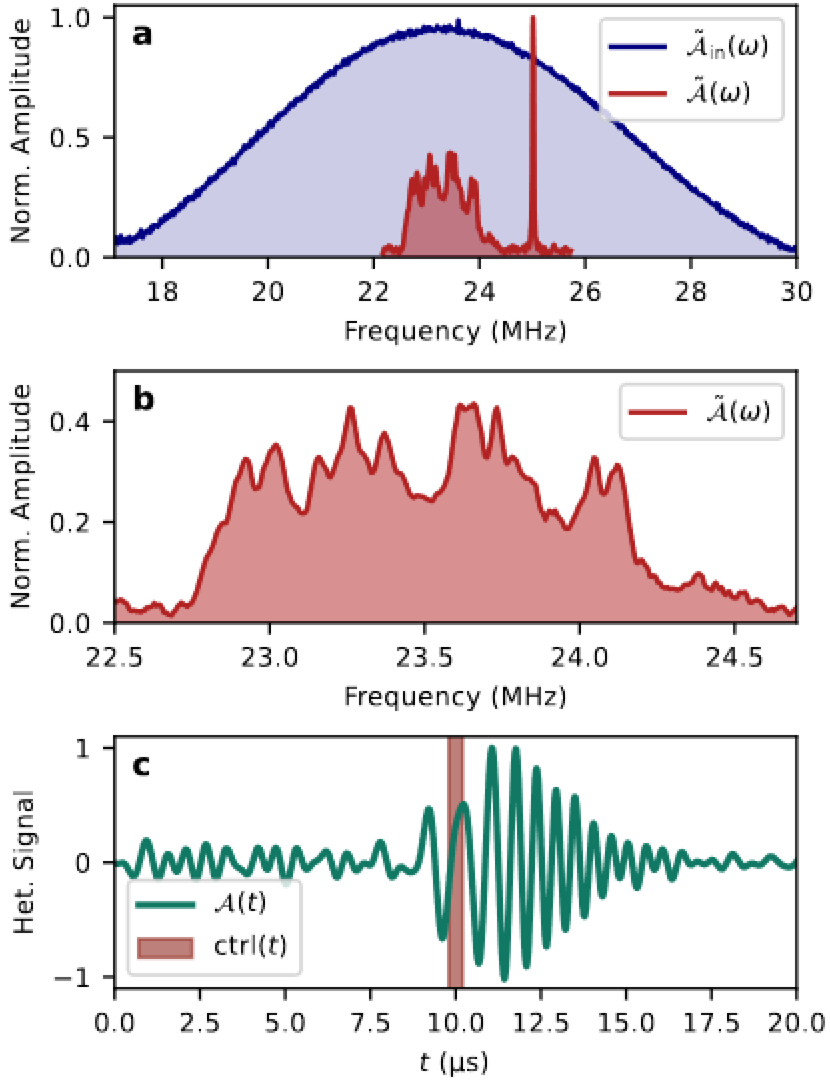
a
Norm. Amplitude
Frequency (MHz)
$\tilde{A}_{in}(\omega)$
$\tilde{A}(\omega)$
b
Norm. Amplitude
Frequency (MHz)
$\tilde{A}(\omega)$
c
Het. Signal
$A(t)$
ctrl(t)
t (µs)

Rydberg blockade tomography

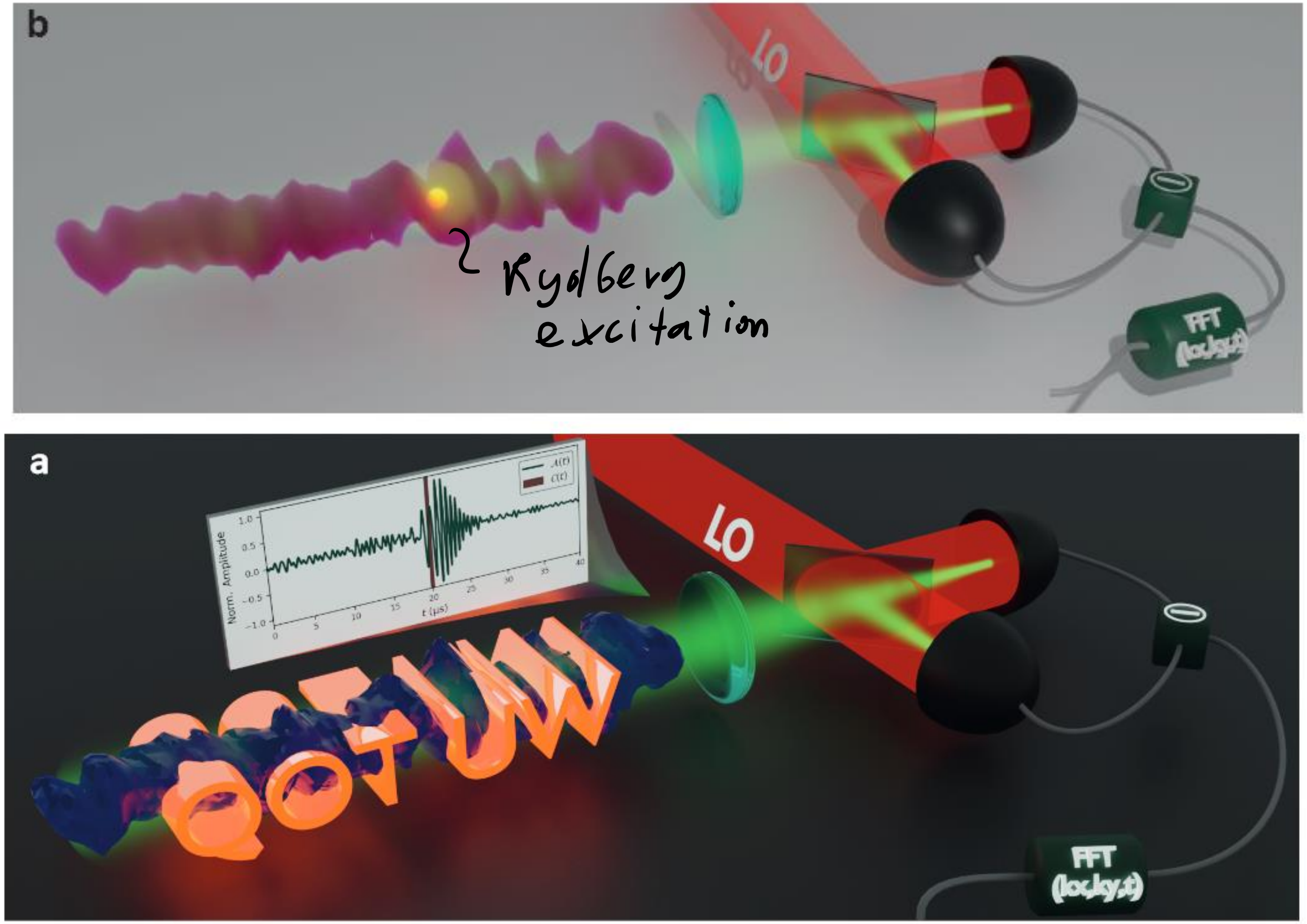

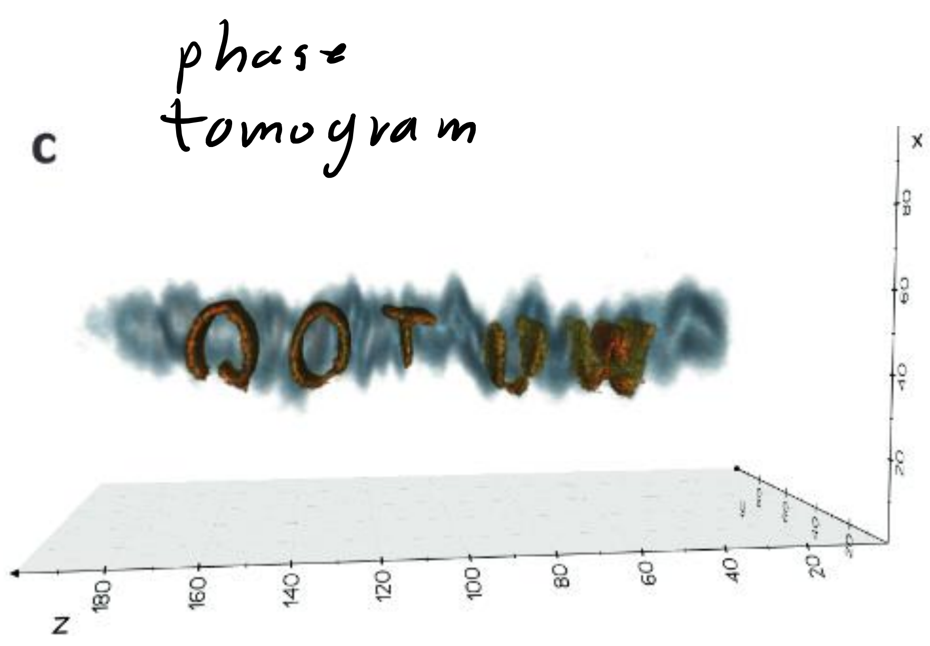

M. Mazelanik, A. Leszczyński, T. Szawełło, **MP**, Comm. Phys. **6**, 165 (2023)

Thank You

QOT Centre for Quantum Optical Technologies
qot.uw.edu.pl

qodl.cent.uw.edu.pl **– lab webpage**

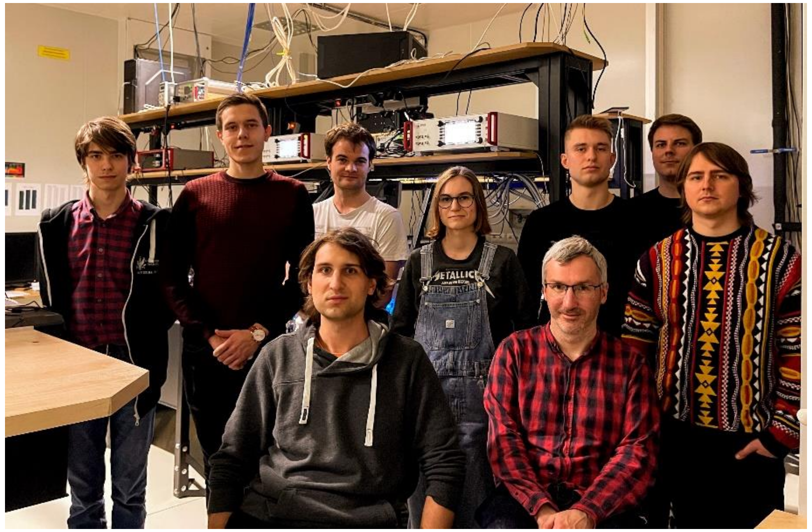

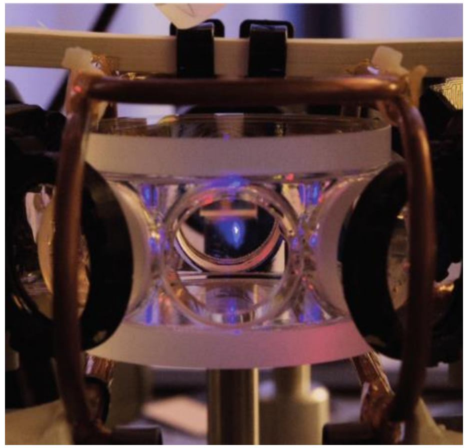

Experimental group leaders:
Wojciech Wasilewski
Michał Parniak
Postdocs:
Mateusz Mazelanik (also at CLEO!)
PhD Students:
Michał Lipka, **Sebastian Borówka**
Students:
Uliana Pylypenko, Marcin Jastrzęnski, Stanisław Kurzyna, Bartosz Niewelt, Jan Nowosielski, Pavel Halavach
Theory Collaborators:
Konrad Banaszek, Rafał Demkowicz-Dobrzański, Krzysztof Jachymski, Rafał Ołdziejewski

The "Quantum Optical Technologies" project (Project No. MAB/2018/4) is carried out within the International Research Agendas programme of the Foundation for Polish Science co-financed by the European Union under the European Regional Development Fund.

NATIONAL SCIENCE CENTRE POLAND

European Funds Smart Growth | Republic of Poland | FNP Foundation for Polish Science | European Union European Regional Development Fund

2021/43/D/ST2/03114